The Dissertation Committee for Charles Ray Chambers Jr.
certifies that this is the approved version of the following dissertation:

DESIGN, SYNTHESIS AND TESTING OF MATERIALS

FOR 157 nm PHOTOLITHOGRAPHY

Committee:

_____
C. Grant Willson, Supervisor

_____
Brent L. Iverson

_____
Eric V. Anslyn

_____
David A. Vanden Bout

_____
Benny D. Freeman

DESIGN, SYNTHESIS AND TESTING OF MATERIALS

FOR 157 nm PHOTOLITHOGRAPHY

by

Charles Ray Chambers Jr., B.S.

Dissertation

Presented to the Faculty of the Graduate School of

The University of Texas at Austin

in Partial Fulfillment

of the Requirements

for the Degree of

Doctor of Philosophy

The University of Texas at Austin
May 2005

Dedicated to my family for all the love and support they have given me.

Acknowledgements

I have really enjoyed my time at The University of Texas at Austin. I have had the opportunity to meet a lot of interesting people and make a lot of good friends. First and foremost I would like to thank Dr. Willson for allowing me to join his group. Dr. Willson's guidance has been invaluable to my development as a chemist and a person.

I thoroughly enjoyed working on the 157 nm project along side Dr. Brian Osborn, Dr. Matt Pinnow, Dr. Raymond Hung, Dr. Hoang Vi Tran, Dr. Brian Trinque, Dr. Ryan Callahan, Dr. Les Carpenter, Takashi Chiba, and Shiro Kusumoto. I consider you all dear friends and hope we can keep in touch.

I was also fortunate enough to work with numerous high school students and undergraduates. Johnathan Downey, Hale McMicheal and Alok Vasudev were outstanding high school students who worked for me a summer and did excellent work. Vanessa Dimas, Leonidas Whalthal, Ryan Odom and Alok Vasudev were the amazing undergraduates that I was able to work with. Alok loved running DRMs so much he came back for more. You are all very intelligent and outstanding with bright futures ahead of you.

The imaging work performed at International SEMATECH was made possible by Will Conley, Danny Miller, Vicki Graffenberg, Shashikant Patel, Georgia Rich, Mike Rodriguez, Jorden Owens and Tony Vander Heyden. Thank you for all your help.

Margaret Rodgers has done a wonderful job keeping everyone in line. She makes sure everything gets done in a timely manner making life easier for us graduate students. Thank you Margaret.

I would like to list all of the things that Kathleen Sparks has done for me but that would take too long. Kathleen you are definitely the heart of the group. I will miss you, please keep in touch.

Finally, I would like to wish good luck to all my friends in the Willson Group.

DESIGN, SYNTHESIS AND TESTING OF MATERIALS

FOR 157 nm PHOTOLITHOGRAPHY

Publication No._____

Charles Ray Chambers Jr., Ph.D.

The University of Texas at Austin, 2005

Supervisor: C. Grant Willson

The microelectronics industries' ability to keep pace with Moore's law (the doubling of the number of transistors per integrated circuit every 18 to 24 months) has been due to advances in the photolithographic process. Shrinking the feature sizes that can be printed has been accomplished by decreasing the exposure wavelength which allows higher resolution and thereby more transistors per area. Currently i-line (365 nm) and deep UV (248 nm) are the most frequently used wavelengths for integrated circuit manufacturing. As device geometries shrink below 100 nm, the lithography for critical layers will be performed at an exposure wavelength of 193 nm. The 193 nm technology is being implemented now. Some "next generation" photolithography will be used to print features down to 45 nm. The technology that has investigated the most for printing the 45 nm node is uses 157 nm as the exposure wavelength. As the move is made from one

exposure wavelength to the next new photoresist materials are required that have a low absorbance at the lower wavelength. Finding materials for 157 nm photolithography was particularly challenging due to the inherently high absorbance of most materials at this short wavelength. It was discovered that the addition of fluorine into organic molecules greatly increased their transparency at 157 nm. Fluorine or other transparency enhancing moieties were therefore incorporated into analogues of the 193 nm photoresist polymers. New fluoro polymers were prepared by free radical copolymerizations of electron deficient olefins with fluorinated and nonfluorinated norbornenes. Unfortunately the transparency requirements were not fully achieved with the 193 nm photoresist polymer analogues. Highly transparent fluorinated norbornene polymers were prepared using metal catalysts. One such polymer is poly(2-(3,3,3-trifluoro-2-trifuoromethyl-2-hydroxypropyl)bicyclo[2.2.1]hept-5-ene) (PNBHFA). It was discovered that PNBHFA has unique dissolution inhibition properties which are reminiscent of the novolac resin used in two component, non-chemically amplified photoresist system used at 365 nm. A more transparent fluoropolymer (Asahi RS001 polymer) was later introduced. Transparent, highly functionalized additives that could be blended with PNBHFA or the Asahi polymer and used to print high resolution, high aspect ratio images at 157 nm were designed, synthesized and tested.

Table of Contents

Table of Figures

CHAPTER 1 — Introduction to Photolithography

Moore's Law

In 1965 Gordon E. Moore, then Director of Research and Development at the Fairchild Semiconductor Division of Fairchild Camera and Instrument Corporation, stated, "The complexity for minimum component cost has increased at a rate of roughly a factor of two per year. Certainly over the short term this rate can be expected to continue, if not to increase. Over the longer term, the rate of increase is a bit more uncertain, although there is no reason to believe it will not remain nearly constant for at least 10 years. That means by 1975, the number of components per integrated circuit for a minimum cost will be 65,000. I believe that such a large circuit can be built on a single wafer" (Moore 1965). The semiconductor industry still follows Moore's law, the doubling of the number of transistors per integrated circuit (IC) every 18 to 24 months, more than 40 years after Gordon Moore's prediction. **Figure 1.1** shows the number of transistors per IC as a function of time. Although Moore's law is more of a guideline than a true law, the industries' strict adherence to Moore's law has enabled computers to shrink dramatically in size from requiring thousands of square feet to house the earliest computer to requiring a small corner of desk space for the computers of today. Following Moore's law has led to increasing computing power and speed over a million times compared to the earliest computers while reducing the cost of computers.

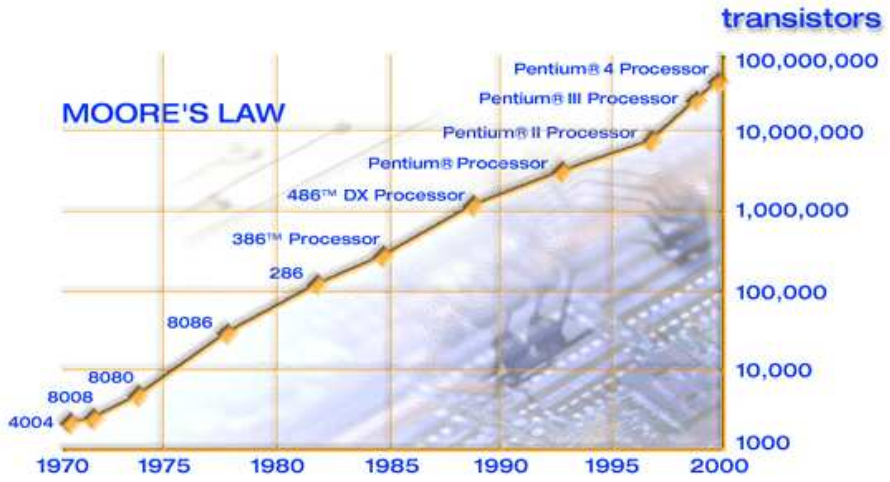

Figure 1.1: Moore's Law Plot of transistors per IC versus year.

The Photolithographic Process

Advances in the photolithographic process are one of the primary reasons the electronics industry has been able to maintain such a rapid development pace. Photolithography accounts for as many as half the process steps required to produce an integrated circuit. A photolithographic step is required before four of the major processes used to construct an IC. Ion implantation, metallization, and chemical vapor deposition all depend on patterning from photolithography. The key component of the photolithographic process is the photoresist. The photoresist serves two major functions: to convert an optical image of a circuit pattern into a 3D relief pattern into a polymer coating through a photochemical reaction which alters its solubility in a developer

solution (photo) and to resist subsequent processes that transfer the relief image into the underlying substrate (resist). **Figure 1.2** shows the photolithographic process.

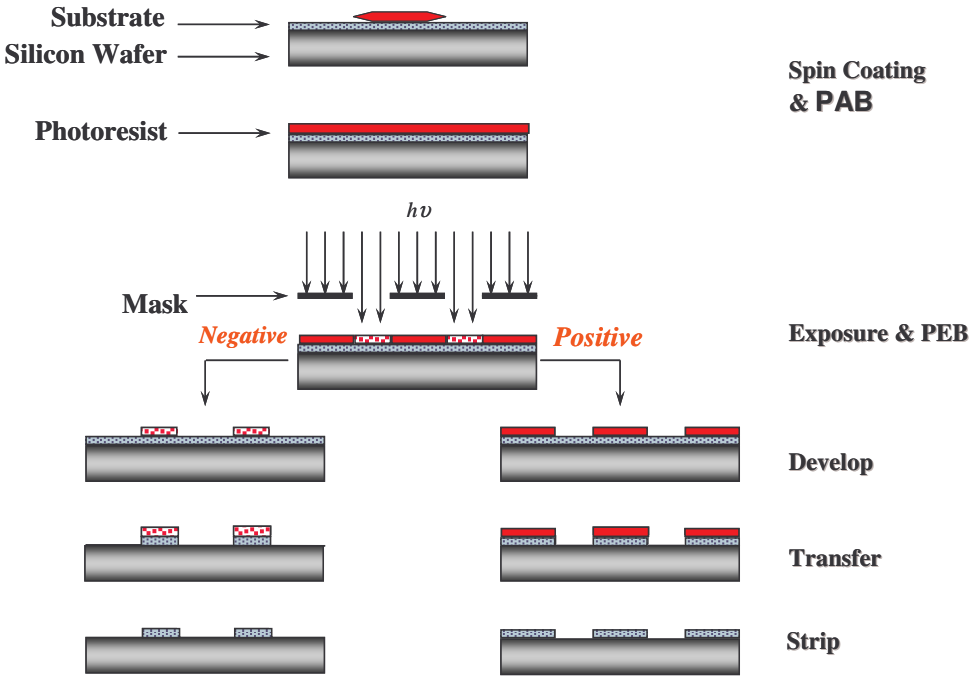

Figure 1.2: The photolithographic process.

The photolithographic process involves seven steps: spin-coating, post application bake (PAB), exposure, post exposure bake (PEB), development, etch and finally, stripping of the resist film. Positive or negative tone photoresists are both used for the pattern transfer. In a positive tone photoresist system the photoresist film is insoluble in developer before exposure but the resist is designed in such a way that after exposure to some wavelength of light, the exposed areas of the photoresist film become base soluble. In the negative tone system the photoresist film is initially soluble but after exposure the

exposed areas of the photoresist film are rendered insoluble in developer. Only positive tone systems will be discussed in this document.

Spin-coating

A photoresist formulation composed of the resist polymer, photoacid generator, a base quencher and an organic casting solvent is deposited onto the middle of a silicon wafer, which is covered with either insulator or conducting layer that is to be patterned. The wafer is then spun at high speeds, forming a thin film of photoresist. The thickness of the spin coated polymer film can be controlled by the concentration of the polymer solution and the wafer velocity during spin casting.

Post Application Bake

The coated wafer is then baked is drive off any residual casting solvent and to densify the film. The temperature range of the post application bake (PAB) is usually between 90-135 ºC. The PAB temperature can be above the T_g of the resist polymer but it must be low enough to avoid thermal degradation of the photoresist polymer or the other photoresist components.

Exposure

The resist-coated wafer is next placed beneath a patterned photomask. Typical photomasks are made of quartz with a patterned chromium coating. The chromium

defines the pattern to be transferred into the photoresist on the wafer. Light of the appropriate wavelength is shined through the patterned photomask. The transparent areas, those without chromium, allow incident light to come into contact with the photoresist film. The exposed areas of the photoresist film undergo a photochemical reaction. The photoresist must be transparent at the exposure wavelength to ensure that the photochemical reactions will occur all throughout the film in the exposed areas.

Post Exposure Bake

After exposure the wafer is again baked, typically between 90-135 ºC. The PEB step drives the thermolytic chemistry that causes the solubility change in the polymer resin. This will be addressed in-depth later. The post exposure bake must be below the T_g of the resist polymer or the features will be distorted.

Development

The most common developer, which has become the industry standard is 0.26 N tetramethylammonium hydroxide (TMAH). This substance is dispensed onto the wafer. Typically the base is in contact with the photoresist film between 20-120 seconds. The TMAH is then spin-coated from the wafer, and the wafer is then rinsed with deionized water. A “hard bake” is sometimes performed after the rinse to remove any residual water. The conditions of the hard bake are similar to those used for the PEB.

Pattern Transfer

The areas of the substrate below the photoresist film that was developed away can be selectively eroded away by free radicals and reactive ions (etch process). The photoresist film is resistant to this process, which allows the pattern in the photoresist film to be transferred to the underlying substrate.

Resist Strip

The final step is to remove the remaining photoresist, which is normally done under oxygen plasma etch conditions. The pattern in the underlying substrate is thus fully revealed, and the process begins again to pattern the next layer of the device.

Non-chemically Amplified Photoresists

The type of positive tone photoresist system used for 436 (*g* line) and 365 nm (*i* line) lithography are termed non-chemically amplified photoresists (**Figure 1.3**). The base resin is novolac, a condensation polymer prepared from formaldehyde and *ortho*, *meta*, and/or *para*- cresol. Since novolac is a phenolic polymer, it is highly soluble in 0.26 N TMAH developer. The rate at which a film of novolac dissolves is dependent on the type of cresol(s) used to prepare the polymer.

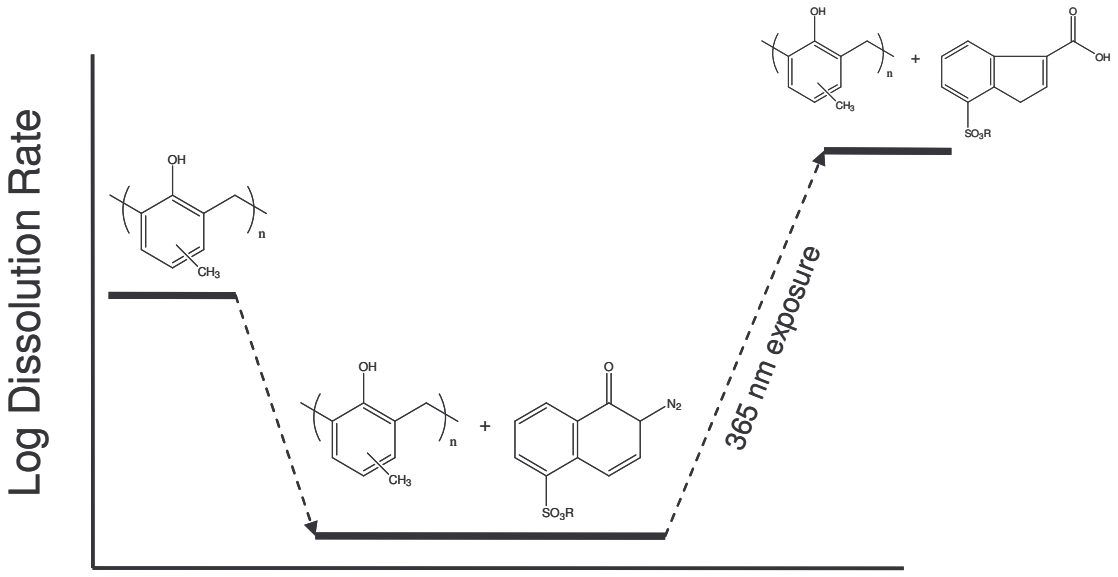

Figure 1.3: Non-chemically amplified photoresist system for i and g line lithography.

A diazonapthoquinone, 20-30 wt%, is blended with the novolac and the films are cast from PGMEA. The resulting film is insoluble in TMAH developer (Kawaba 1996). The sulfonate functionality of the diazonapthoquinone hydrogen bonds with the phenolic hydrogen to raise the effective pK_a of the acidic species in the film rendering the photoresist film insoluble in 0.26N TMAH developer. The mechanism of the inhibition of the dissolution of novolac by the diazonapthoquinone has been extensively investigated. (McAdams 2000). The film is exposed to ca. 200 mJ/cm^2 at 405 or 365 nm using a mercury arc lamp and appropriate band pass filters that block all unwanted wavelengths.

During exposure the diazonapthoquinone, a photoactive compound (PAC), undergoes the Wolff rearrangement to give a ketene, which reacts with water to form a

carboxylic acid. The rearrangement renders the exposed areas of the film soluble in TMAH developer. In fact, the formation of the carboxylic acid promotes the dissolution rate of the exposed areas making them dissolve at a faster rate than a film of pure novolac. The best features of this system are the low cost of the materials, the fact that the system works well and is very simplistic. Today this system is used for the photolithographic steps used in the back end, or noncritical layers, of IC fabrication.

Chemically Amplified Photoresists

The exposure source for i and g line was a mercury arc lamp. In the beginning of 248 nm photolithography the mercury arc lamp was still the exposure source. The output of the mercury arc lamp is strong at 436 nm and 365 nm but at 248 nm the output is weak. It was obvious that a resist system with increased sensitivity over that of non-chemically amplified system was required to sustain productivity. For this reason chemically amplified photoresists were created in the early 1980s (**Figure 1.4**) (Ito 1982; Frechet 1983; Willson 1986).

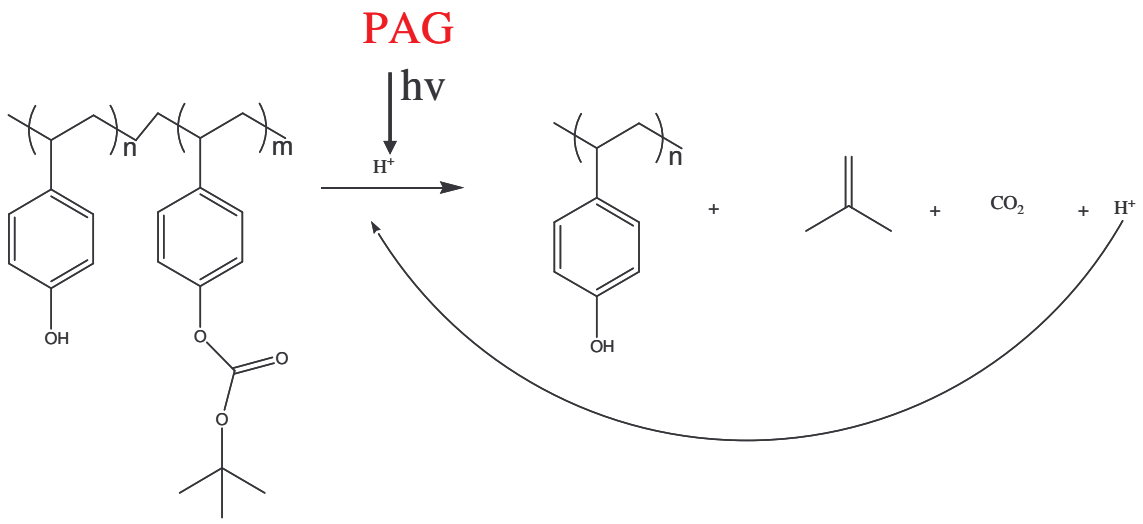

Figure 1.4: Chemically amplified photoresist system used for 248 nm lithography.

Novolac, which is highly absorbing at 248 nm, is replaced by the more transparent phenolic resin, poly (*p*-hydroxystyrene), (PHS). A critical fraction of the acidic functional groups of PHS are blocked by acid labile *tert*-butyl carbonate groups, which render the polymer insoluble in TMAH developer. The PAC for the non-chemically amplified system is a photoacid generator (PAG).

The photoacid generator generates a super acidic species (pK_a = -9) during exposure. The acid catalyzes the thermolysis of the *tert*-butyl carbonate protecting group, exposing the phenolic site during the post exposure bake, producing isobutene and carbon dioxide as volatile byproducts, and acid is regenerated and catalyzes the decomposition of another *tert*-butyl carbonate group. The exposed areas thus become soluble in developer. This acid-catalyzed resist system requires a lower exposure dose, typically

well below 50 mJ/cm^2, to promote the required solubility change. The thermal decomposition of the *tert*-butyl carbonate occurs at around 200 ºC, which is above the T_g of the polymer. The acid-catalyzed thermolysis of *tert*-butyl carbonate occurs rapidly at 100 ºC, which, well below the T_g of PHS.

Today KrF excimer laser is the exposure source for 248 nm photolithography. At the next wavelength (193 nm) an ArF laser is the exposure source for photolithography. For 193 nm lithography, PHS was replaced by acrylate based copolymers or cyclic olefin-maleic anhydride (COMA) (**Figure 1.5**) copolymers (Ito 2000) because PHS is too highly absorbing at 193 nm. The acidic group was changed from phenol to a carboxylic acid and the acid-labile protecting group *tert*-butyl carbonate was replaced with *tert*-butyl ester. The deprotection chemistry that occurs here during the post exposure bake is the same.

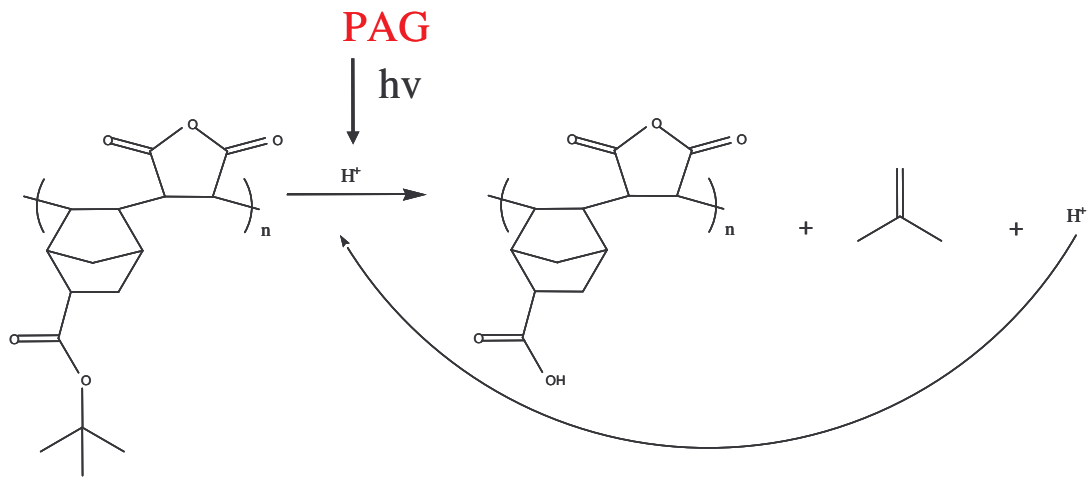

Figure 1.5: COMA copolymer photoresist system for 193 nm photolithography.

Photoacid Generator (PAG)

Several types of compounds have been designed to produce acid upon UV irradiation (Shirai 1998). The most commonly used PAGs for photolithography are onium salts. The photolysis mechanism of sulphonium salts is shown in **Figure 1.6** (Dektar 1990). The carbon-sulfur bond is cleaved homolytically by UV irradiation resulting in an aryl radical and sulfur radical cation. Hydrogen abstraction by the sulfur radical cation followed by protonation of the counter ion generates the photoacid and the other resulting byproducts (i.e., diphenyl sulfide, etc.).

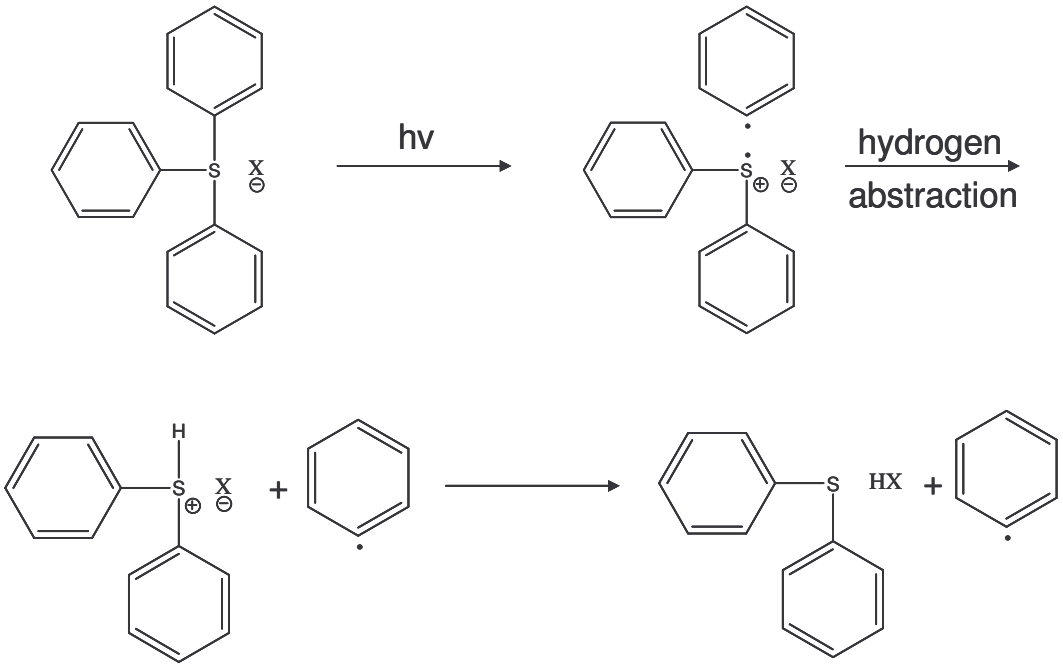

Figure 1.6: Mechanism of sulphonium PAG photolysis.

Resolution Limits

The principle reason photolithography has enabled the microelectronics industry to keep pace with Moore's Law can be explained by use of the Rayleigh equation (**Eqn. 1.1**) (Mack 1997).

$$R = k\frac{\lambda}{NA} \qquad \textbf{Eqn. 1.1}$$

R = resolution limit

k = constant of photoresist

λ = exposure wavelength

NA = numerical aperture

The resolution limit, or minimum feature size that can be printed, is reduced by either decreasing the exposure wavelength, or by increasing the numerical aperture. The numerical aperture is determined by the lens system of the stepper. Optical engineers work on the optics systems in steppers to increase the numerical aperture. Resist chemists are responsible for developing new polymers or base resins that to support shorter exposure wave lengths. The new polymer must be transparent at the exposure wavelength and undergo the chemistry required for pattern transfer.

The reason three different polymers are used as the base resins for 365, 248 and 193 nm photoresists is due to high absorbance values of the old resist polymer at the new lower exposure wavelength. It is critical that photons are able to penetrate all the way

through the resist film to the underlying substrate. If the photoresist is not sufficiently transparent at the exposure wavelength then the photochemistry that changes the polymers solubility characteristics will not take place in the regions near the substrate where no photons were able to penetrate. **Figure 1.7** compares the imaging performance of transparent and opaque photoresist materials.

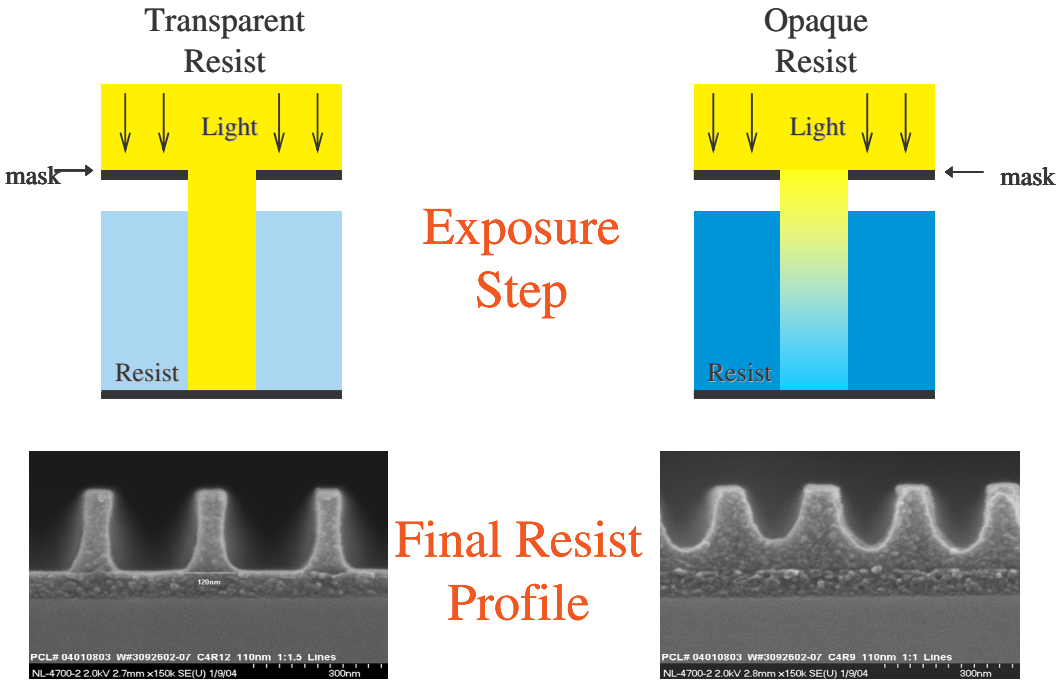

Figure 1.7: Imaging performance of a transparent and opaque photoresist.

Photolithographers work to adapt the photoresist materials to the demands that result from decreasing the exposure wavelength. A photoresist must be quite transparent at the exposure wavelength, have a T_g above the PEB (90-130 ºC), be resistant to the

reactive ion etch process, have an acid labile solubility switch and form a film that adheres to the wafer surface.

Photoresist Design

Photoresist polymers can be broken down into four modules (**Figure 1.8**). The backbone of the polymer tethers the functional monomers together and provides the mechanical properties of the resin such as T_g.

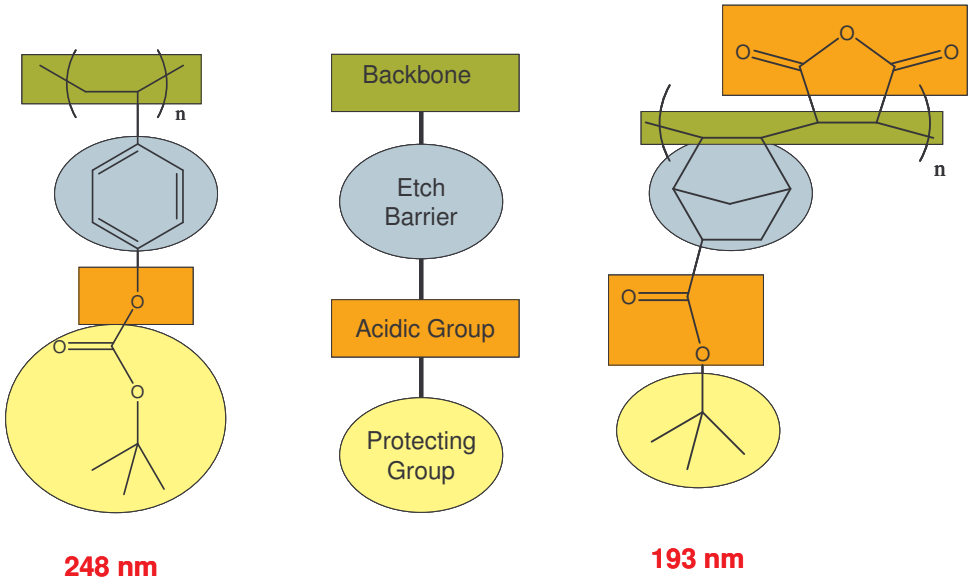

Figure 1.8: Modules of 248 nm and 193 nm photoresists.

The etch barrier provides resistance to the reactive ion etch process. An empirically derived relationship between polymer structure and etch rate, the Onishi parameter, can be used to approximate the etch resistance of photoresist materials. Equation 1.2 demonstrates that increasing the carbon content while decreasing the oxygen or hydrogen content, decreases the etch rate (Gokan 1983).

$$Rate_{etch} \alpha \frac{N_T}{N_C - N_O}$$ **Eqn. 1.2**

N_T = total number of atoms

N_C = total number of carbon atoms

N_O = total number of oxygen atoms

One way of increasing the carbon in the polymer is to introduce unsaturation. The aromatic rings in PHS provide the etch resistance for the 248 nm photoresist. The alicyclic norbornene structure provides the etch resistance for 193 nm photoresists.

The acidic group imparts base solubility and also promotes adhesion to the silicon wafer. The most commonly used acidic groups are the phenols, pK_a of 11, used in 365 and 248 nm resist polymers, and carboxylic acids, pK_a of 4, used for 193 nm resist polymers. In chemically amplified photoresist systems, an acid protecting labile group masks some fraction of the acidic groups that are appended to the base polymer resin. Acetals, *tert*-butyl carbonates and *tert*-butyl esters are the most widely used protecting groups.

Design of 157 nm Photoresist

The wavelength to be used in future fabrication of semiconductor devices could be 157 nm, which is the output of an F_2 excimer laser. Finding materials to be used for photolithography at this wavelength is particularly challenging due to the high absorbance of most compounds in this region of the VUV. Even air and water are very highly absorbing at 157 nm. **Figure 1.8** shows the absorbance of 248 and 193 nm photoresists as well as several common polymers. Polystyrene, PMMA and polynorbornene are all highly absorbing at 157 nm. **Figure 1.8** also shows that fluoropolymers are somewhat transparent at 157 nm (Kunz 1999). Incorporation of fluorine into one or more of the four photoresist modules could be used to achieve a photoresist base resin that is transparent at 157 nm.

	Wavelength (nm)		
	157.6	**193**	**248**
248 resist	6.84		**0.37**
193 resist	6.86	**0.47**	
Polystyrene	6.20		
Polynorbornene	6.10		
PMMA	5.69		
Fluorocarbon	0.70		

Figure 1.9: Absorbance (μm^{-1}) at 157 nm of common polymers

The modular approach (Brodsky 2000) was used to design a 157 nm photoresist (**Figure 1.9**). Since the polymer backbone is a determined by the method of polymerization, there was some uncertainty about the polymer backbone. In 193 nm resists, the etch barrier was changed from an aromatic ring, at 248 nm, to a norbornene derivative. Fluorination of the norbornene to impart transparency at 157 nm was the next logical evolution of the etch barrier. The acid groups that can be used are either the bis trifluoromethyl carbinol, with a pK_a similar to phenol; or a carboxylic acid with sufficient fluorination to improve transparency. The acetal, *tert*-butyl carbonate and *tert*-butyl ester solubility switching groups that were used at 248 and 193 nm can also be used for 157 nm photolithography.

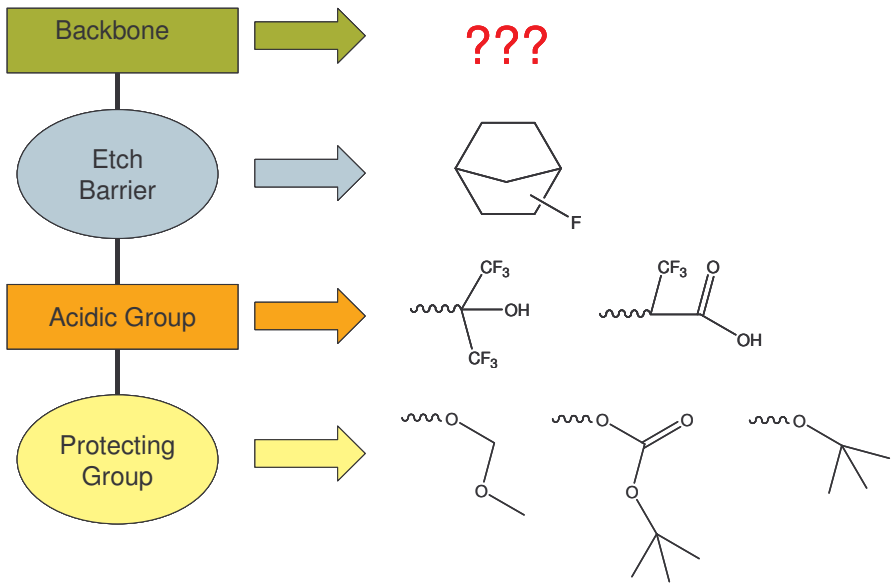

Figure 1.10: Modular approach to 157 nm photoresist design

Synthesis and Absorbance of Fluorinated Norbornenes

The easiest way to incorporate fluorine into norbonenes is through Diels-Alder reactions of fluorinated dieneophiles with cyclopentadiene (**Figure 1.10**). Several fluorinated norbornenes were prepared (Hung 2003) (Ito 1997). These olefins were hydrogenated, to represent what the monomer would be like after incorporation into a polymer, and the gas phase absorbance measured at 157 nm (Osborn 2004). **Figure 1.11** show the gas phase absorbance for several norbornanes. The fluorinated norbornanes were several orders of magnitude more transparent than norbornane. Methods to incorporate the fluorinated norbornenes into photoresist polymers then became the challenge.

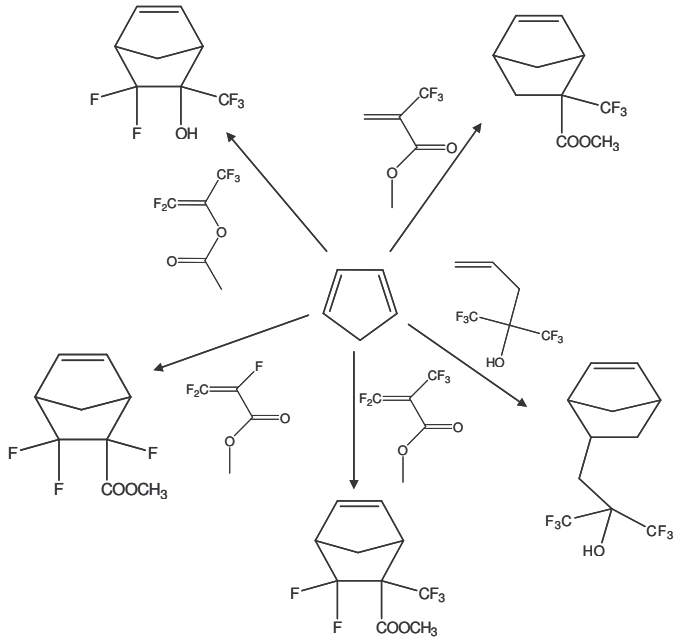

Figure 1.11: Diels Alder synthesis of fluorinated norbornenes.

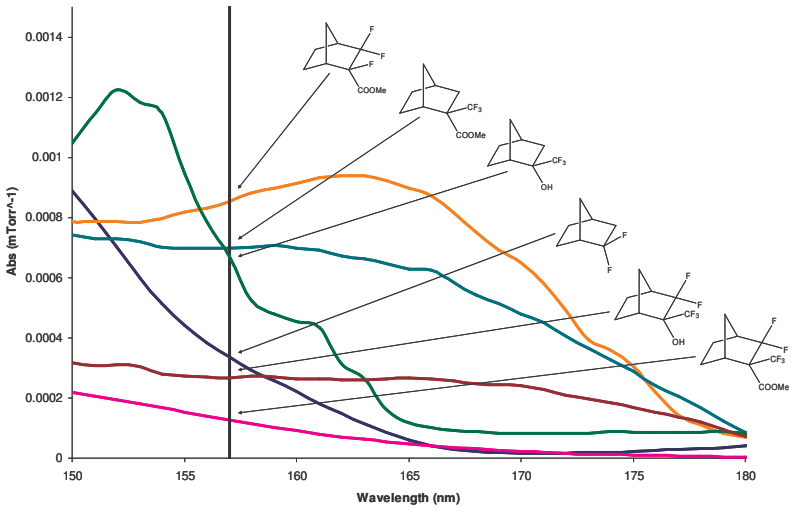

Figure 1.12: Gas phase absorbance of fluorinated norbornanes.

CHAPTER 2 — Free Radical Polymerization of Norbornenes

Radical polymerization is favored over metal catalyzed polymerization for photoresist synthesis for several reasons. Metal catalysts are expensive and even trace amounts of metal contamination can cause a drastic decrease in polymer transparency. More importantly, residual metal contamination in a photoresist can diffuse into the silicon substrate, destroying its semiconductive properties. The resist polymers used for both 248 nm and 193 nm photolithography are prepared by free radical polymerization. Free radical polymerization would be the ideal method for the polymerization of the transparent fluorinated norbornenes to prepare photoresist polymers that are transparent at 157 nm.

Simulations predicted that an absorbance of 0.7 μm^{-1} was required for imaging at 157 nm in 300 nm thick photoresist films. Initial imaging experiments were conducted in thinner films, 130-150 nm, which means the phototresist films could have higher absorbance values. The initial target absorbance for the photoresist base resin was 1.4 μm^{-1}.

Free Radical Polymerization of Norbornenes

Unfortunately, attempts to homopolymerize norbornenes radically using AIBN gave poor yields of low molecular weight oligomers (Gaylord 1977). However, norbornene-2-carboxylic acid was homopolymerized in 80 mol% di-*tert*-butyl peroxide. The polymerization was carried out neat using di-*tert*-butyl peroxide initiator at 135 °C

(Okoroanyanwu 1997). Poly(2-(3,3,3-trifluoro-2-trifluoromethyl-2-hydroxypropyl) bicycle[2.2.1.]hept-5-ene) (PNBHFA) (**2.1**) can also be polymerized using di-*tert*-butyl peroxide (Hung 2003). In theory, the PNBHFA made with radical initiator should be more transparent than the polymer synthesized via metal catalyzed addition polymerization. In reality, the radically polymerized PNBHFA was found to have higher absorbance at 157 nm than the same polymer prepared by metal catalyst (**Figure 2.1**).

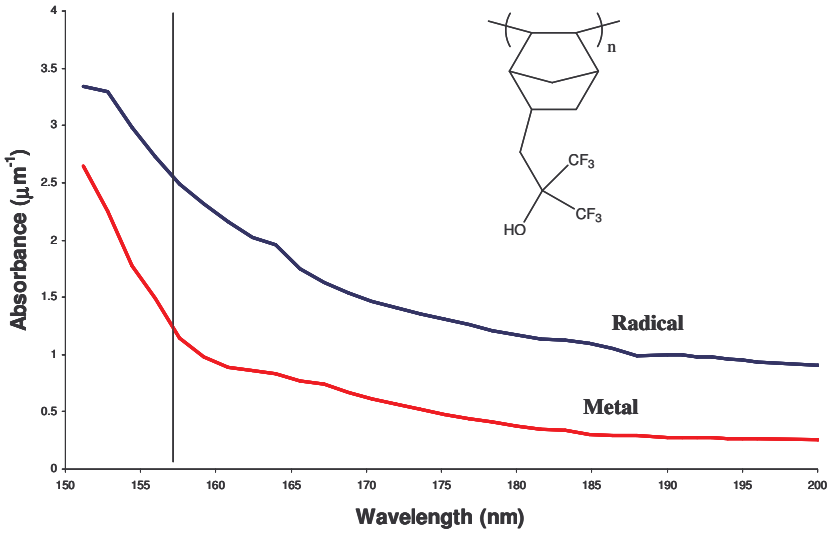

Figure 2.1: Absorbance of PNBHFA prepared by metal catalyst and free radical polymerization.

The origin of this higher absorbance was unclear, until the polymers were characterized by Matrix Assisted Laser Desorption Ionization (MALDI). The number and complexity of the peaks in the MALDI spectrum (**Figure 2.2**) shows that the **2.1,** prepared by radical initiator, was not as clean as the polymer prepared using the metal

catalyst. The MALDI also shows the PNBHFA prepared by free radical homopolymerization also had a much lower molecular weight which means more end groups are present. The end groups have been shown to contribute to the absorbance of polymers prepared by free radical polymerization (Ishikawa 2004). Despite the higher absorbance of polynorbornenes radically prepared by di-*tert*-butyl peroxide, a copolymer of 2-trifluoromethyl bicycle[2.2.1]hept-5-ene-2-carboxylate *tert*-butyl ester (NBTBECF3) and NBHFA (**2.2**), was successfully imaged at 157 nm (**Figure 2.3**). The performance penalty of this highly absorbing polymer was an exposure dose of 47 mJ/cm^2, which is relatively high for a chemically amplified photoresist. Improving this metric of imaging performance would require more transparent materials.

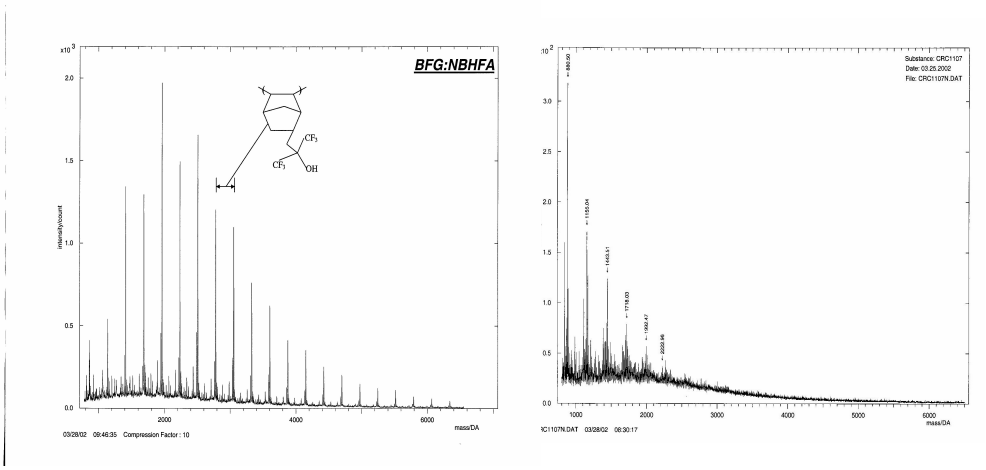

Figure 2.2: MALDI of PNBHFA (2.1) prepared by metal catalyst and free radical polymerization.

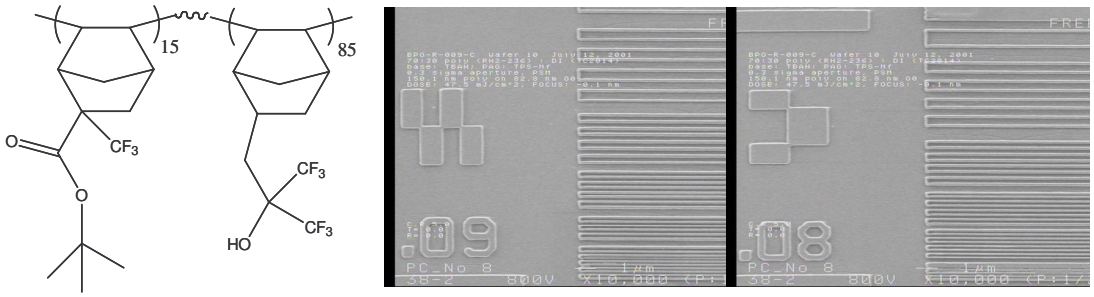

2.2

Figure 2.3: Imaging at 157 nm with copolymer 2.2.

Cyclic Olefin – Maleic Anhydride Copolymers

Cyclic Olefic-Maleic Anhydride (COMA) copolymers are used in commercial 193 nm photoresists. Such polymers (**Figure 2.4**) are prepared by the free radical mediated copolymerization of norbornenes and maleic anhydride using 2,2'-azo-*bis*(2-methylpropionitrile) (AIBN) as the initiator. If the norbornene is non-functionalized, a 1:1 alternating copolymer is formed due to the electron rich nature of the norbornene olefin and the electron deficient nature of the maleic anhydride (MA) olefin.

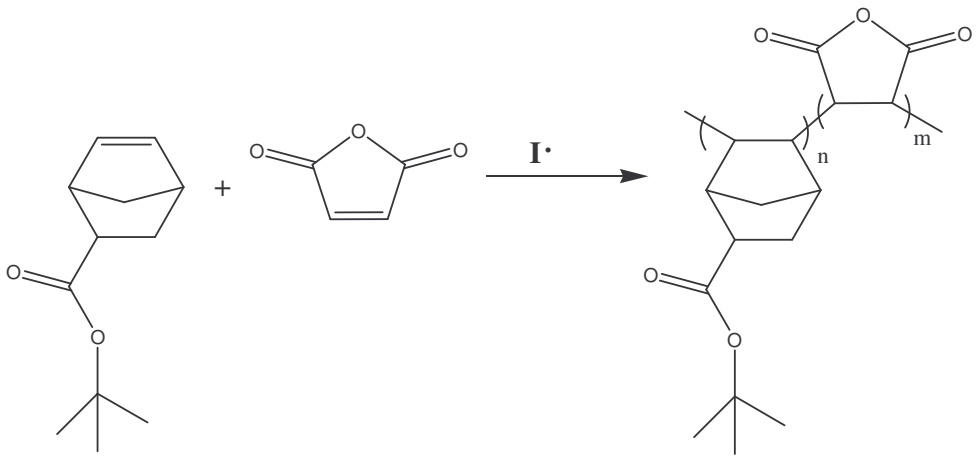

Figure 2.4: Preparation of COMA copolymers

Substitution at the 2 position of the norbornene causes the resulting copolymer to have slightly higher maleic anhydride incorporation (Ito 2000). Unfortunately, COMA polymers are not transparent enough at 157 nm to be used as a photoresist, with a reported absorbance of 6.86 μm^{-1}. Since spectroscopic studies (Kunz 1999) led to the observation that fluorinated hydrocarbons have the potential to provide the necessary transparency for 157 nm photoresists, the search for a 157 nm photoresist resin began with a survey of possible, transparent monomers.

The goal was to find transparent copolymers for 157 nm that imitate the COMA system. Fluorination of norbornanes has been shown to decrease their absorbance at 157 nm (Hung 2002) (Trinque 2003) (Osborn 2004). The fluorination of norbornenes also substantially reduces the electron density of the olefin. In order to form alternating copolymers with fluorinated norbornenes, highly electron deficient comonomers are

required. The examined comonomers were electron deficient and possessed some degree of transparency-enhancing functionality.

Alfrey–Price Q & e Scheme

Initially, the idea was to use the Alfrey-Price Q & e scheme to aid in the selection of the viable comonomers. Unfortunately, the calculated Q & e values were not received until after the possible comonomers were tested. Ultimately the Q & e values were determined to be of little practical use, we believe this to be true because the Q & e scheme does not take into account the steric hindrance of the olefins. The Alfrey-Price Q & e scheme assigns two values per olefin that relay its reactivity towards free radical copolymerization, compared to two reactivity ratio values for a pair of olefins. The Q value describes the resonance stabilization of the monomer and radical. The e value describes the polar interactions of the monomer and radical. The Q and e values are related to reactivity ratios by the following equations:

$$r_1 = \frac{Q_1}{Q_2} \exp(-e_1[e_1-e_2]) \qquad \textbf{Eqn. 2.1}$$

$$r_2 = \frac{Q_2}{Q_1} \exp(-e_2[e_2-e_1]) \qquad \textbf{Eqn. 2.2}$$

Styrene was chosen as a baseline reference and arbitrarily given the values Q = 1.0 and e = -0.8. Tables of Q & e values have been generated relative to the reactivity

ratios of styrene with other monomers. The best method for forming an alternating copolymer requires monomers with similar Q values, and similar but opposite sign e values (Allcock 1990). The Q & e values for the fluorinated norbonenes and several highly promising, electron deficient comonomers were not found in the literature. Prof. Dixon of Pacific Northwest National Labs (PNNL) (now University of Alabama) agreed to calculate the Q & e values for norbornene, several fluorinated norbornenes, as well as some promising electron deficient comonomers (**Figure 2.5**).

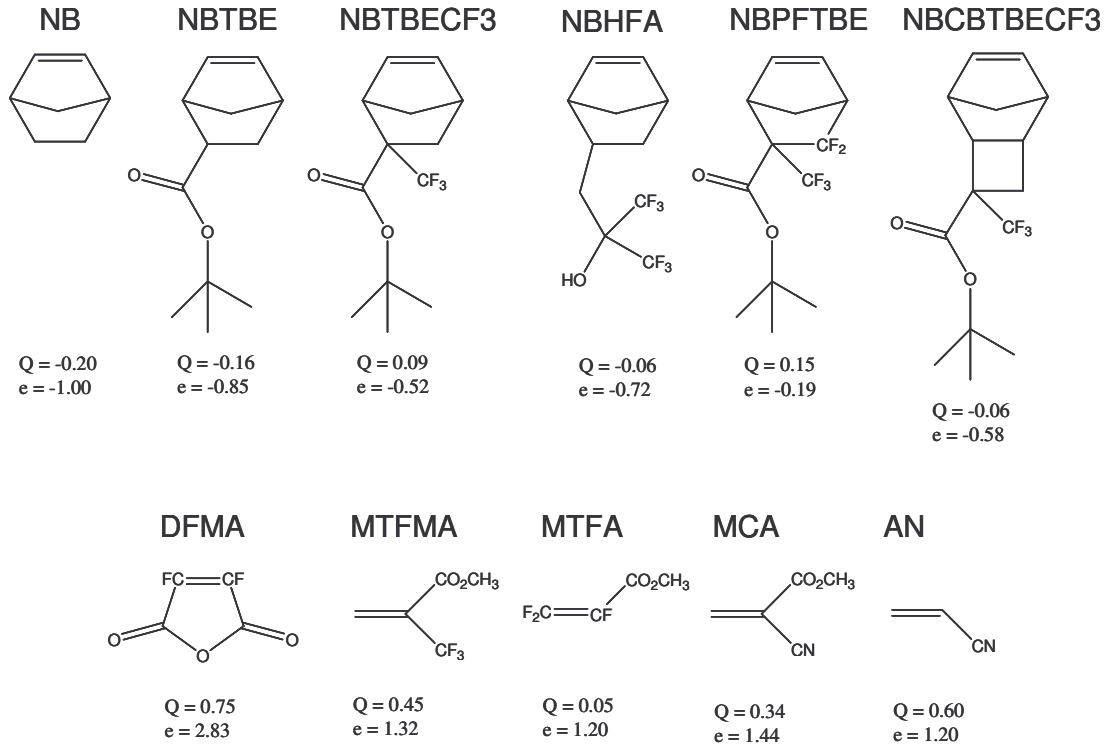

Figure 2.5: Calculated Q and e values (Dixon 2001).

Radical Copolymerization Procedure

Potentially transparent, electron deficient comonomers were evaluated empirically by polymerizing them with norbornene (NB). If the polymerization was successful then the monomer was polymerized with the *tert*-butyl ester of norbornene-2-carboxylic acid (NBTBE). Then, the monomer was copolymerized with the *tert*-butyl ester of 2-trifluoromethyl norbornene-2-carboxylic acid (NBTBECF3).

Polymerizations were typically carried out using equimolar amounts of each monomer and 10 mol% AIBN (or other similar azo radical initiators) or *tert*-butyl peroxide. The reactions were degassed by three freeze-pump-thaw cycles, with N_2 back filling, before being heated to 70-75°C. Polymers were purified by precipitation of polymer solutions into a beaker of rapidly stirring solvent that the monomer but not the polymer was soluble in. The percent incorporation of the NBTBE and NBTBECF3 monomers into the resultant polymers was determined by thermogravimetric analysis (TGA).

Fluorinated Analogues to COMA Copolymers

The copolymerization of MA with both norbornene, and norbornenes substituted at the 2 position (such as NBTBE) is well documented. There was no literature precedence for the polymerization of MA with a norbornene that has geminal substitution at the 2 position (**Figure 2.6**). This polymer was the first 157 nm analogue to typical 193 nm COMA photoresists**.** The copolymerization of MA and NBTBECF3 (**2.3**) produced a

modest yield of low molecular weight oligomers (M_w < 1500) with a high polydispersity. The absorbance and the imaging performance of the oligomers were first examined at 193 nm (**Figure 2.7**).

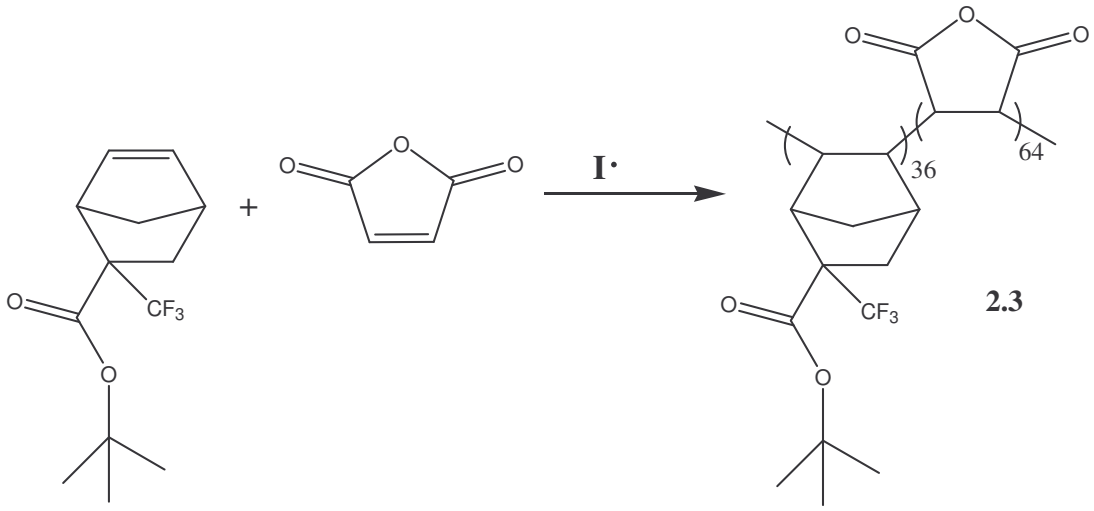

Figure 2.6: Preparation of copolymer 2.3

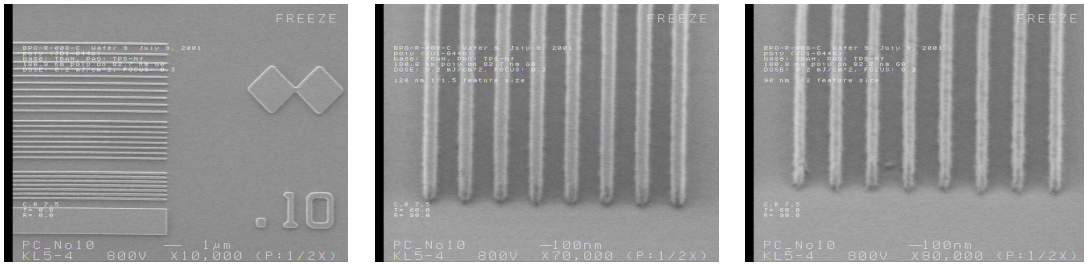

Figure 2.7: Imaging at 193 nm with copolymer 2.3.

The fluorinated analogue was 20% more transparent than the non-fluorinated COMA polymer. The polymer imaged to provide excellent features, with steep sidewalls, little top loss and no residual polymer in the exposed areas. This polymer demonstrates that 157 nm resists are backwards compatible at 193 nm, and have the potential to also be high performance materials at 193 nm. Unfortunately, the polymer absorbance was too high for use as a 157 nm photoresist polymer. It was obvious that the electron deficient olefin component would also need to have some transparency enhancing functionality in order to decrease the overall polymer absorbance.

Difluoromaleic anhydride (DFMA) and trifluoromethyl maleic anhydride (TFMMA) were both attractive electron deficient olefins to audition for copolymerization with norbornene (**Figure 2.8**). The fluorine should increase the transparency and electron deficiency of the olefins relative to MA. The free radical polymerization of DFMA and styrene has been reported. The incorporation of the DFMA in the polymer ranges from 50 to 20% depending on the conditions of the polymerization reaction (Regel 1980). No literature precedent for the free radical polymerization of TFMMA has been found.

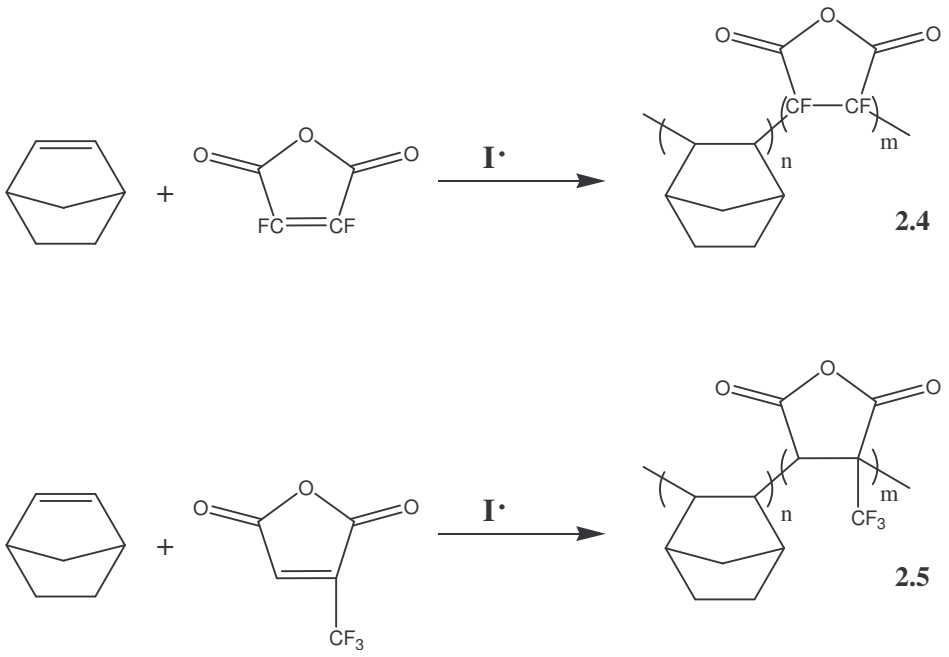

Figure 2.8: Preparation of copolymers 2.4 and 2.5

The polymerizations were performed neat (monomers and initiator only) and resulted in low yields, typically less than 10%, of low molecular weight oligomers (M_w less than 1000). Both DFMA and TFMMA are sterically hindered, which could explain the low yields and molecular weights. Alternative electron deficient comonomers to replace the maleic anhydride derivatives were then sought.

Copolymerization of Norbornenes and Fluorinated, Olefinic Gases

The most transparent, radically initiated norbornene copolymers reported are tetrafluoroethylene (TFE)-NB copolymers (**Figure 2.9**). TFE-NB copolymers composed

of up to fifty percent TFE with an absorbance of 1.1 μm^{-1} at 157 nm and a T_g of over 150 ºC have been reported (Hung 2001) (Crawford 2000).

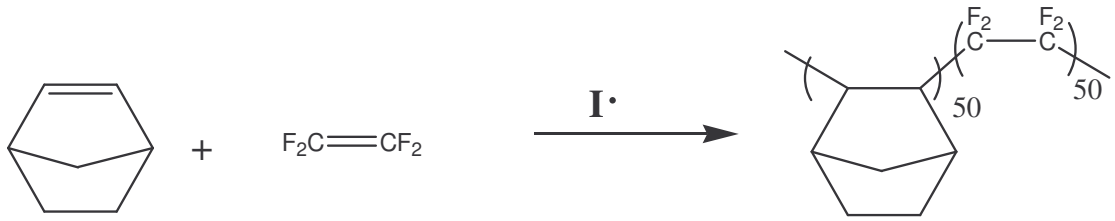

Figure 2.9: Copolymerization of tetrafluoroethylene and NB.

Due to the dangers associated with working with TFE, it disproportionates explosively, special equipment is required to work with TFE. For this reason a collaborative effort was established with Professor Darryl D. DesMateau's research group at Clemson University where there is a laboratory equipped to work with TFE. Professor DesMarteau's group focused on TFE-NB copolymers and we collaboratively investigated several alternative fluorinated gases. Attempts were then made to copolymerize norbornene with trifluoropropene (TFP), hexafluoropropene (HFP), and hexafluorocyclobutene (HFCB) (**Figure 2.10**).

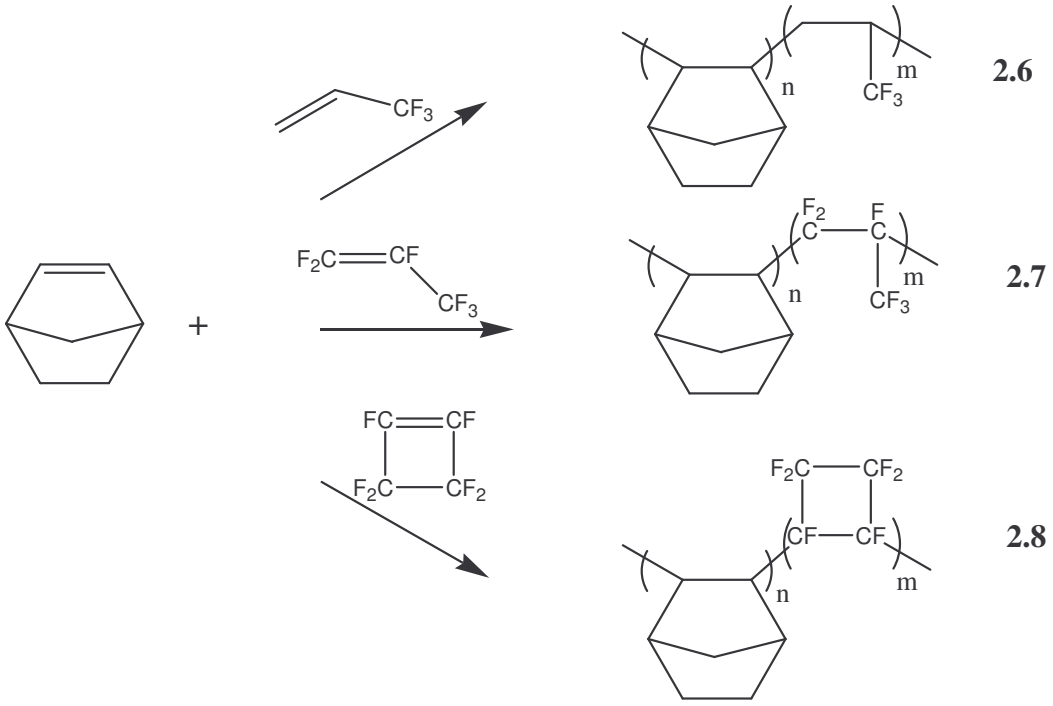

Figure 2.10: Free radical copolymerization of fluorinated gasses with norbornene.

The polymerization reactions were performed in a 22 mL stainless steel Parr reactor. Norbornene, initiator and solvent were added to the Parr reactor. Trichlorotrifluoroethane, *tert*-butyl alcohol or a mixture of the two were used as solvents. The Parr reactor was connected to the lecture bottle containing the fluorinated gas. The entire system was deoxygenated before the fluorinated gas was condensed in the Parr reactor using liquid nitrogen.

The free radical homopolymerization of TFP has been reported (Goldschmidt 1951) but the copolymerization of TFP has not. The transparency and electron

withdrawing power of the trifluoromethyl group made TFP an attractive electron deficient olefin to attempt copolymerization with NB and NBTBE. Unfortunately, only low molecular weight oligomers with a T_g below room temperature were formed upon polymerization of TFP and NB. Although the access to the olefin in HFP is much more sterically encumbered than in TFP, it was felt that the higher electron deficiency of the olefin would allow for higher molecular weights when copolymerized with norbornene. However, no polymer was produced by the attempted copolymerization of HFP and norbornene.

Copolymers of NBTBE and HFCB were prepared using *tert*-butyl peroxide and reaction temperatures above 150 ºC. Polymer **2.8** was primarily composed of NBTBE and has a high absorbance similar to the norbornenes that were homopolymerized using di-*tert*-butyl peroxide. The transparency of the norbornene–TFE copolymers were far superior to the NB copolymers that were formed using TFP or HFCB (Hung 2001) (Crawford 2000).

Copolymerization of Norbornenes and Fluorinated Acrylates

Methyl 2-trifluoromethylacrylate (MTFMA) has received attention as a monomer candidate to be used in resist material preparation. In the 1980s, anionically prepared poly(methyl-2-trifluoromethylacrylate) was investigated as a resist resin for e-beam lithography due to its ability to undergo main-chain scission upon exposure to radiation (Ito 1982). It was reported that MTFMA would not free radically homopolymerize;

however, alternating copolymers of methyl methacrylate (MMA) and MTFMA could be prepared if a large excess of the MTFMA was present (Ito 1982). It was later reported that the MTFMA would free radical homopolymerize in low conversions using AIBN or benzoyl peroxide and long reaction times (Iwatsuki 1984). The comparison of the absorbance values of poly(MTFMA) and poly(MMA) in **Figure 2.11** confirms the transparency enhancing effect of the trifluoromethyl group (Trinque 2003). Incorporating the MTFMA into a copolymer with a transparent NB monomer should give a transparent polymer with higher resistance than the MTFMA homopolymer. The copolymerization of TFMMA with NB and NBTBE were both successful (**Figure 2.12**).

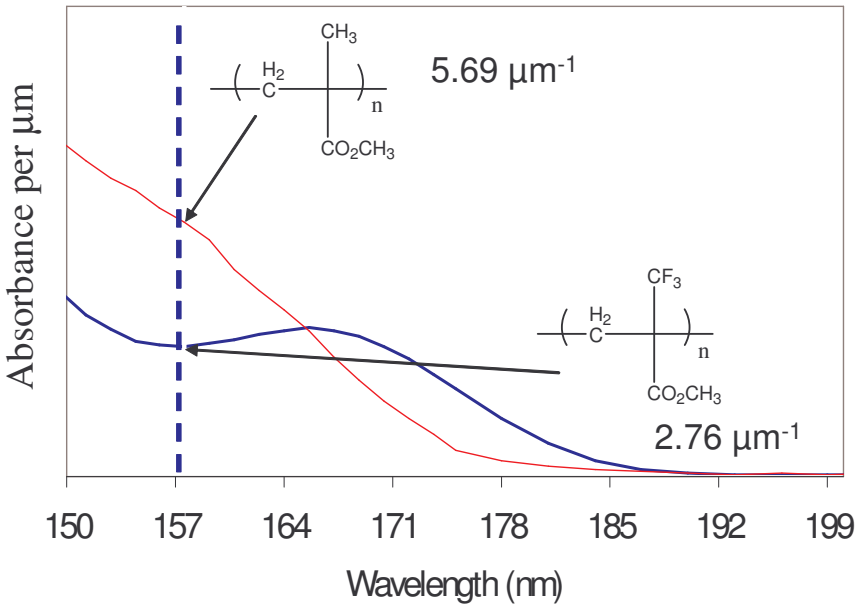

Figure 2.11: Absorbance values of poly(MTFMA) and poly(MMA).

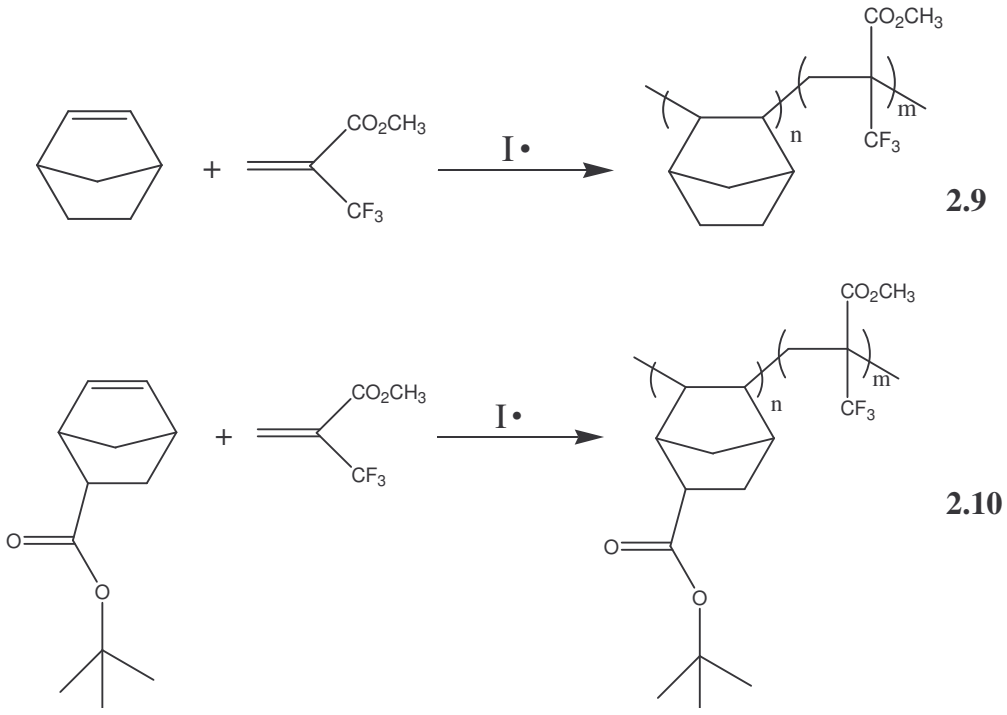

Figure 2.12: Preparation of copolymers 2.4 and 2.5.

The yield of the initial polymerization of MTFMA and NB (**2.9**) was 70%. When MTFMA is copolymerized with NBTBE (**2.10**) the yields drop to 50%. The TGA data for polymer **2.10** showed the composition of the polymer to be 60% MTFMA and 40% NBTBE. Initially, this result was not believed to be reliable because the MTFMA does not free radically homopolymerize. Yet, this polymer has MTFMA-MTFMA linkages, a result that was later reported by IBM (Ito 2001). Anionically prepared poly(2-trifluoromethylacrylates) was investigated as potential 157 nm photoresist polymers. The discovery that MTFMA and norbornenes would copolymerize shifted the focus from

MTFMA homopolymers, to the copolymers as possible 157 nm photoresist polymers. Moderate imaging success was achieved using MTFMA-NB copolymer systems (**Figure 2.13**). The absorbance and imaging results of free radically prepared MTFMA-NB copolymers has been reported (Trinque 2003).

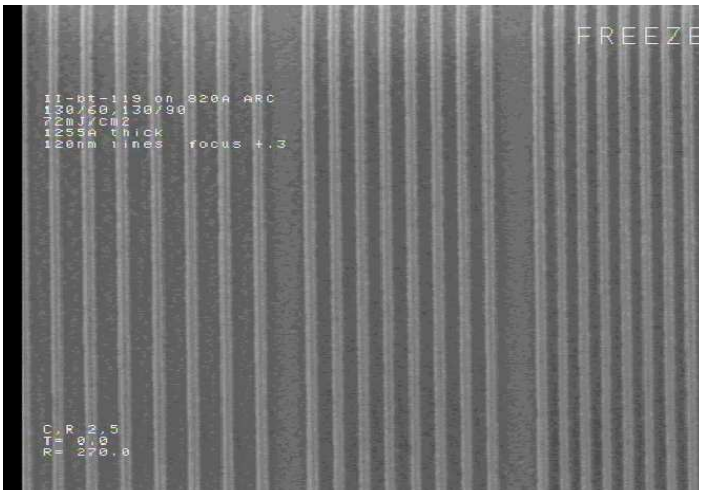

Figure 2.13: Imaging at 157 nm with MTFMA-NB copolymer (Trinque 2003).

Another fluorinated, electron deficient acrylate that was investigated as an comonomer was methyl trifluoroacrylate (MTFA). MTFA was reported to undergo free radical polymerization with 1,1,2,3,4,4-hexafluoro-1,3-butadiene and n-alkylvinyl ethers to form the terpolymer (Zurkova 1987). The results from the copolymerization of MTFA with NB, NBTBE and NBTBECF3 (**Figure 2.14**) were very comparable to the results of the copolymerization of these norbornenes with MTFMA.

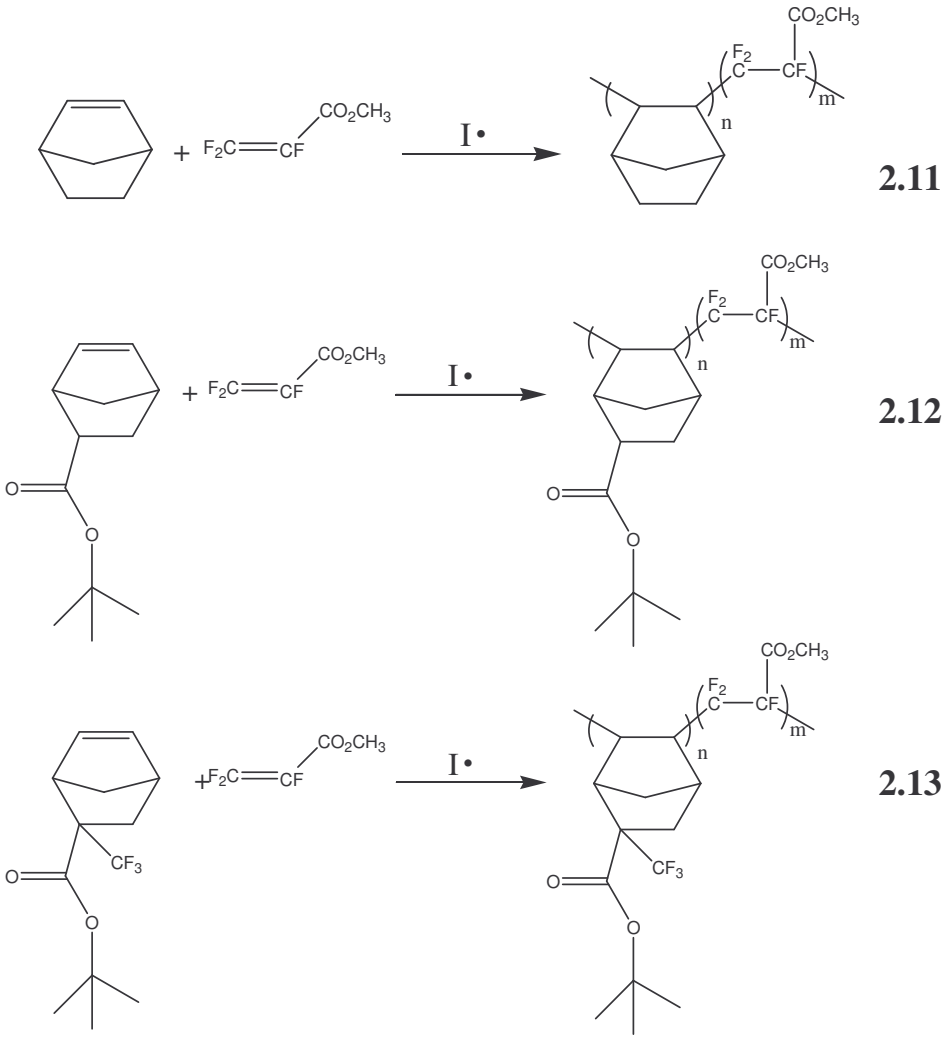

Figure 2.14: Preparation of copolymers 2.10, 2.11 and 2.12.

The 60:40 copolymer ratio was again observed for the copolymerization of the acrylate with NBTBE. The polymer yields also decrease dramatically from the **2.11** to **2.12** and no **2.13** was formed.

Copolymerization of Norbornenes and Vinyl Cyano Monomers

Early in the 157 nm photoresist project it was discovered that poly(methyl 2-cyanoacrylate) has a lower absorbance at 157 nm than poly(methyl methacrylate) (**Figure 2.15**).

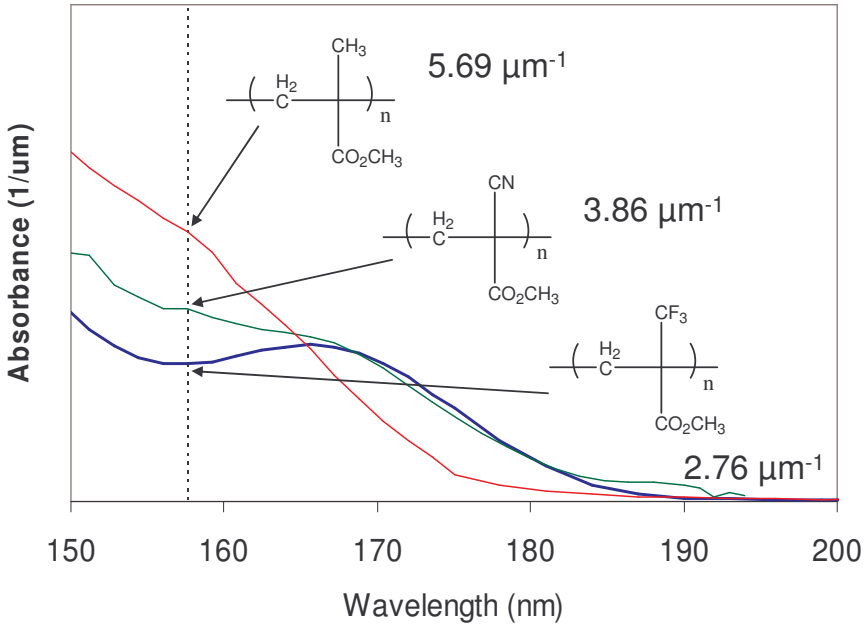

Figure 2.15: Absorbance values of poly(MTFMA),poly(MMA) and poly(MCA).

Most of the effort to find transparent materials for 157 nm photoresists was focused on fluorinated materials. The possibility of transparent materials containing the cyano functionality had not been explored. Methyl-2-cyanoacrylate (MCA) and acrylonitrile (AN) were attractive monomers to copolymerize with NB, NBTBE, and NBTBECF3 (**Figures 2.16 and 2.17**). Transparent copolymers prepared using either of these two

monomers would be attractive due to their availability and synthetic accessibility compared to that of the fluorinated monomers.

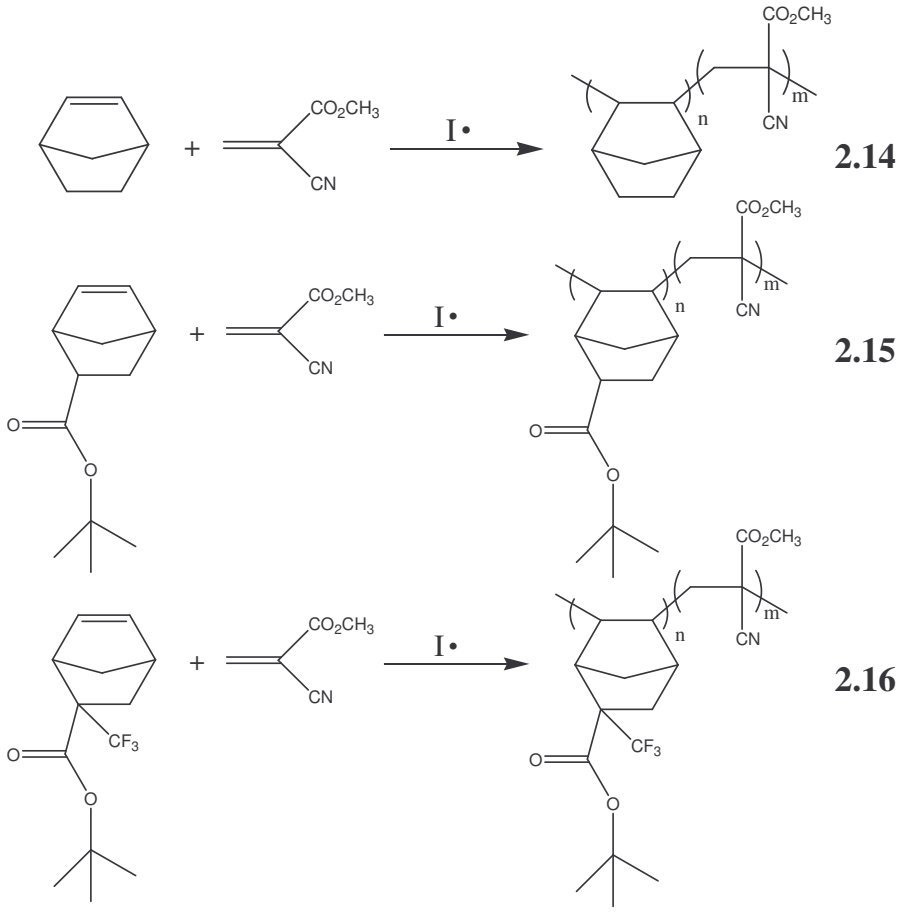

Figure 2.16: Preparation of copolymers 2.14, 2.15 and 2.16.

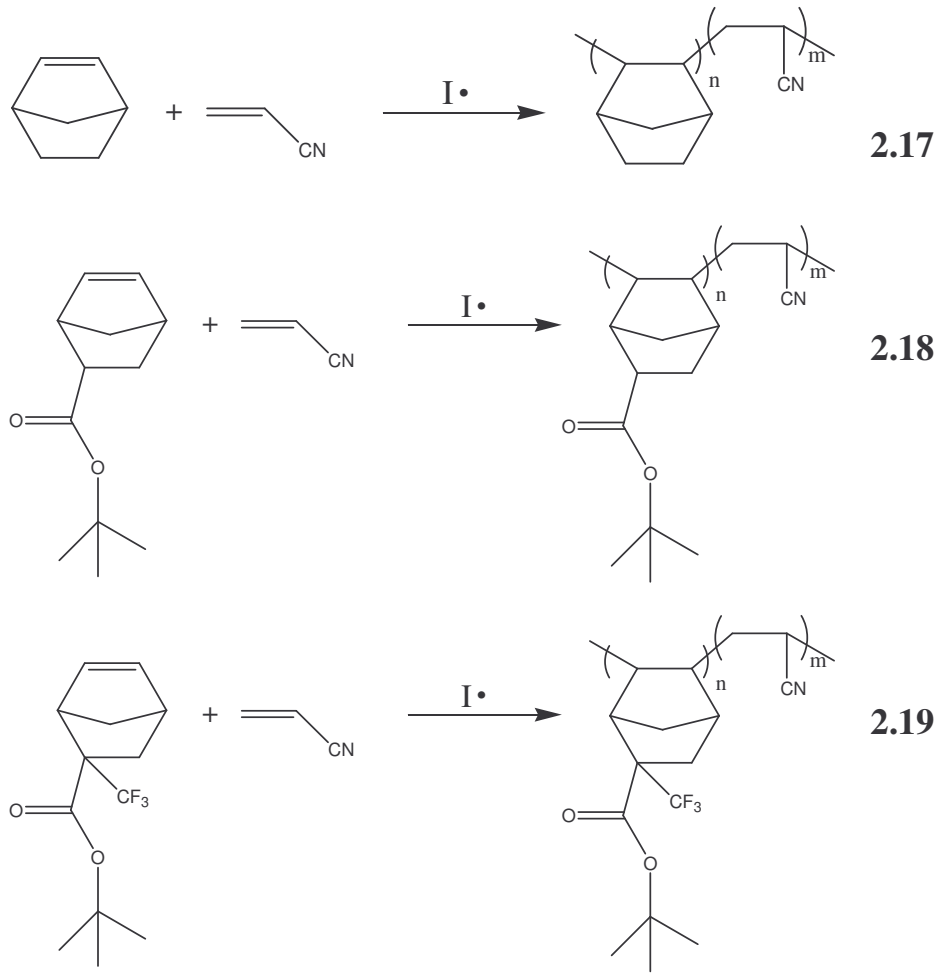

Figure 2.17: Preparation of copolymers 2.17, 2.18 and 2.19.

The free radical homopolymerization of MCA has been reported (Canale 1960, Bevington 1976). The anionic polymerization of MCA is the basis for the adhesive, "Super Glue." The anionic polymerization can be initiated by trace amounts of water or other weak bases. Care must be taken to ensure the reaction vessel, solvent and the other reactants (comonomers and initiators) are dry when free radically polymerizing MCA to

prevent unwanted homopolymerization. The free radical copolymerization of MCA and NB was initially performed neat. The viscosity of the reaction quickly increased and prevented efficient mixing, resulting in a very high polydispersity of 4.5. A solvent, 1,4-dioxane, was used in the copolymerization of MCA and NBTBE to allow more homogeneity, leading to lower polymer polydispersity.

The polydispersity of this copolymer was found to be considerable lower (1.9) than the copolymer **2.14**. The reaction yield was higher, over 60%, compared to the yields achieved with the fluorinated acrylates under the same reaction conditions. The composition of copolymer **2.15** was determined to be 32% NBTBE by TGA. All three of the acrylates investigated polymerized with NBTBE in an approximately 2:1 ratio. Unlike the fluorinated acrylates, CMA did copolymerize with NBTBECF3 to give a 20% yield. Only 21% NBTBECF3 was incorporated into the copolymer **2.16**. Considering the cost and copolymerization results of CMA versus that of MTFMA and MTFA, from an viable reaction standpoint, CMA was the most attractive of the three acrylates tested. Unfortunately, the target absorbance of 1.4 μm^{-1} was not achieved with any of the acrylate-NB copolymers.

The copolymerization of AN and the methyl ester of norbornene-2-carboxylic acid (NBME) has been reported. Starting with a 1:1 molar concentration of both monomers, 23.5% incorporation of the NBME was observed at low conversion (Judge 1959). The copolymerization of AN with either NB or NBTBE had low yields (40 and 27%) compared to the copolymers prepared with MCA, but the yields were still better

than the copolymers prepared from MTFMA or TFA. Copolymer **2.18** was composed of 32% NBTBE. Copolymer **2.19** was composed of 14.5% NBTBECF3 and was prepared with a 13% yield. The best copolymerization results (yield and incorporation of NBTBECF3) were achieved with MCA.

Imaging of Acrylate-Norbornene Copolymers

The copolymers of MTFA and MCA with NBTBE were contact printed at 248 nm (**Figure 2.18**). Contact printing is can be used as a rudimentary form of optical imaging, used to evaluate whether a photoresist will image upon exposure or not. No lens system is used in contact printing, the wafer is in contact with the photomask as 248 nm light is shined through the mask.

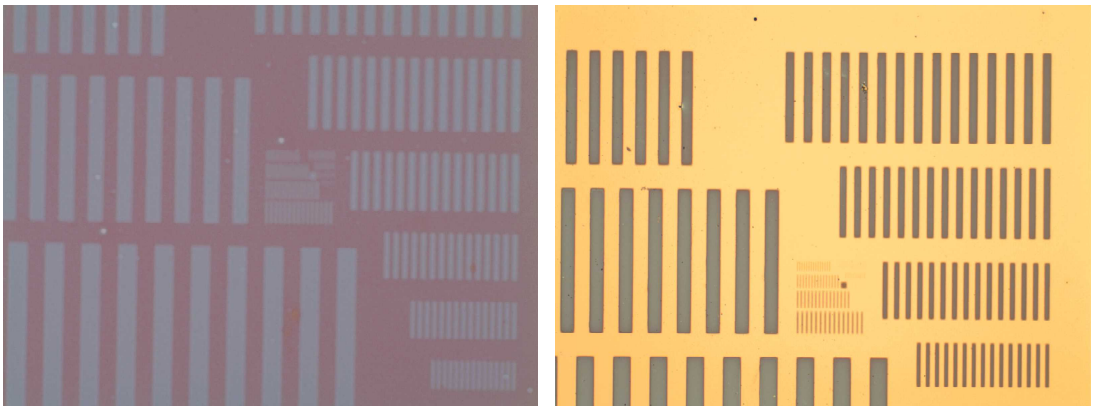

Figure 2.18: 248 nm contact printing with 3.12 and 3.15 with 6 wt% PAG.

Absorbance of Acrylate-Norbornene Copolymers

Figure 2.19 shows the VASE absorbance spectra for several of the norbornene copolymers.

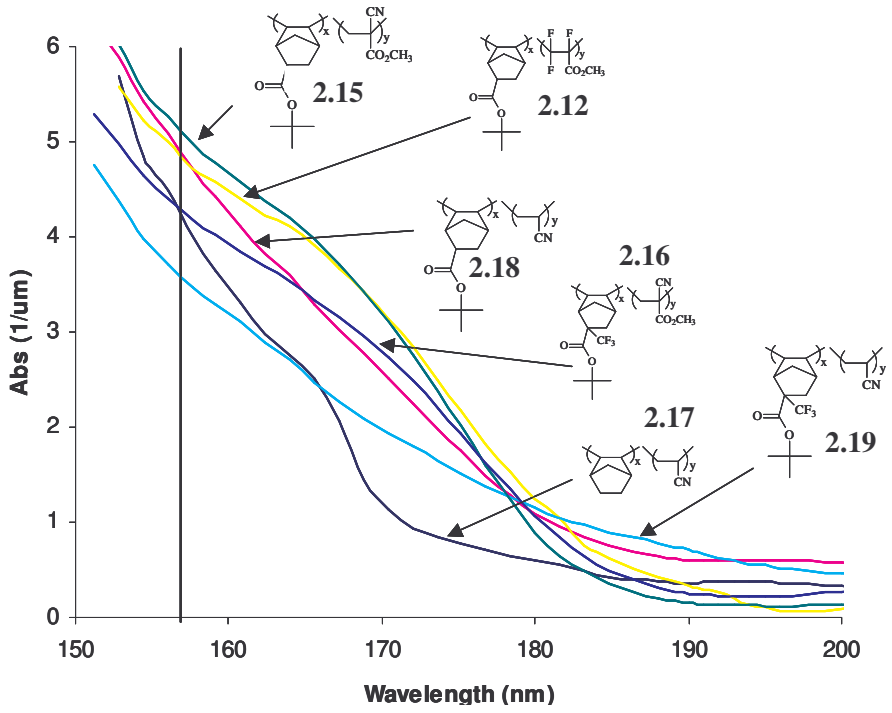

Figure 2.19: VASE data for acrylate-norbornene and acrylonitrile-norbornene copolymers.

The VASE spectra show that the copolymer **2.19** is the most transparent (3.6 μm^{-1}) of those tested, but the lack of a modifiable functional group on the acrylonitrile monomer limits the polymer's potential use as a 157 nm photoresist. The target absorbance of 1.4 μm^{-1} was not achieved by the free radical copolymerization of the fluorinated norbornenes. A copolymer of MTFMA and NBHFA with an absorbance of

2.18 μm^{-1} has been reported (Trinque 2003). The large difference in absorbance explains why only the MTFMA-NB free radically prepared copolymers was further investigated as possible 157 nm photoresist resins within our group. Absorbance values of 1.4 μm^{-1} or below μm^{-1} were achieved with polymers prepared by metal catalyzed vinyl addition (Tran 2002). Absorbance value around 1.6 μm^{-1} for the fully formulated resist (polymer, PAG, base quencher etc.) were believed to be required for optimum imaging performance in 130 to 150 nm thick films at 157 nm.

CHAPTER 3 — Dissolution Inhibitors for 157 nm Photolithography

Despite the advantages of preparing polymers via free radical initiation, the transparency required for high resolution imaging at 157 nm (absorbance $\leq 1.4\ \mu m^{-1}$) was not achieved. The search for a transparent base resin shifted to polymers prepared using transition metal catalysts. The three polymerizations pathways investigated were: ROMP (ring opening metathesis polymerization) (Osborn 2004), carbon monoxide copolymerization, and metal catalyzed vinyl addition polymerization (Tran 2002). Polymers prepared by carbon dioxide copolymerization or vinyl addition polymerization showed the most promise as base resins for 157 nm photoresists.

Carbon Monoxide Copolymers

The copolymerization of carbon monoxide with fluorinated 2-(3,3,3-trifluoro-2-trifuoromethyl-2-hydroxypropyl)bicyclo[2.2.1]heptane-5-ene (NBHFA) and 2-trifluoromethyl bicyclo[2.2.1]hept-5-ene-2-carboxylic acid *tert*-butyl etster (NBTBECF3) for 157 nm photoresist materials has been previously reported (Tran 2001). The polymerization is carried out using a catalyst system similar to the one used for the production of Carilon® by Shell (Drent 1991). A palladium catalyst with two bidentate chelating ligands, two weakly or non coordinating anions and an oxidant (benzoquinone in methanol) was used to prepare copolymers of carbon dioxide and **NBHFA** or **NBTBECF3** (**Figure 3.1**). The bidentate ligand, 2,2'-bipyridine, and the anion, tosyl,

were chosen because of previous experience working with Drent's Catalyst (Yamada 2000).

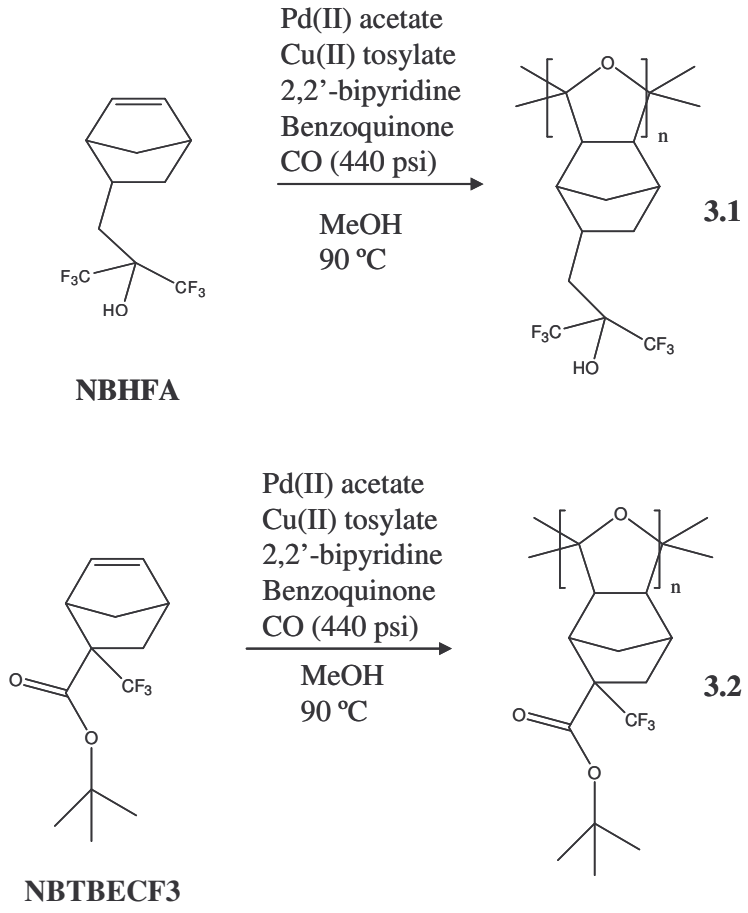

Figure 3.1: Copolymerization of carbon monoxide and NBHFA and NBTBECF3.

Terpolymers were prepared and successfully imaged at 157 nm. **Figure 3.2** shows the terpolymer, its absorbance at 157 nm and the images achieved. No swelling or residue in the exposed areas of the wafer was observed (Hung 2001). Despite the imaging success with this system, there were two major obstacles to overcome; the obvious

roughness of the printed features and the surprisingly high absorbance of the carbon monoxide copolymers.

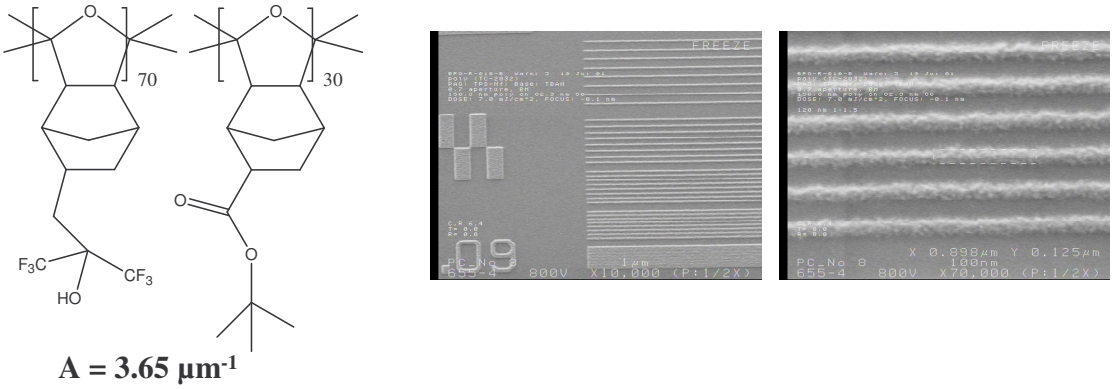

Figure 3.2: Absorbance and imaging at 157 nm of CO-co-NBHFA-co-NBTBE terpolymer.

The carbon monoxide terpolymer used to print the images in **Figure 3.2** had a M_w of 1600 and to improve the severe roughness observed, a terpolymer with higher molecular weight was required. Introduction of a crosslinker into the polymerization reaction was thought the ideal way to increase the molecular weight of the terpolymer. Three types of crosslinkers were examined: terminal olefins, alicyclic dienes, and compounds composed of two norbornene rings tethered together. The results from the crosslinker experiments are summarized in **Table 3.1**.

Table 3.1: Results from cross linkers tested in the carbon monoxide copolymerization.

Cross linker		%	GPC			Cross
Structure	Mole %	Yield	Mw	Mn	PD	linked
	20	88	740	540	1.37	No
	20	81	1090	650	1.68	No
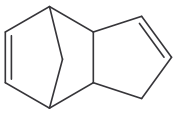	20	80	940	630	1.49	No
	20	90	4040	940	4.33	Yes
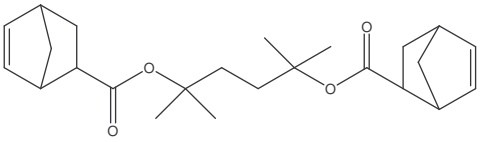	20	high	6450	1490	4.33	Yes
	10	83	5990	1390	4.31	Yes

The reactions were carried out using 80 mol% of bicyclo[2.2.1]hept-5-ene-2-carboxylic acid *tert*-butyl or methyl etster (NBTBE or NBME) as the monomer and 20 mol% of crosslinker unless otherwise noted. For the terminal olefins, 1,7-octadiene and 1,13-tetradecadiene were used as crosslinkers. A terminal olefin peak corresponding to 1,7-octadiene was still observed in the resulting polymer by ^{1}H-NMR, even after purification. The NMR study suggests that only one side of the olefin reacted because free 1,7-octadiene is too volatile to remain in the polymer both during and after the purification

process. Furthermore, GPC analyses showed no cross linking. Increasing the length of the crosslinker by using 1,13-tetredecadiene did lead to increased molecular weights.

Next, alicyclic dienes were tested as crosslinkers. While reactions with dicyclopentadiene failed to increase the molecular weight, norbornadiene did give higher molecular weight polymer. However, the polymer had very low solubility in organic solvents.

Finally, a crosslinker consisting of two norbornene rings tethered together was investigated. This compound had been used as a crosslinker previously within the group. When 20 mol% of the crosslinker was employed, the reaction produced some insoluble solid. The polymerization using 10 mol% of this crosslinker yielded polymer having an M_w of 6000. Two imageable polymers were prepared using 10 mol% of the crosslinker, but some insoluble solid was formed. Even after attempts at purification the polymer was dark brown and formed a slightly turbid solution when dissolved in solvent.

The feed of crosslinker in the reaction was likely too high. Reducing the crosslinker amount to 5 mol% eliminated the formation of the insoluble materials, but the polymers were still dark in color. A new, more transparent crosslinker (**3.3**) was synthesized by a Diels-Alder reaction of 2,2,3,3,4,4,5,5-octafluorohexamethylene diacrylate with cyclopentadiene.

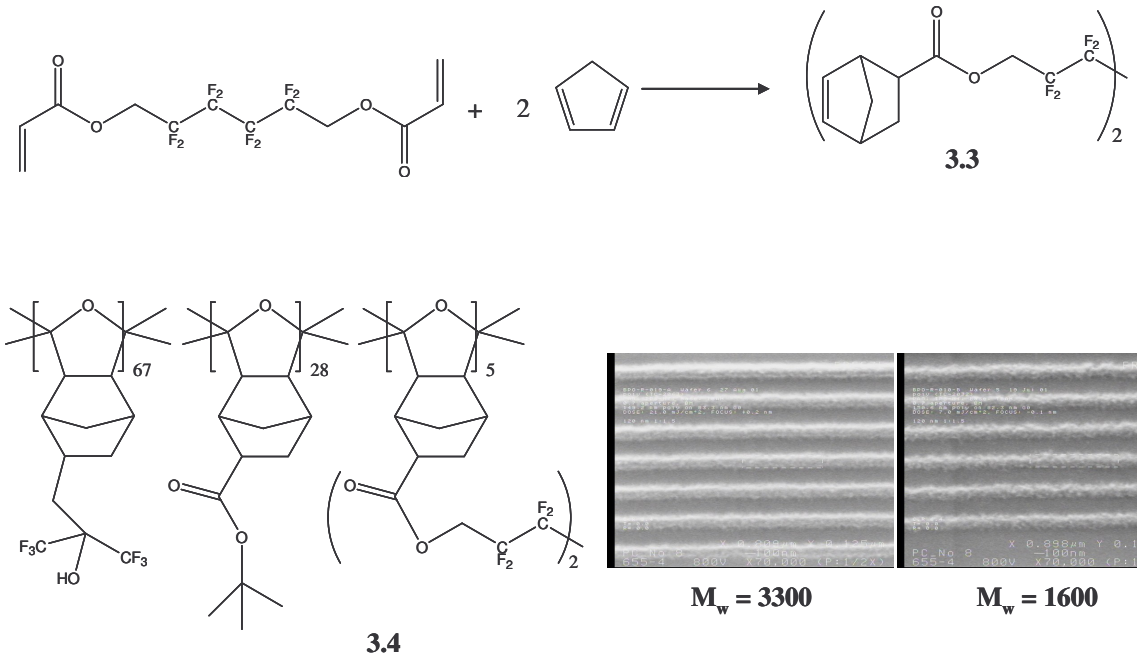

Figure 3.3: synthesis of crosslinker and imaging at 157 nm of CO copolymer with and without 3.3.

The higher molecular weight version of carbon monoxide-**co**-NBHFA-*co*-NBTBE terpolymer prepared using **3.3** as a crosslinker (polymer **3.4**) was successfully synthesized and imaged at 157 nm (**Figure 3.3**). The line edge roughness is significantly reduced in the features formed from the higher molecular weight polymer. Unfortunately, significant line edge roughness was still observed and further increases in the molecular weight of the carbon monoxide terpolymers would only reduce but not eliminate this line edge roughness and led to crosslinking or gel formation.

According to simulation data the target absorbance for a 157 nm photoresist base resin was 1.4 μm^{-1} or lower. Carbon monoxide copolymer **3.1** has an absorbance of 2.6

μm^{-1} which is more than an order of magnitude higher than the target absorbance. The significantly high absorbance of the carbon monoxide copolymers prepared from the highly transparent fluorinated norbornene monomers was surprising. To investigate the origin this absorbance, carbon monoxide copolymer **3.1** was studied. The polymer has an M_n of 1360, while the molecular weight of one repeat unit is 302 amu. The average repeating unit is 4.5 (= 1360/302) and the MALDI mass spectrum of **3.1** is shown in **Figure 3.4**.

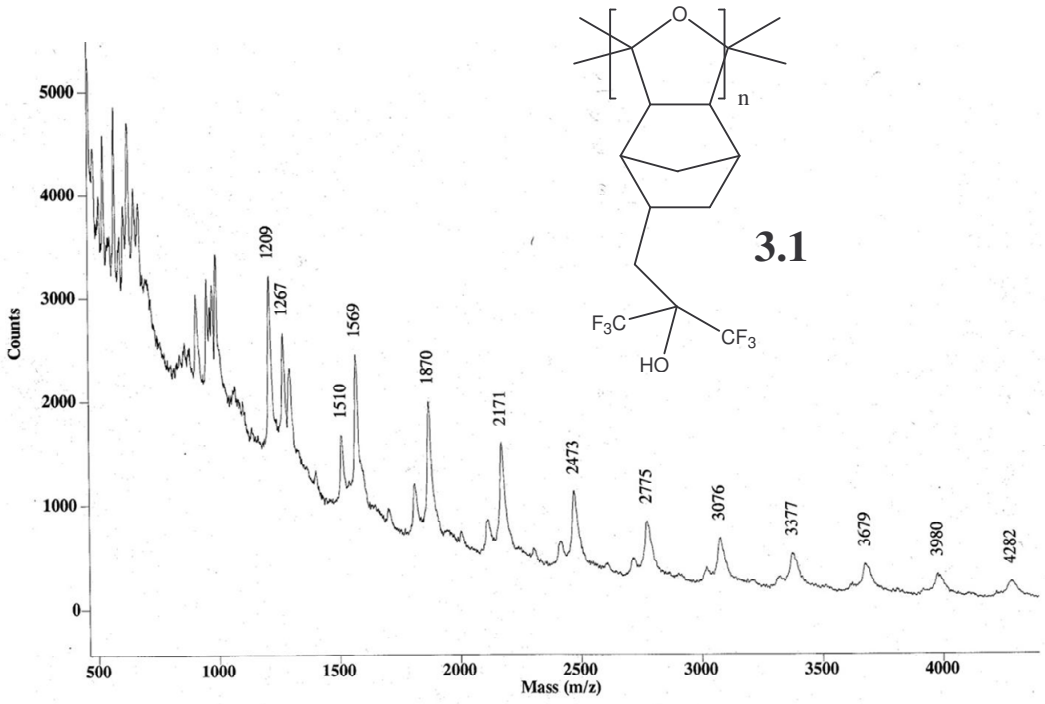

Figure 3.4: MALDI spectrum of copolymer 3.1.

The data agree with the molecular weight of the repeating unit, and show that this polymer contains two families of polymers. ^{1}H NMR (**Figure 3.5**) shows methoxy group at 3.6 ppm (integration 5.0) and hexafluoroalcohol at 7.8 ppm (integration 8.8).

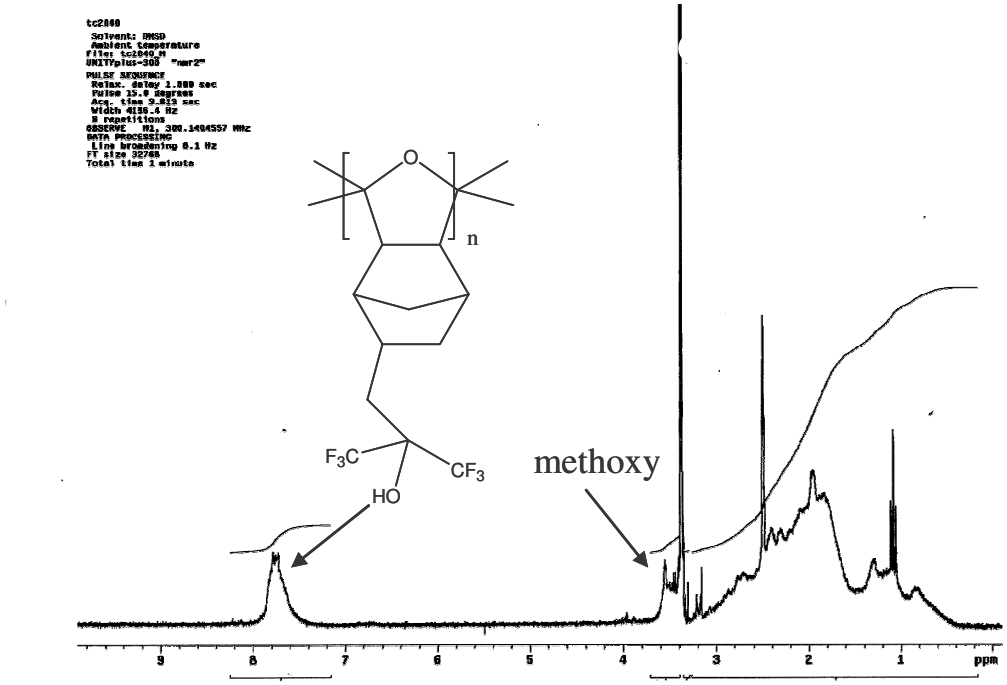

Figure 3.5: 1H NMR spectrum of copolymer 3.1.

These values roughly correspond to one methoxy group per one polymer molecule. ^{13}C NMR spectra (**Figure 3.6**) taken using a relaxing agent, chromium acac, show a weak ketone peak around 210 ppm, ester and lactone carbonyl peaks between 180-170 ppm,

weak olefinic peaks around 150 ppm, a strong quartet (CF_3) and a broad peak (ketal) around 120 ppm, weak olefinic peaks around 110 ppm, a singlet peak at 76 ppm, and broad multiplet including solvent peaks 64-26 ppm.

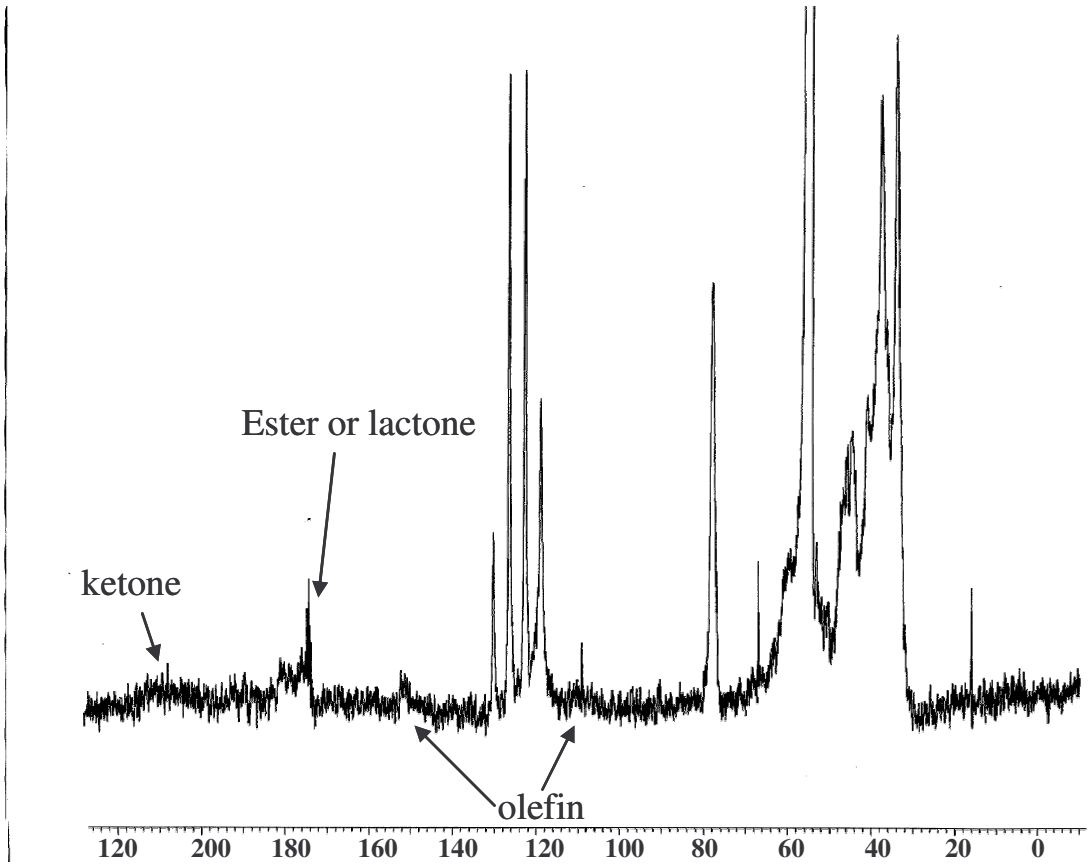

Figure 3.6: 13C NMR spectrum of copolymer 3.1.

IR data showed a carbonyl group indicating lactone and ester and olefinic stretch at 1620 cm^{-1} (**Figure 3.7**).

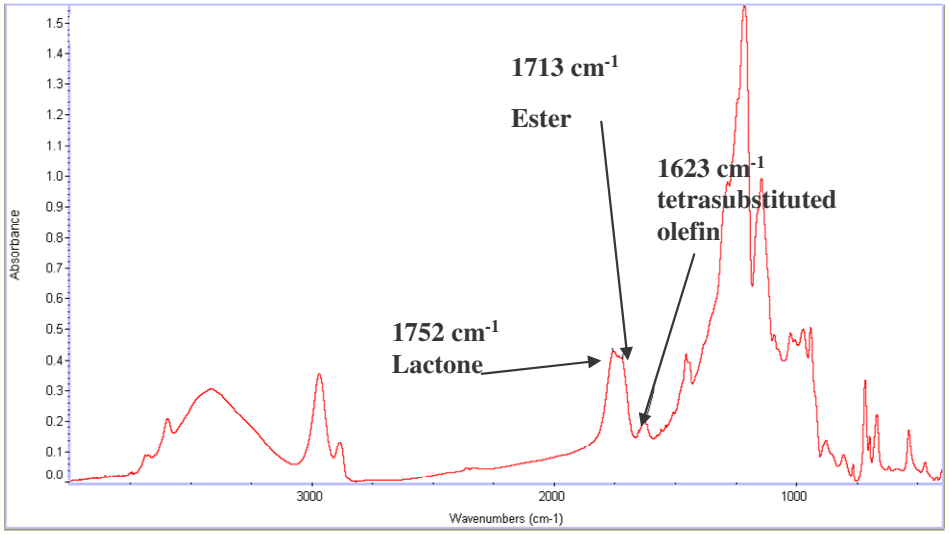

Figure 3.7: IR spectrum of copolymer 3.1.

Most of the data agree with the structure proposed in **Figure 3.8** although the weak ketone peak observed in ^{13}C NMR is not observed. These are not the only possibilities for the polymer structure. For example, the double bond in the proposed structure can be located between the other norbornene ring and the carbon of the ether linkage. The 3,3,3-trifluoro-2-hydroxy-2-(trifluoromethyl)propyl group can be located on either norbornane bridge carbon opposite of the polymer backbone.

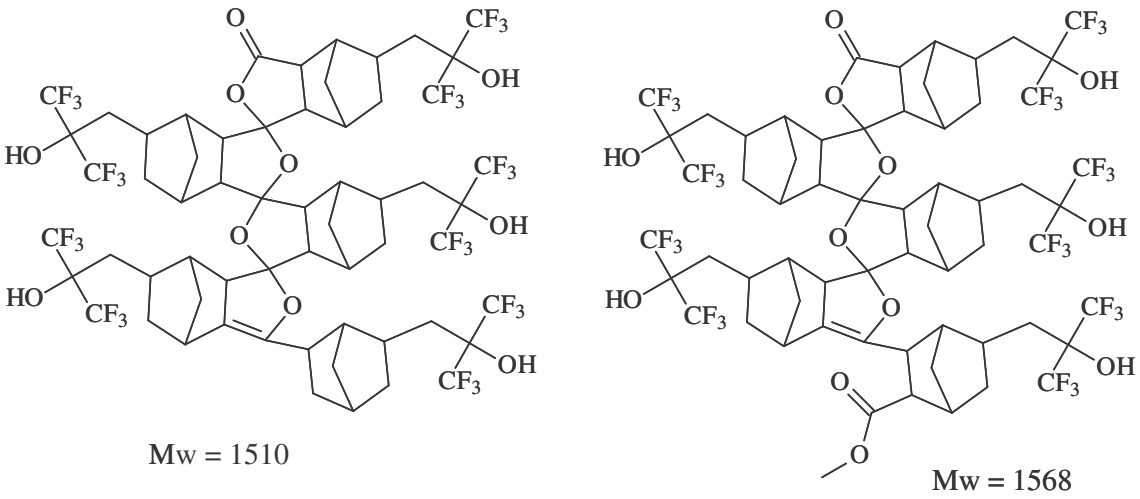

Figure 3.8: Proposed structure of copolymer 3.1.

The formation of such structures might be explained by the mechanism shown in **Figure 3.9**. The mechanism to form a spiroketal is consistent with the mechanisms proposed in the literature (Drent 1996).

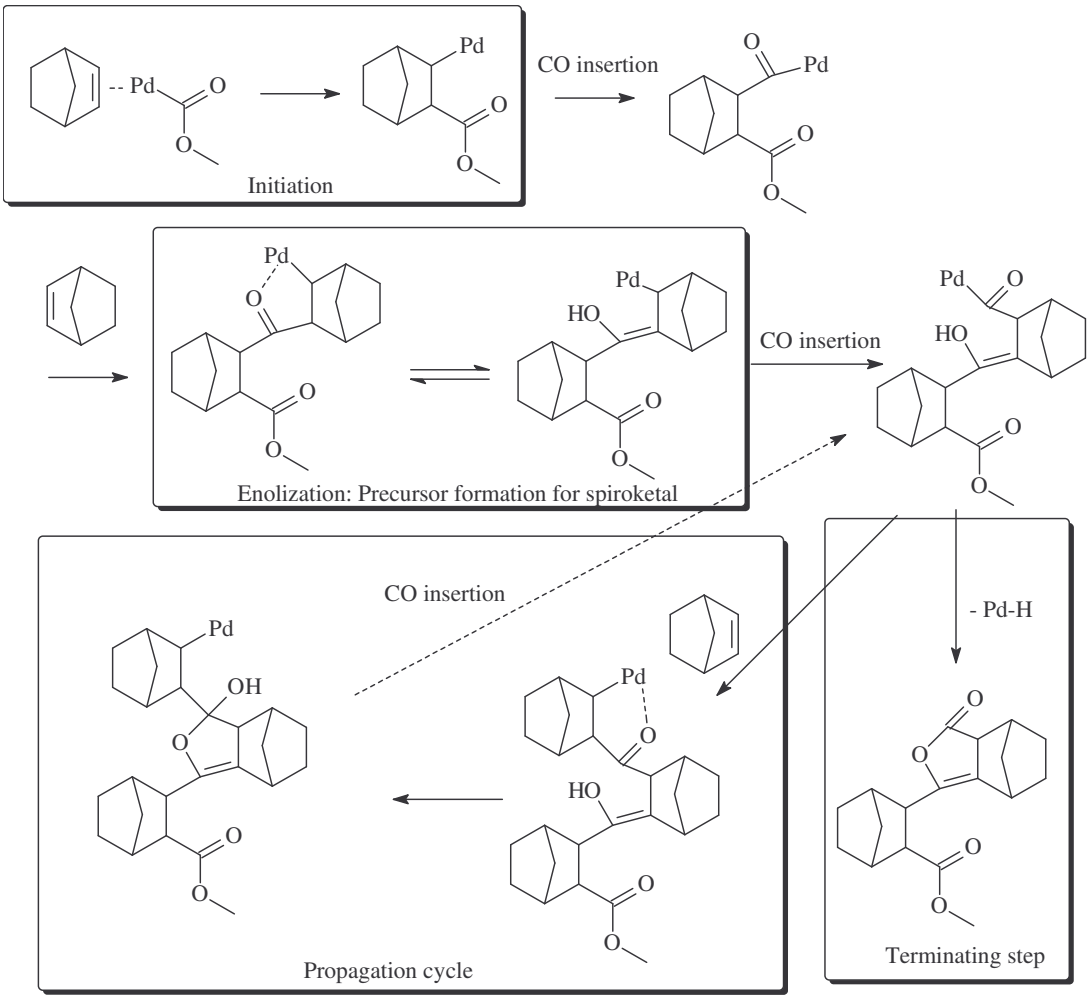

Figure 3.9: Proposed mechanism of CO copolymerization.

The existence of a carbonyl group, known to absorb at 157 nm, is observed. The copolymer was then reacted with a borane-THF complex. This reagent reduced a number of these lactone groups, but not all of them, as indicated by IR (**Figure 3.10**). The absorbance at of this copolymer at 157 nm improved from 2.6 to 2.2 μm^{-1}.

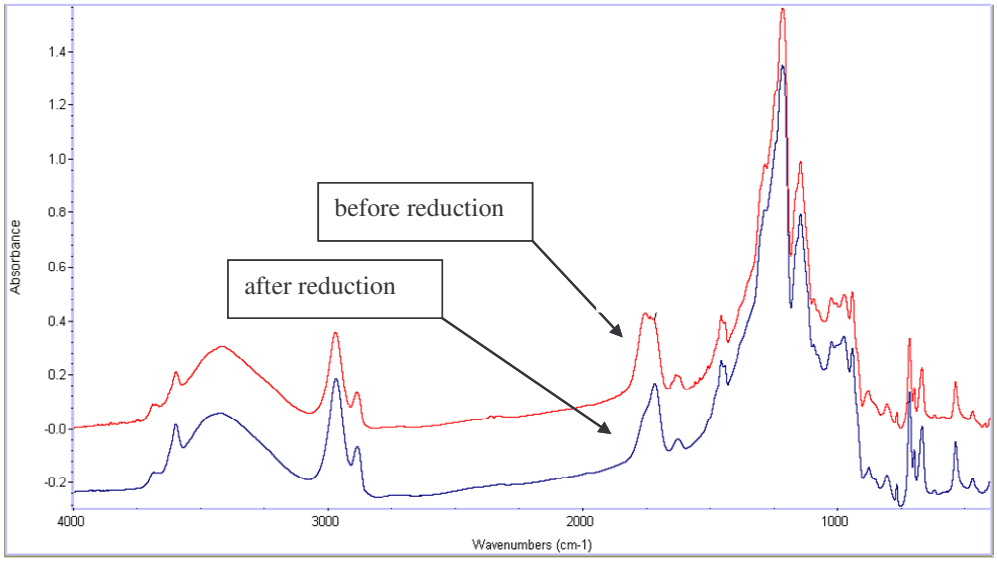

Figure 3.10: IR spectrum of copolymer 3.1 before and after borane reduction.

Despite the improvement the target absorbance of 1.4 μm^{-1} was still not achieved. Since the carbon monoxide polymers were low molecular weight the effect of the absorbing end groups could not be over come. It was clear that the carbon monoxide copolymers and terpolymers would not provide the necessary transparency necessary for a 157 nm base resin. The low molecular weight copolymers would find significant use as dissolution inhibitors (DI) in 157 nm photoresists.

PNBHFA Polymers

The norbornene-based polymer that received the most attention as a potential base resin was poly(2-(3,3,3-trifluoro-2-trifuoromethyl-2-hydroxypropyl)bicyclo[2.2.1]

heptane-5-ene) (PNBHFA) prepared by a metal catalyzed vinyl addition polymerization (Tran 2002). This homopolymer has an absorbance of 1.14 μm^{-1} at 157 nm, as compared to 2.2 μm^{-1} for polymer **3.1,** which was prepared using the same monomer. With the discovery of a polymer that met our transparency requirements (absorbance $\leq$ 1.4 μm^{-1}) the focus shifted toward our imaging goals. The three imaging goals were 130 nm lines printed in a 100 nm thick resist film, 100 nm lines printed in a 130 nm thick resist film, 130 nm lines printed in a 250 nm thick film and 100 nm lines printed in a 300 nm thick film. These goals were set by our funding agency International SEMATECH. To achieve these goals copolymers of PNBHFA with some fraction of the hexafluorocarbinol acidic sites blocked by either a *tert*-butyl carbonate or an acetal protecting groups were prepared, as analogues of partially *tert*-butyl carbonate protected poly(*para*-hydroxystyrene) (PHS) used at 248 nm (**Figure 3.11**).

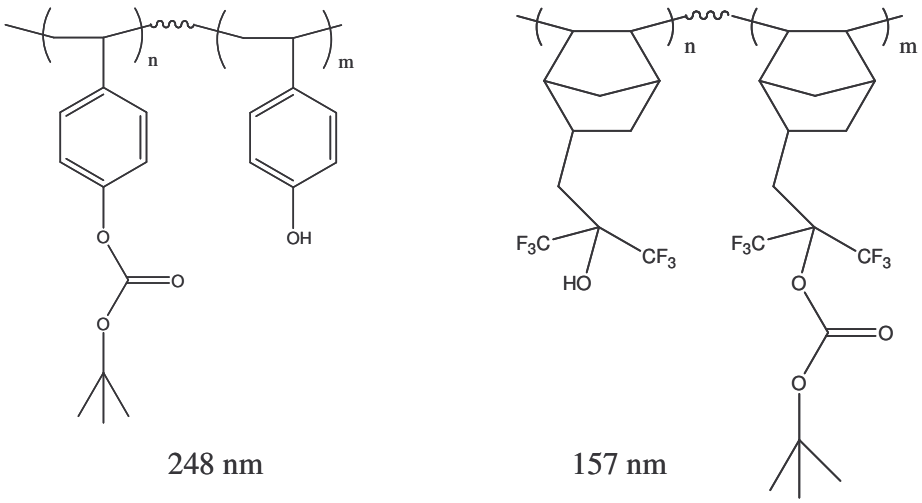

Figure 3.11: 248 and 157 nm photoresists polymers with *tert*-butyl carbonate switching group.

The copolymers were prepared by either copolymerizing protected and unprotected PNBHFA or by protection of the homopolymer. Too little protecting group incorporation renders the polymer partially soluble in the 0.26 N TMAH and some portion of the unexposed resist film will dissolve (Hung 2002). Too high an incorporation of a protecting group likewise has negative consequences: an increase in the polymers absorbance and thus the required exposure dose which leads to reduced imaging performance of the resist.

Carbon Dioxide Copolymers as Dissolution Inhibitors (DIs)

The dissolution inhibitor (DI) project began with a PNBHFA copolymer containing only 8% of the *tert*-butyl carbonate protecting group. Not enough of the acid sites were blocked to render the polymer insoluble in 0.26 TMAH. Rather than trying to incorporate more protecting group into the polymer, carbon monoxide copolymers were blended with the copolymer to adjust the overall percentage of protected sites in the blend. The goal was to use the carbon monoxide copolymers to reder the partially protected PNBHFA base insoluble. Both 5 and 10 wt% of polymers **3.2** and **3.5** were blended with the copolymer and the dissolution rates of the resulting polymer films measured. Figure **3.12** shows that by increasing the loadings of **3.2** and **3.5** that the dissolution rate of the film slowed until the film was completely insoluble at a loading of approximately 10 wt%.

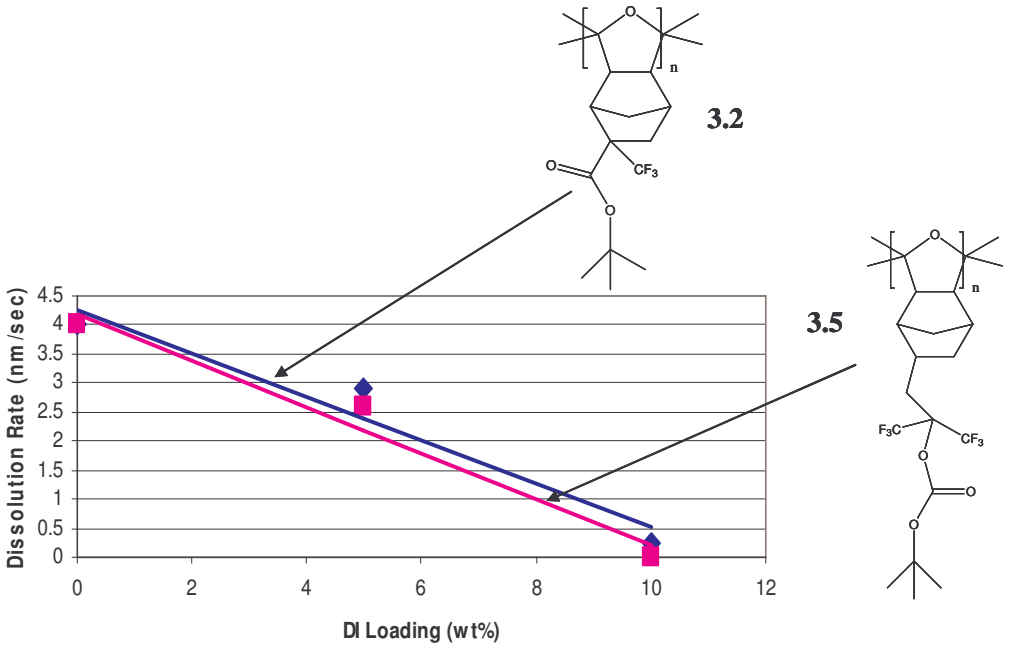

Figure 3.12: Dissolution Inhibition of carbon monoxide copolymers 3.2 and 3.5 blended with 8% tert-butyl carbonate protected PNBHFA.

Substantial imaging success was achieved using a 90:10 blend of 8% *tert*-butyl carbonate protected PNBHFA and polymer **3.5.** (**Figure 3.13**) (Hung 2002). The 80 nm lines were printed in a 100 nm thick film which exceeded our goal of 130 nm lines. These 157 nm images were the best in the world when they were printed. The reason such high resolution features could be printed using this system can be explained by looking at the use of DIs at 193 nm.

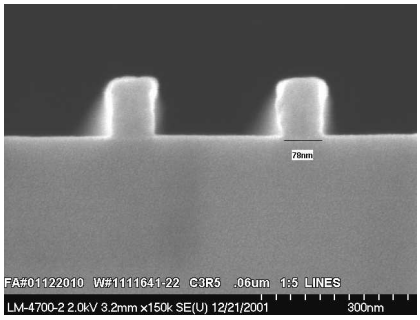

Figure 3.13: Imaging at 157nm of 90:10 blend of 8% *t*-butyl carbonate protected PNBHFA and 3.5.

Dissolution inhibitors were used in 193 nm photoresists to improve the contrast and thus improve lithographic performance (Ito 2000). A typical DI used for 193 nm was *tert*-butyl cholate which contains an acid labile *tert*-butyl ester protecting group. **Figure 3.14** shows the imaging results of a photoresist with and without added carbon monoxide copolymer. The carbon dioxide copolymer performs well as a DI and improves the contrast of the printed features.

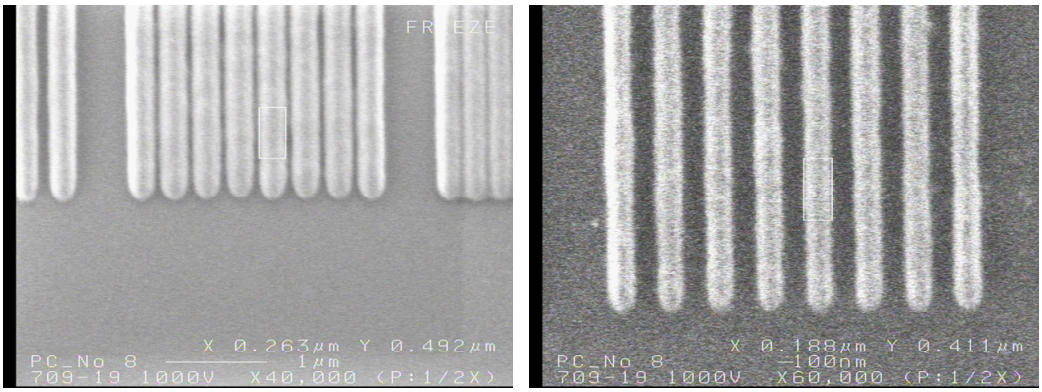

130 nm 1:1.5
without DI

130 nm 1:1.5
with DI

Figure 3.14: Imaging at 157nm of a resist with and without 3.5 added as a DI.

The carbon monoxide copolymers worked well as DIs. The improved contrast achieved by adding the dissolution inhibitor was the reason we were able to achieve the first of our goals. Unfotunately, the high absorbance of the carbon monoxide-norbornene copolymers was still problematic.

Monomeric Dissolution Inhibitors in Partially Protected PNBHFA

Transparent, monomeric additives were sought to replace the carbon monoxide-norbornene copolymers as DIs for partially protected PNBHFA. Monomeric dissolution inhibitors were proposed as a better alternative to polymeric DIs because they are easier to purify and less likely to phase separate. The first such compounds investigated were derivatives of commercially available tetrafluorohydroquinone and 1,3 or 1,4-bis(2-hydroxyhexafluoroisopropyl)benzene (1,3- or 1,4-HFAB). Although all three compounds

are aromatic, they were still of interest due to their fluorine content. The synthesis of these compounds is shown in **Figure 3.15**. The tert-butyl carbonate based DIs were prepared by the N,N-dimethylaminopyridine catalyzed reaction of the alcohols with 2 equivalents of di-*tert*-butyl-dicarbonate (bisBOC) (McKean 1988).

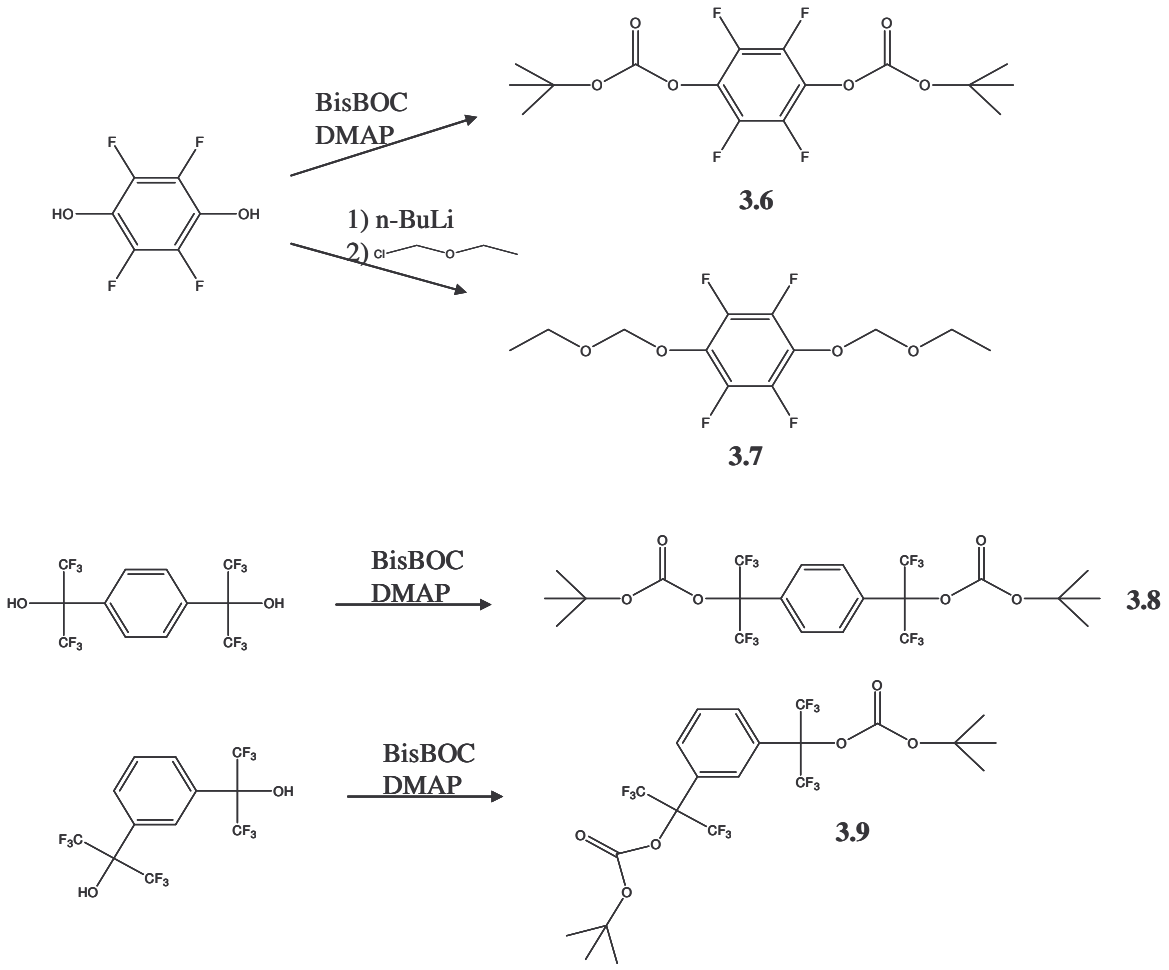

Figure 3.15: Synthesis of fluorinated aromatic DIs.

Films with differing concentrations of 1,4-bis(*tert*-butoxy)tetrafluorobenzene in 8% *tert*-butyl carbonate protected PNBHFA were prepared and their absorbance measured at 157 nm. The initial absorbance of the polymer was 1.68 μm^{-1}. The 20 wt% loading of 1,4-bis(*tert*-butoxy)tetrafluorobenzene led to an increase in absorbance to 1.93 μm^{-1}, loadings greater than 20 wt% resulted in phase separation. Dissolution rates were measured for films with loadings between 0 to 20 wt% 3.. It was determined that 1,4-bis(*tert*-butoxy)tetrafluorobenzene had no inhibitive effect on the dissolution rate of 8% *tert*-butyl carbonate protected PNBHFA.

The dissolution inhibitor 1,4-bis-*tert*-butoxycarbonyloxy tetrafluorobenzene (**3.6**) was insoluble in all of the typical organic solvents used for spin coating photoresist films. A 95:5 mixture of polymer and **3.6** could be prepared if the polymer and DI were combined before the 2-heptanone was added. Unfortunately, the 5 wt% loading was not enough to inhibit dissolution of 8% *tert*-butyl carbonate protected PNBHFA. The methyl-ethyl acetal derivative of tertrafluororhydroquinone (**3.7**) was prepared for improved solubility; however, a 10 wt% loading of **3.7** had no effect on the dissolution rate of the polymer either.

The first HFAB derivatives synthesized were 1,3-bis(2-*tert*-butyl carbonate hexafluoroisopropyl)benzene (**3.8**) and 1,4-bis(2-*tert*-butyl carbonate hexafluoroisopropyl)benzene (**3.9**). Compound **3.9** had very poor solubility in all common casting solvents. Compound **3.8** was moderately soluble in propylene glycol methyl ether acetate (PGMEA) and 10 wt% of **3.8** was sufficient to render 8% *tert*-butyl

carbonate protected PNBHFA insoluble in 0.26 N TMAH. **Table 3.2** shows the results of the dissolution measurements conducted in 8% *tert*-butyl carbonate protected PNBHFA.

Table 3.2: Summary of DIs in 8% tert-butyl carbonate protected PNBHFA.

DI	wt%	Thickness (nm)		Average loss (nm)
		Initial	Developed	
none	0	1080 1080	605 595	480
3.5	5	1130 1140	815 830	310
3.5	10	1195 1210	1200 1210	0
3.2	5	1140 1135	785 790	350
3.2	10	1185 1180	1160 1150	30
1,4-bis(*tert*-butoxy)tetrafluorobenzene	5	1105 1095	630 625	470
1,4-bis(tert-butoxy)tetrafluorobenzene	10	1090 1100	605 610	490
3.6	5	1135 1135	900 905	230
3.8	10	1195 1205	1175 1170	28

The DIs were an effective way to modify the dissolution characteristics and render the partially protected PNBHFA polymer insoluble in 0.26 N TMAH developer. The next logical step was to test the effect DIs would have on the PNBHFA homopolymer.

Inhibition of the PNBHFA Homopolymer

With the success achieved using inhibitors to fine tune the dissolution rate of the 8% *tert*-butyl carbonate protected PNBHFA, it seemed plausible to use a DI to inhibit the NBHFA homopolymer. The resulting photoresist would contain three components: PNBHFA, DI and PAG. This type of system would combine the best features of the chemically amplified and non-chemically amplified photoresist systems. The simplicity of the two component non-chemically amplified system would be combined with the high sensitivity of the chemically amplified system and greatly ease the formulation process. The main problem with a photoresist polymer that requires partial protection by an acid labile group is determining the percent incorporation of the acid labile group that gives the optimum imaging performance. Typically several copolymers with varying degrees of incorporation of the acid labile group are synthesized and tested. The use of a DI in unprotected PNBHFA would eliminate the need to synthesize a wide variety of copolymers.

Early in the 157 nm project PNBHFA was prepared in our group and later became commercially available. A sample was generously donated by Dr. Ralph Dammel of AZ Clariant Microelectronics. Any experiments using PNBHFA for a potential 157 nm photoresist would carry more weight in industry if they were conducted using the commercially available resin.

It was important to understand the dissolution characteristics of PNBHFA relative to novolac. In order to test the dissolution inhibition response of the polymer, two model compounds were synthesized from bisphenol A (**Figure 3.16**).

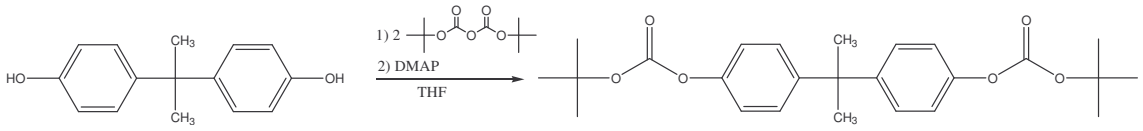

3.10

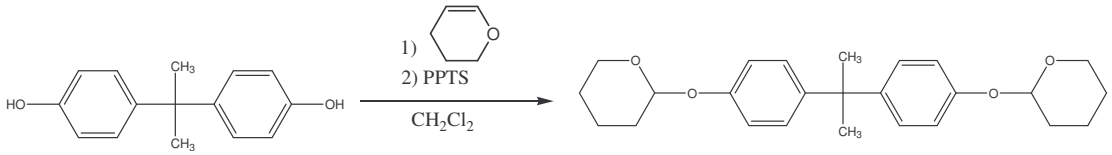

3.11

Figure 3.16: Synthesis of Bisphenol A based model DIs.

The di-*tert*-butyl carbonate of bisphenol A (**3.10**) was prepared by the N,N-dimethyl aminopyridine catalyzed reaction of bisphenol A with di-*tert*-butyl dicarbonate (McKean 1988). The diacetal (**3.11**) was synthesized by the acid-catalyzed reaction of bisphenol A with 3,4-dihydro-2H-pyran (Schlegel 1989).

The dissolution inhibition effects of these two compounds and a diazonapthoquinone (TDQ), long used by IBM in their 365 nm non-chemically amplified photoresist (Clecak 1983), were studied in both PNBHFA and novolac (**Figure 3.17**).

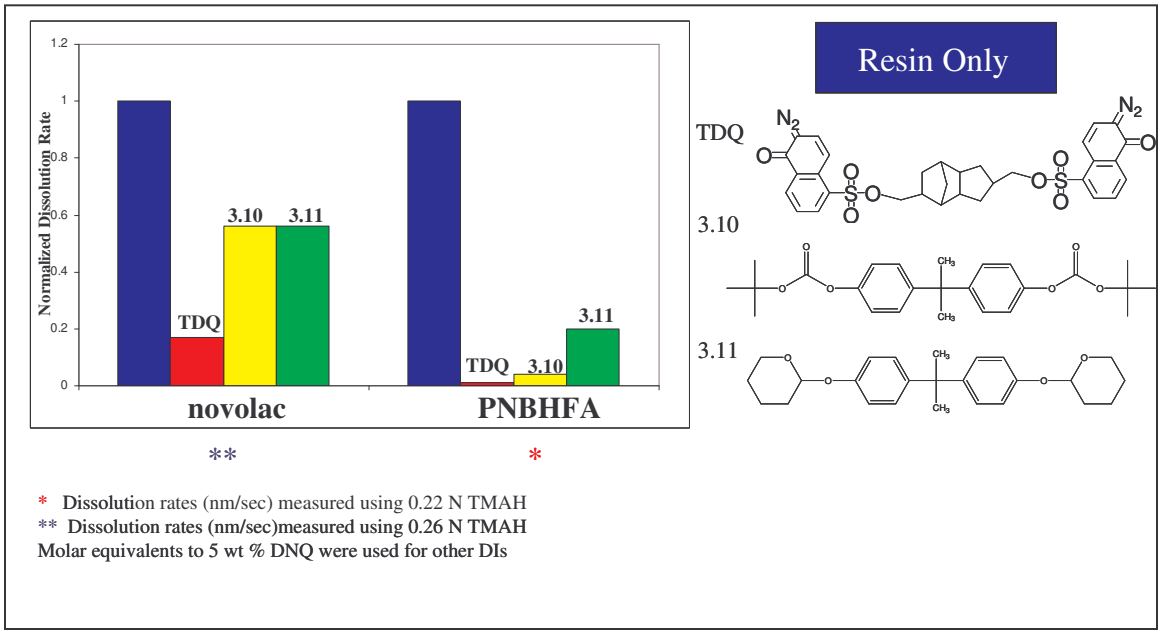

Figure 3.17: Dissolution inhibition study of equimolar amounts of TDQ, 3.10 and 3.11 in novolac and PNBHFA.

TDQ (5 wt%) and the other DIs (equimolar amounts equivalent to TDQ) were added to samples of the both polymers. In order to fairly compare the inhibiting effects of acetal, carbonate and sulfonate groups, the same number of the inhibiting functional groups were present in each formulation. Since the dissolution rates of novolac (40 nm/s) and PNBHFA (340 nm/s) are so different measures were taken to normalized the dissolution rates of the two polymers. A more dilute developer was used for PNBHFA and all the dissolution rates were divided by the dissolution rate of the base polymer. All three functional groups showed strong inhibition effects on the dissolution rate of PNBHFA. The PNBHFA polymer had a dissolution response to the acetal stronger than that of novolac. The acetal has very little effect on novolac but showed a sizable effect on the

dissolution rate of PNBHFA. The PNBHFA polymer dissolves at a rate of 182 nm/s in 0.22 N TMAH. The added acetal slowed that rate down to 36 nm/s. The carbonate had a much greater impact on the dissolution rate of the PNBHFA than it did on the dissolution rates of novolac. The carbonate slowed the dissolution rate from 182 to 7 nm/s. TDQ was the best of the three dissolution inhibitor tested in PNBHFA. A Meyerhofer plot (Meyerhofer 1980) comparing the dissolution rates (DR) of the exposed and unexposed photoresist films containing different weight percent loadings of TDQ (1,3, and 5 wt%) in novolac and PNBHFA was prepared (**Figure 3.18**).

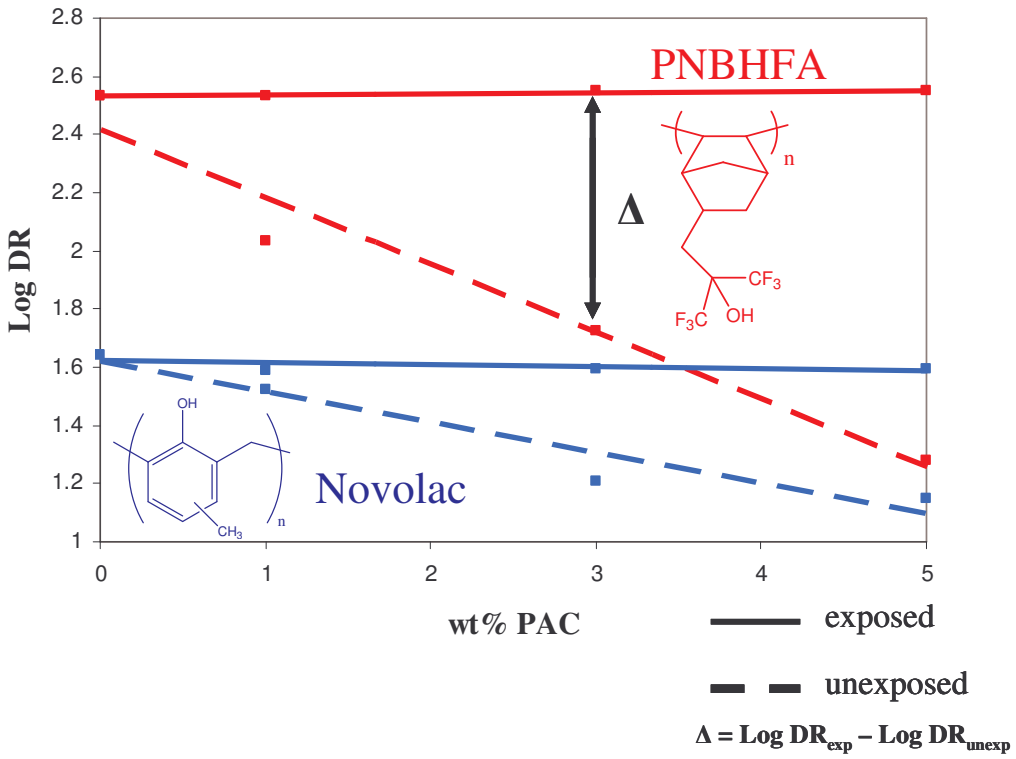

Figure 3.18: Meyerhofer plot of TDQ in novolac and PNBHFA.

The Log $DR_{exposed}$ –Log $DR_{unexposed}$ (Δ) was then compared for the TDQ-novolac and TDQ-PNBHFA systems. The Δ for the TDQ-novolac system is two orders of magnitude at a TDQ loading of 25-30 wt% and is the basis for IBM's i-line resists (Clecak 1983).

The inhibition effect of TDQ in PNBHFA was orders of magnitude better than in novolac. The dissolution properties of novolac make it very useful for i-line resists and it is the standard to which all other polymers are compared. At 5 wt% loading of TDQ in PNBHFA, two orders of magnitude difference between the exposed and unexposed dissolution rates (Δ) was achieved. Novolac, by comparison, requires around 30 wt% of TDQ to achieve the same two orders of magnitude rate difference. Much effort has been expended to find polymers with dissolution inhibition characteristics similar to that of novolac. Although PHS, a 248 nm photoresist polymer, is a structural isomer of novolac, no inhibition of PHS has been demonstrated. The discovery of the effect TDQ has on the dissolution properties of PNBHFA was very exciting, especially considering how transparent PNBHFA is at both 193 and 248 nm. Any photoresist system based on PNBHFA would easily be backwards compatible to those two wavelengths. It was hoped that the well-understood properties of novolac could be used as a reference to guide studies of PNBHFA.

Unfortunately, TDQ is too opaque for use at 157 nm (**Figure 3.19**), so it was decided to further investigate the carbonate-based DIs.

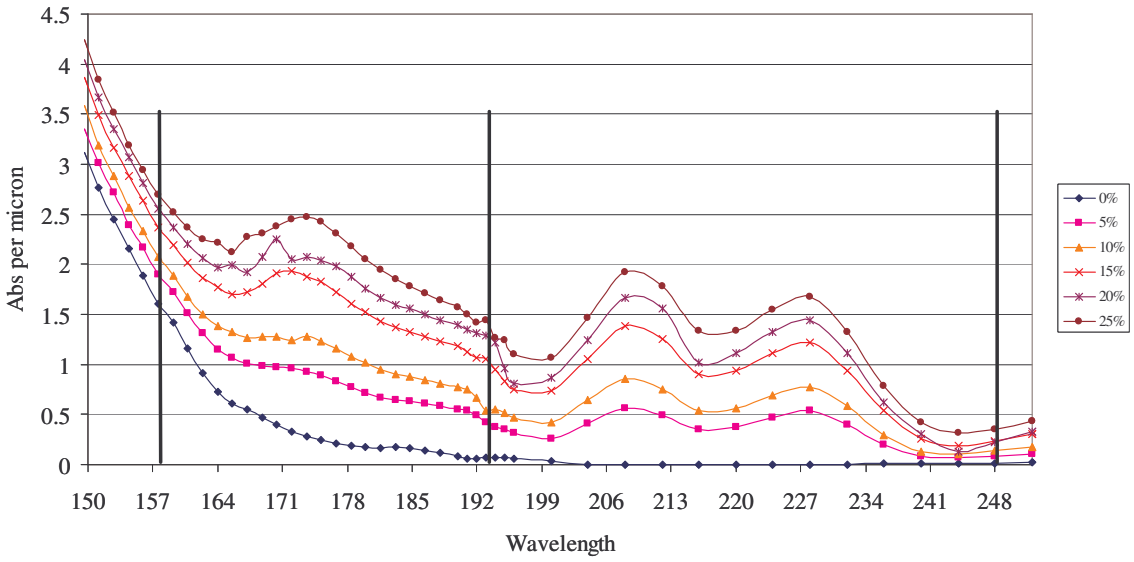

Figure 3.19: Absorbance of different 0 to 25 wt% loadings of TDQ in PNBHFA.

The *tert*-butyl carbonate based DI **3.10** was also efficient at inhibiting the dissolution rate of PNBHFA**.** A Meyerhofer plot of **3.10** in novolac and PNBHFA (**Figure 3.20**) with 1 wt% of a photoacid generator (PAG) was prepared. The Δ of **3.10** in PNBHFA was orders of magnitude greater than in **3.10** in novolac.

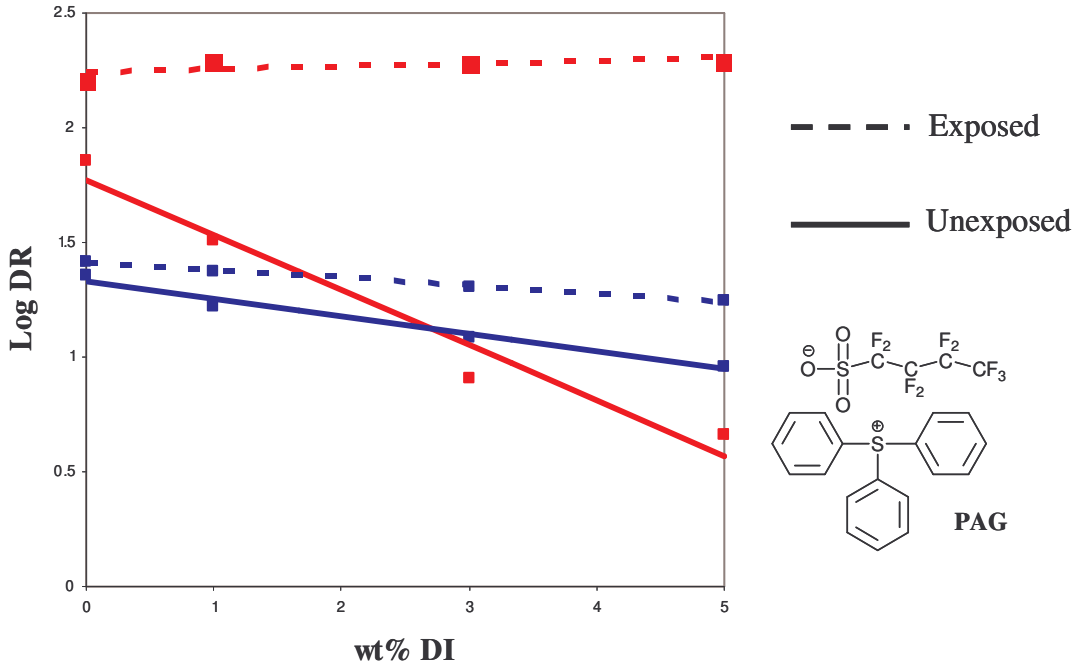

Figure 3.20: Meyerhofer plot of 3.10 and 2 wt% PAG in novolac and PNBHFA.

Imaging at 248 nm using **3.10** in PNBHFA is shown in **Figure 3.21**. Beautiful features with straight side walls were achieved using **3.10** as a DI for PNBHFA. This results demonstrated that a three component system with PNBHFA, DI and PAG could be used to print high resolution features.

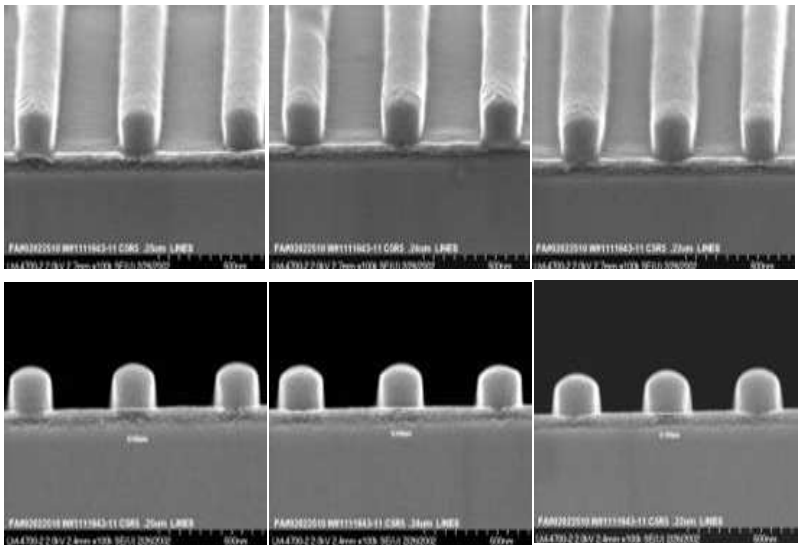

Figure 3.21: Imaging at 248 nm of 10 wt% 3.10 and 2 wt% PAG in PNBHFA.

Unfortunately, **3.10** was also too opaque for use at 157 nm. However, there was an inspiration for the design of a transparent carbonate-based DI for 157 nm based on the transparency and acidity of the hexafluorocarbinol functional group.

HFAB Analogues as DIs

The hydrogenation of 1,4-HFAB with rhodium on carbon at high pressure (500 psi H_2) and temperatures (150ºC) was reported (Maruno 1996). The same procedure was used to prepare **3.12** and **3.13**. The bis-*tert*-butyl carbonate of **3.12** and **3.13** were prepared (**Figure 3.22**).

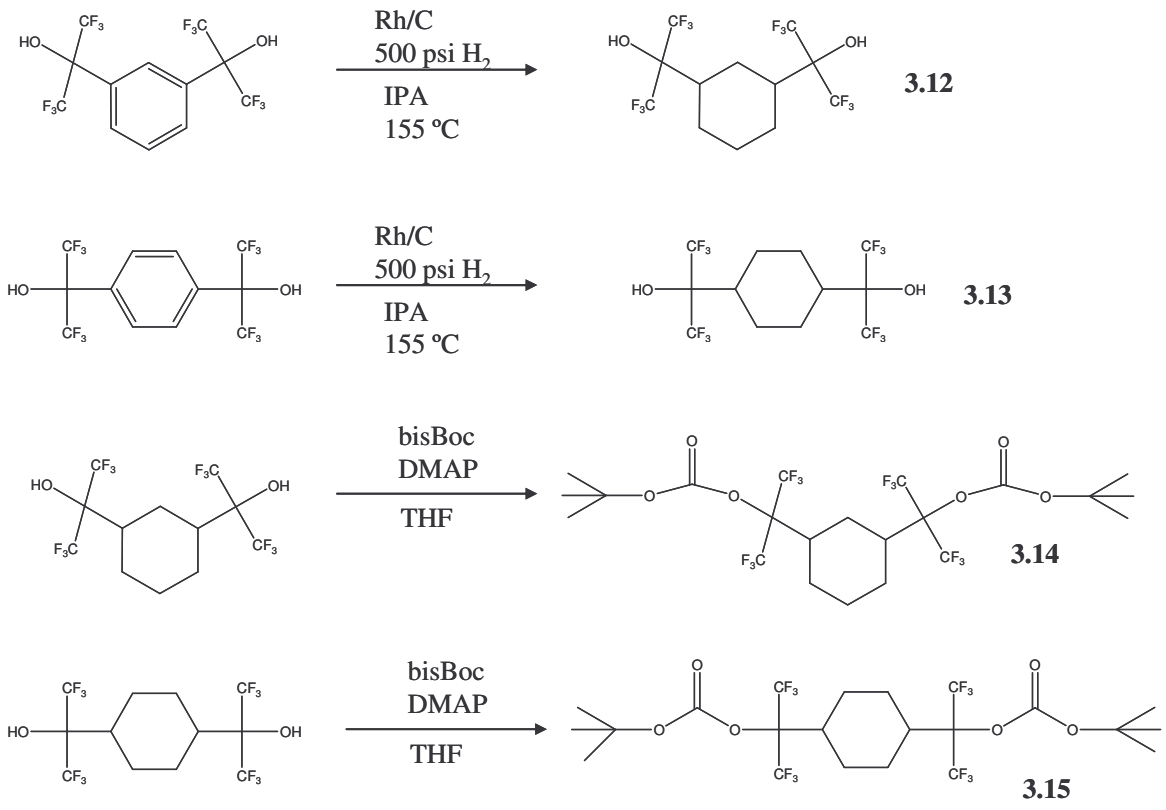

Figure 3.22: Synthesis of transparent DIs based on hydrogenated 1,3 and 1,4-HFAB.

Dissolution inhibitor **3.15** had higher solubility in both the common casting solvents 2-heptanone and PGMEA compared to the nonhydrogenated version (**3.9**). The absorbance at different loadings of **3.14** in PNBHFA was measured, in fact, only a minor increase in absorbance was observed. A 30 wt% loading gave an absorbance of 1.2 μm^{-1} compared to 1.14 μm^{-1} for PNBHFA by itself. The DI **3.14** had a higher solubility in 2-heptanone and PGMEA versus that of **3.15**. Imaging at 157 nm was performed using a 15 wt% loading of **3.14** in PNBHFA (**Figure 3.23**) and 110 nm 1:2 lines and spaces in 130 nm

thick photoresist were achieved. This was just short of our goal of 100 nm lines in a 130 nm thick film. The imaging performance severely deteriorated while trying to print smaller features or attempting to print in thicker photoresist films. To over come this investigation of DIs with three or more inhibiting functional groups then began. The use of DIs with three or more inhibiting functional groups has been shown to improve imaging performance (Trefonas 1987).

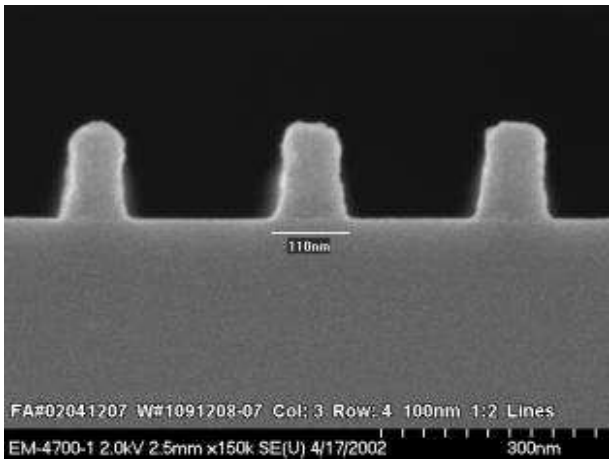

Figure 3.23: Imaging at 157 nm of 15 wt% 3.14 and 2 wt% PAG in PNBHFA.

Figure 3.24 shows the several analogues of 1,3-HFAB. The first redesigned DIs were prepared by the bromination of 1,3-HFAB, followed by methyl-ethyl acetal protection of its alcohols. The Grignard was prepared and reacted with either hexafluoroacetone or ethyl trifluroacetate, followed by an acidic work up to give **3.18**

(Soulen 1989) and **3.20**. The *tert*-butyl carbonate protected derivatives, **3.19** and **3.21**, were prepared and tested by contact printing in PNBHFA. (**Figure 3.25**).

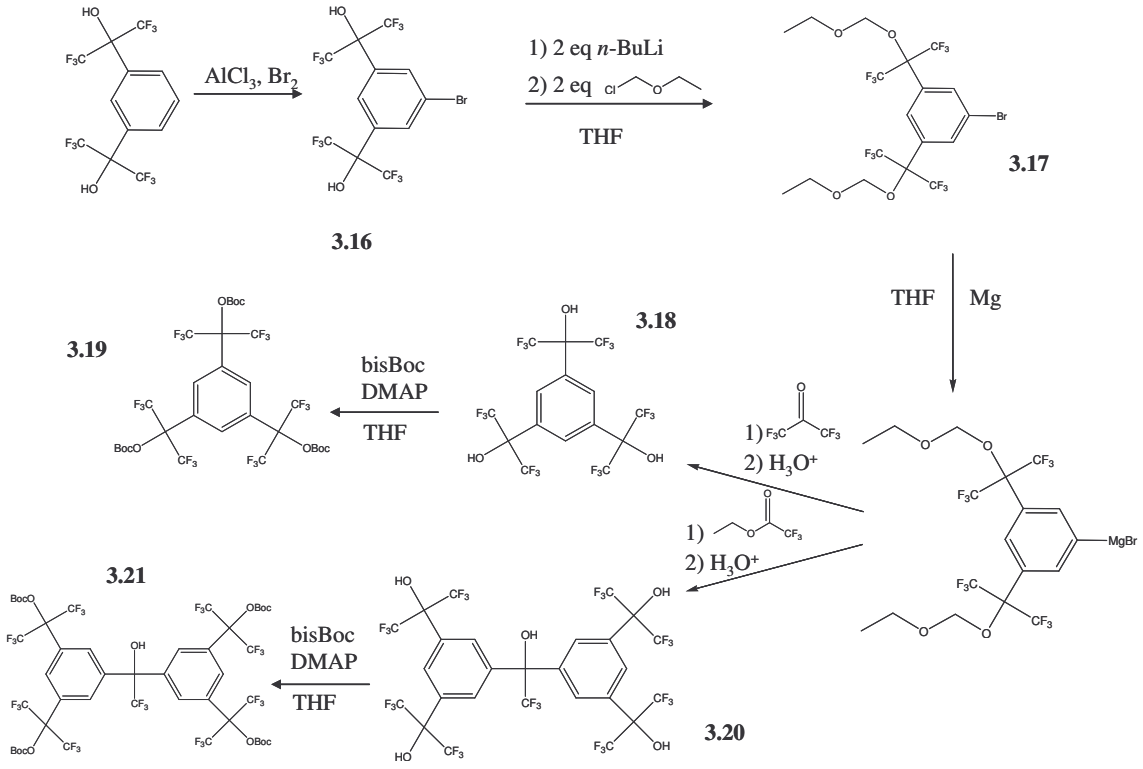

Figure 3.24: Synthesis of DI analogues of 1,3-HFAB.

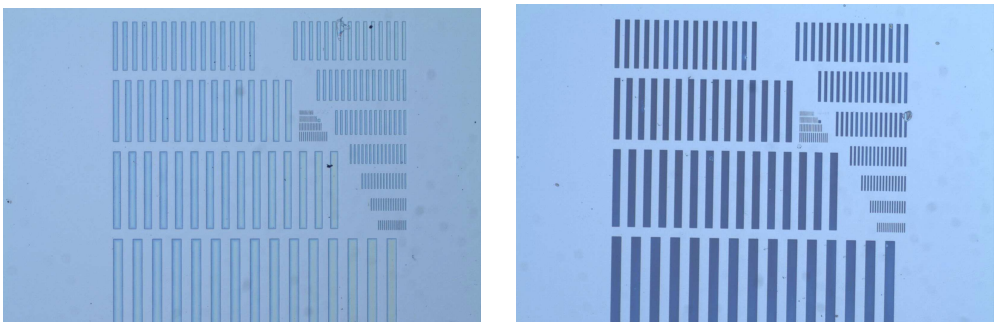

Figure 3.25: Contact printing images at 248 nm of 10 wt% 3.19 (left) and 3.21(right) with 2 wt% PAG in PNBHFA.

The aromaticity of these DIs lends them for a prohibitively high absorbance at 157 nm. Removal of this aromaticity was accomplished via hydrogenation of the DIs using the same procedure used to prepare **3.12** and **3.13,** and then incorporating the *tert*-butyl carbonate functionality.

Unfortunately, these hydrogenation attempts failed. The reaction temperature and pressure were increased to 200 ºC and 1000 psi of H_2, but only starting material was recovered. Even dissolving metal reductions using sodium or lithium in liquid ammonia were unsuccessful in reducing these aromatic rings. Samples of **3.18** and **3.20** were given to Central Glass Company. Even with their proprietary hydrogenation techniques, Central Glass could only achieve 50% hydrogenation. Since the difference between the hydrogenated and nonhydrogenated compounds is only a few hydrogen atoms, separation of the two is nearly impossible with conventional purification techniques. It was decided to circumvent this need for hydrogenation by synthesizing DIs that were based on the transparent, fluorinated norbornenes.

Fluorinated Norbornene-based Dissolution Inhibitors

To help achieve a large Δ, NBTBECF3 monomer was chosen for the first norbornene-based DI. Earlier work showed that ester functionalities had weaker dissolution inhibition characteristics than the corresponding carbonates. The Δs achieved in the non-chemically amplified photoresist system and the PNBHFA- *tert*-butyl carbonate based DI systems were around two orders of magnitude. The same two order of magnitude Δ was desired. The weaker dissolution inhibition effect of the esters was to be compensated for by the incorporation of three inhibiting groups into the DI structure. The alcohol of NBTBECF3 (**3.22**), prepared by hydroboration of the alkene (Knight 1968), would be prepared and two of these alcohols linked together by an inhibiting functionality. **Figure 3.26** shows the synthetic scheme for the preparation of DIs with sulfate (**3.23**) and carbonate (**3.24**) linkers.

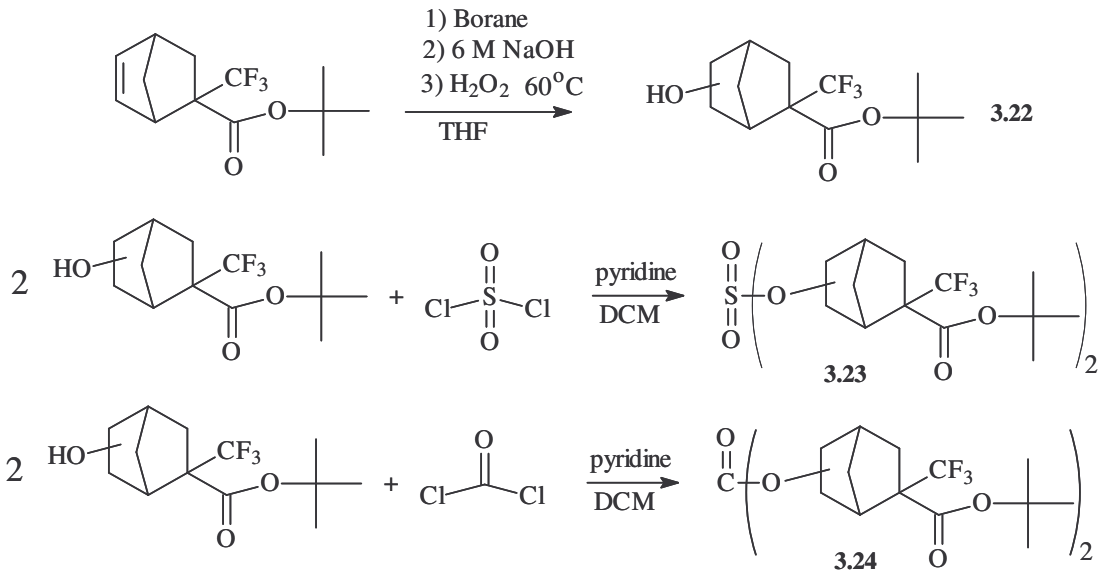

Figure 3.26: Synthesis of DIs based on NBTBECF3.

After seeing the inhibition effect of TDQ due to its sulfonate groups in PNBHFA, the gas phase absorbance of several sulfur-containing compounds was investigated (**Figure 3.27**) (Osborn 2004). The sulfate and sulfite functional groups were chosen as they could link two molecules of compound **3.22** together.

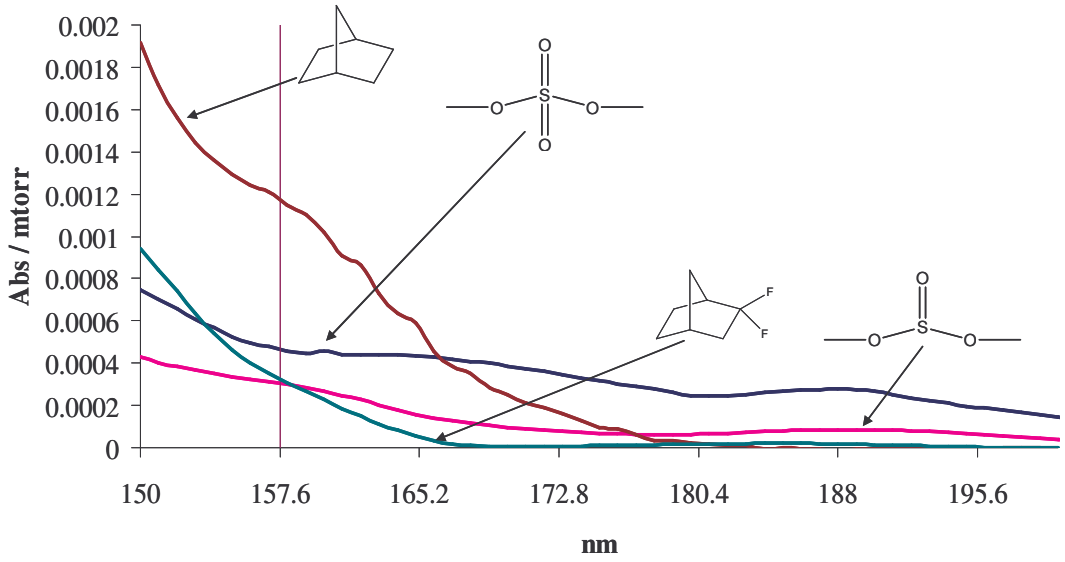

Figure 3.27: Gas phase absorbance of dimethyl sulfate and dimethyl sulfite versus the most opaque and transparent norbornanes.

The sulfate was chosen over the sulfite because its higher hydrolytic stability, which is critical for the development step. The yield for the synthesis of **3.23** was (15%) A Meyerhofer plot was prepared to test the dissolution inhibition of **3.23** with 1 wt% PAG in PNBHFA (**Figure 3.28**).While this DI had a strong inhibiting effect on the dissolution rate of the polymer, the post-exposure slope is negative. This indicates that post-exposure, the DI is inhibiting the polymer's dissolution rate. The negative slope of the exposed line causes the Δ to be slightly over an order of magnitude but well short of the two orders of magnitude sought.

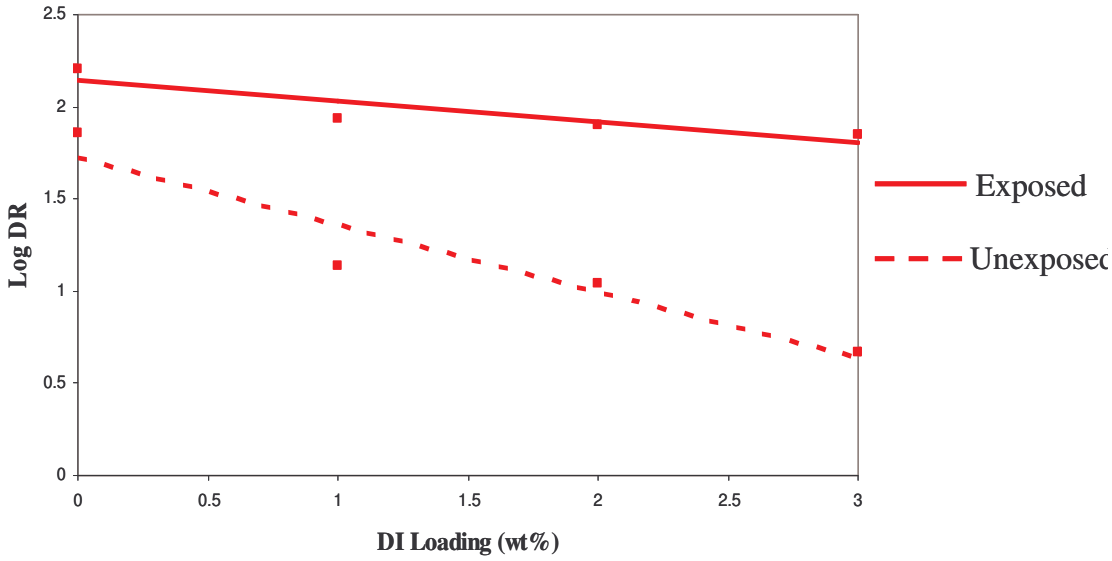

Figure 3.28: Meyerhofer plot of 3.23 and 1 wt% PAG in PNBHFA.

A Meyerhofer plot of **3.24** in PNBHFA was prepared (**Figure 3.29**). The Δ using **3.24** is greater than two orders of magnetude but imaging with **3.24** in PNBHFA was problematic. The images had severe top loss, an indication that the DI is not strongly inhibiting the resist dissolution rate. The reason for the poor imaging performance was investigated.

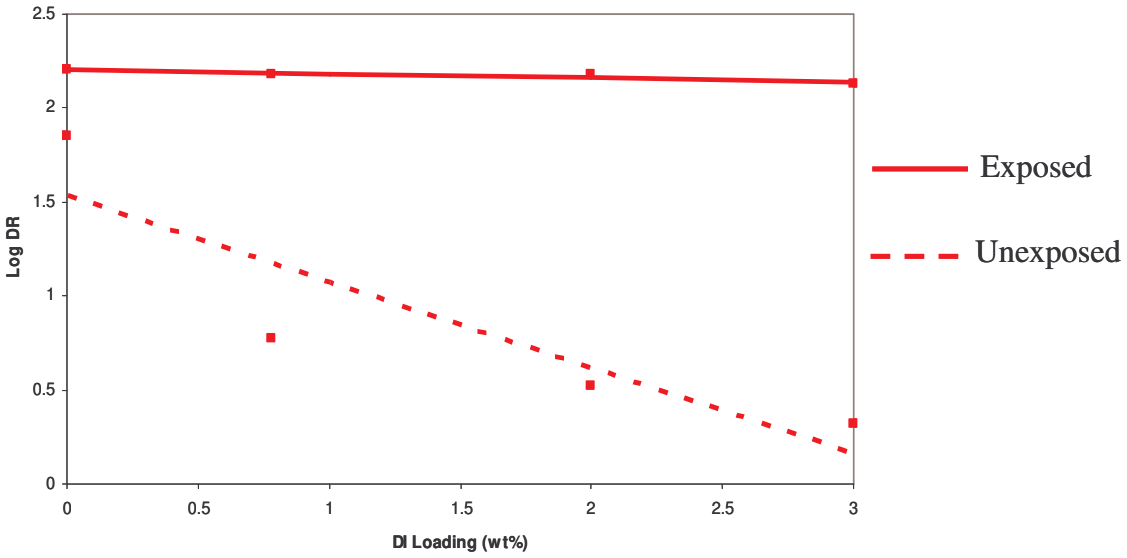

Figure 3.29: Meyerhofer plot of 3.24 and 1 wt% PAG in PNBHFA.

An IR experiment of a film cast from glyme shed some light on why the DI had such poor imaging performance. The wafer was baked at 130 °C and reflectance IR used to monitor the carbonyl signal intensity over time. **Figure 3.30** shows the carbonyl region of the IR spectrum. The spectrum shows the disappearance of both the ester and carbonate carbonyl peaks.

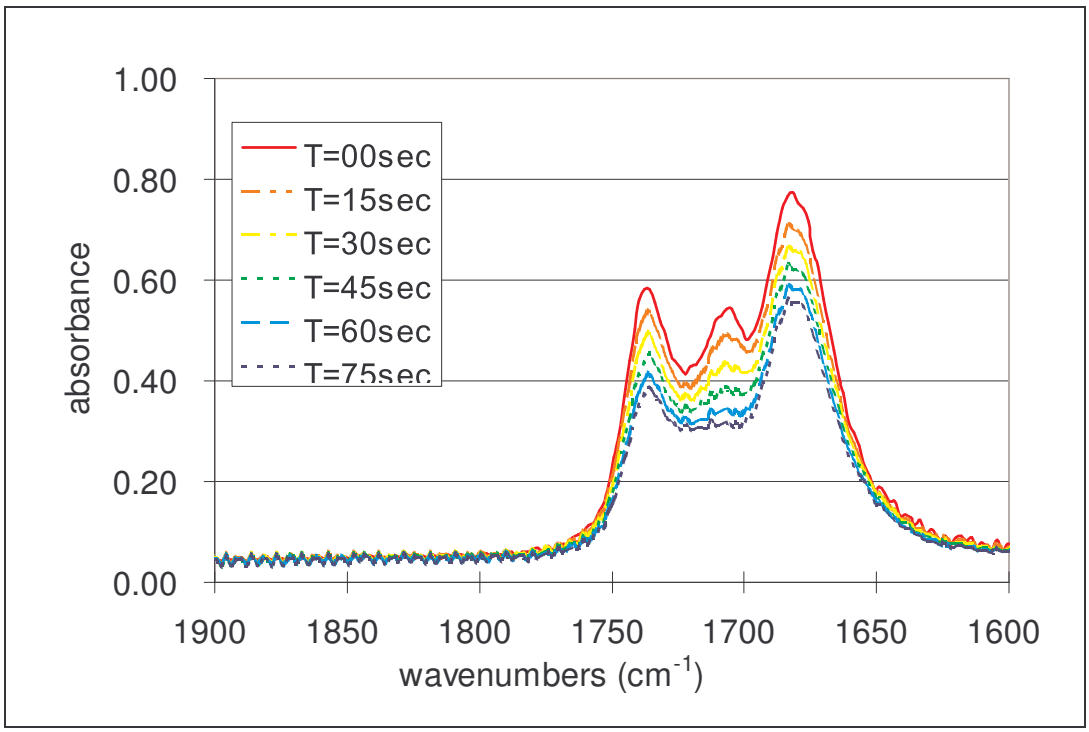

Figure 3.30: Carbonyl region of an IR spectrum a film containing 3.24 and PNBHFA at 130 ºC.

The observed carbonyl loss was likely due to one of two reasons. The first possibility is a carbocation could have formed by the cleavage of the oxygen-norbornene bond. Norbornenes are well known to readily form carbocations, which are stabilized through rearrangements. However, since **3.24** has two strong electron-withdrawing groups on the ring, which would destabilize any carbocation formation, this seemed unlikely. The second possibility is that **3.24** was volatilizing out of the film during the bake step. Since **3.24** is a large molecule, this too seemed unlikely.

In order to completely eliminate the possibility of carbocation formation, **3.27** was synthesized (**Figure 3.31**). The methylene groups in **3.27** removes the carbonate linkage from the norbornene, thus eliminating the possibility of any such carbocation formation.

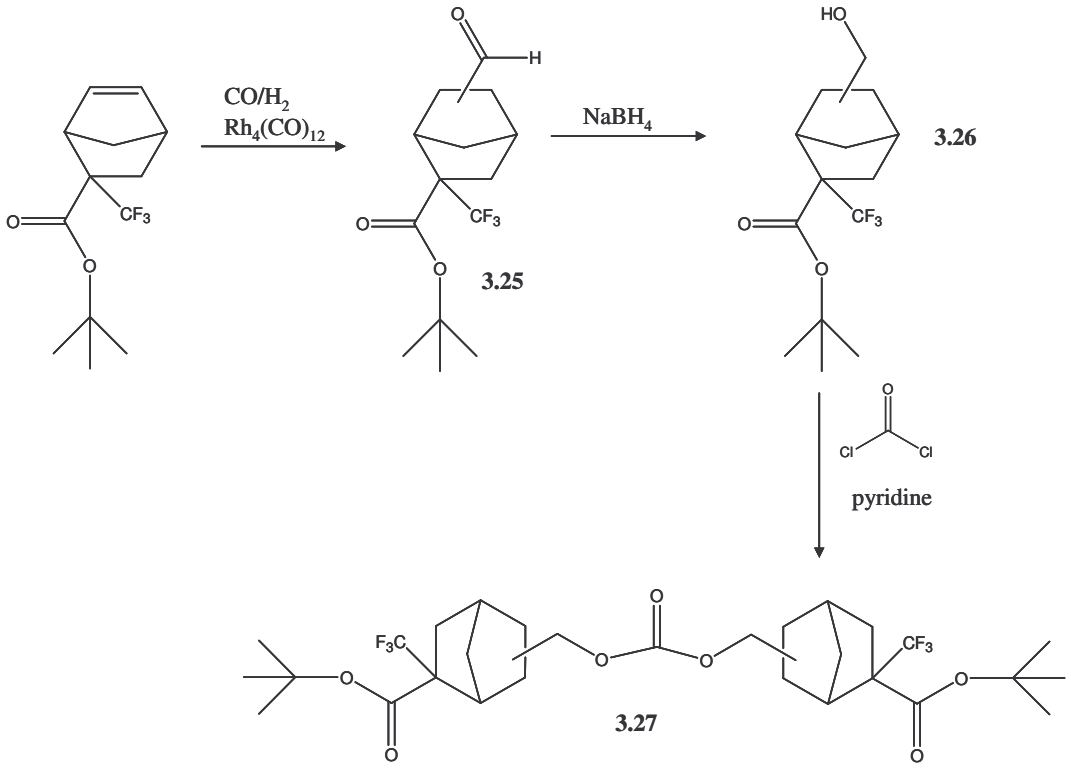

Figure 3.31: Synthesis of analogue of DI 3.24 with methylene spacer.

A Meyerhofer plot of **3.27** in PNBHFA was prepared (**Figure 3.32**). The Δ was only slightly lower than that observed with **3.24**.

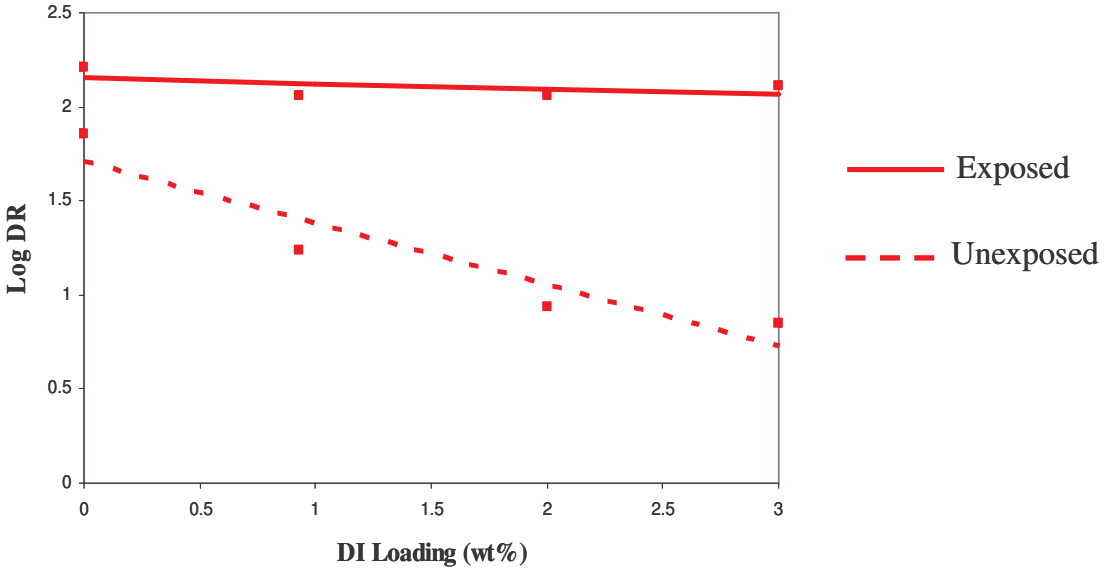

Figure 3.32: Meyerhofer plot of 3.27 and 1 wt% PAG in novolac and PNBHFA.

Top loss was again observed when attempting to image using **3.27**. This observed top loss led to another IR experiment. A salt plated was suspented above a wafer coated with a film of **3.27** in PNBHFA. The wafer was heated to 130 °C and the subliming species was collected on the salt plate and its IR measured. The sublimation species was identified as **3.27,** conclusively proving that the imaging problems encountered were a result of a surprisingly high volatility of these DIs.

The most likely reason the DIs showed strong inhibition effects in the Meyerhofer plots, but poor imaging performance is likely due to the difference in film thickness. Dissolution rate measurements are made on films that are approximately one

micron thick. Most imaging at 157 nm is performed on films that are less than 130-150 nm thick. It is much easier for the DIs to volatilize out of the thin film.

Despite the strong dissolution inhibition effect observed using the norbornene based DIs no major progress towards our goals of imaging in 130, 250 and 300 nm thick films was made. The volatility of the fluorinated compounds was a major concern that had to be addressed. Two ways to decrease the volatility of the fluorinated norbornenes were to increase the weight of the DIs and the introduction of polar groups.

PNBHFA Oligomers as Dissolution Inhibitors

Partially protected oligomers of PNBHFA were considered as DIs for several reasons. Imaging success was achieved using the carbon dioxide copolymers as DIs. The volatility of the monomeric DIs was a major problem. The use of oligomeric PNBHFA would eliminate this problem. The oligomers are large enough to prevent the sublimation problem encountered with the monomeric DIs. Oligomers with only partial incorporation of an acid labile inhibiting group would have free alcohols which should also further prevent sublimation. The *tert*-butyl carbonate based DIs reported earlier had Δs greater than two orders of magnitude.

Oligomeric PNBHFA was provided by Dr. Ralph Dammel of AZ Clariant Microelectronics. The oligomers were first reacted with di-*tert*-butyl dicarbonate using catalytic DMAP. The oligomers were 82% *tert*-butyl carbonate protected (**3.28**).

Comparison of the contrast curves prepared with the monomeric **3.14**. A contrast curve shows the thickness change (by development) versus exposure dose and is a metric used to judge the imaging capability of a photoresist. The contrast curve of DI **3.14** and the oligomeric DI **3.28** in PNBHFA is shown in **Figure 3.33**.

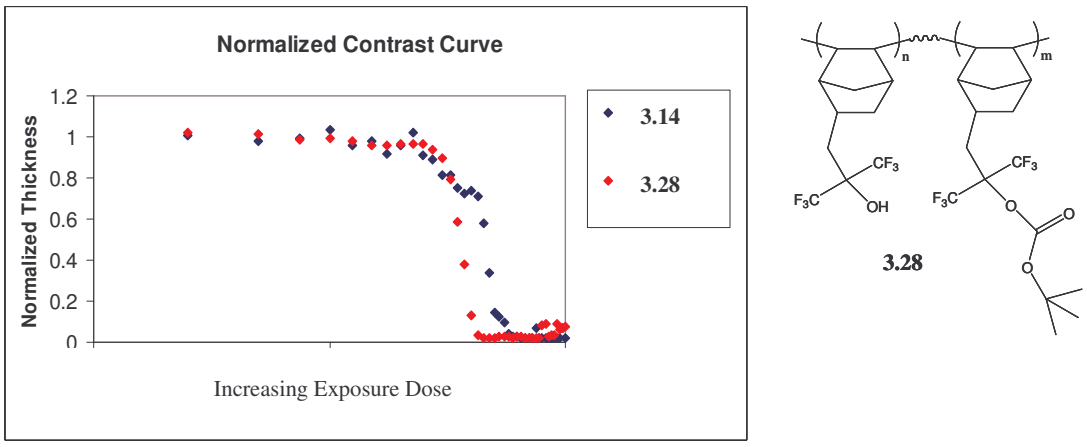

Figure 3.33: Contrast curve of 3.14 and 3.28 with 2 wt% PAG in PNBHFA.

Both curves show some top loss before the threshold dose is reached. The slope of the curve in the region where most of the thickness change occurred is much sharper for the oligomers, an indication of a higher contrast system.

The Asahi Glass Polymer

In 2002, at the SPIE (International Society for Optical Engineering) conference, the Asahi Glass Company announced a new fluorinated cyclopolymer that was a highly

transparent resin with the astounding absorbance of 0.3 μm^{-1} at 157 nm. The polymer that is commercially available has 20% incorporation of a acetal protecting group and has an absorbance of 0.7 μm^{-1} at 157 nm (Kodama 2002). Exploring the dissolution characteristics of the Asahi polymer made it was necessary to remove the MOM protecting group, using trifluoroacetic acid in water (**Figure 3.34**).

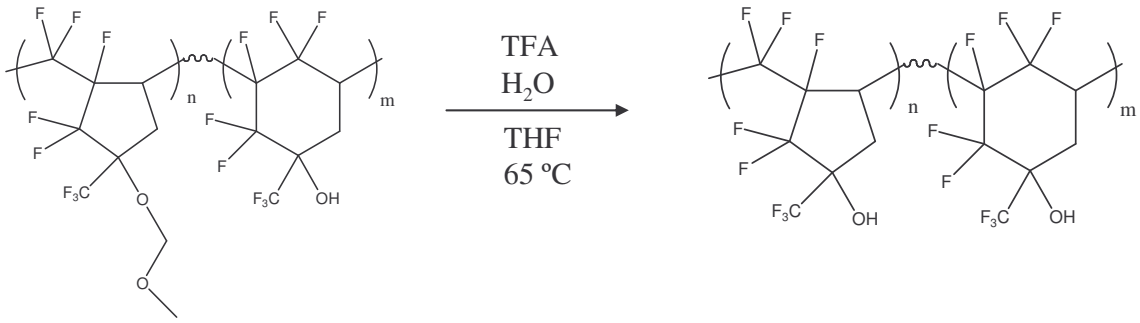

Figure 3.34: Deprotection of the acetal protected Asahi polymer.

The vast majority of the work with DIs for 157 nm photolithography centered around PNBHFA and, while the Asahi polymer has superior transparency, it lacks the dissolution inhibition and etch resistance properties of PNBHFA. **Figure 3.35** compares the dissolution inhibition properties of TDQ in both polymers.

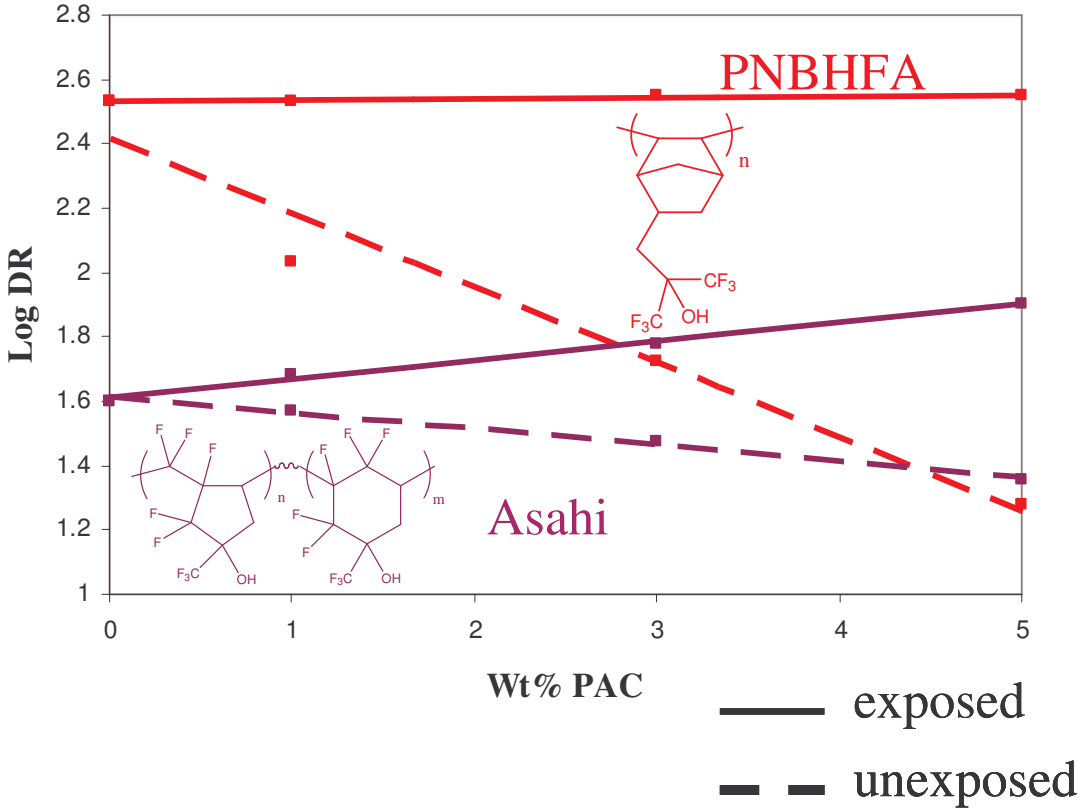

Figure 3.35: Meyerhofer plot of TDQ in the Asahi polymer and PNBHFA.

The Δ at 5 wt% loading of the DI is an order of magnitude in PNBHFA. This value is more than twice as large as the effect the DI has on the Asahi polymer. The difference between the exposed and unexposed dissolution rates of PNBHFA is due almost entirely to the inhibition effect of the DI on the unexposed film. The difference between the exposed and unexposed dissolution rates of the Asahi polymer is due to slight inhibition in the unexposed film and the acceleration of the dissolution rate in the

exposed areas. The DI has a reduced inhibiting effect on the dissolution rate of the Asahi polymer.

A high contrast photoresist was achieved by using 25 wt% of the oligomeric DI **3.28** in the Asahi polymer (**Figure 3.36**).

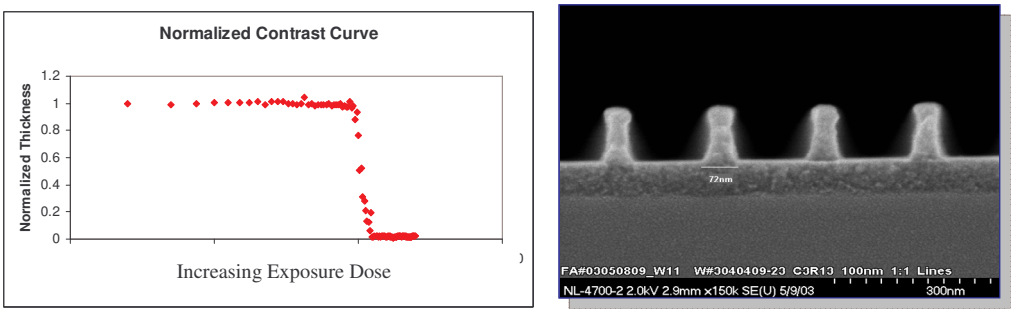

Figure 3.36: Contrast curve and imaging at 157 nm for 25 wt% 3.28 and 5 wt% PAG in the Asahi polymer.

The contrast curve shows that no top loss occurred before the threshold dose was reached. The slope of the curve in the region where the thickness change occurs is high, meaning the system has high contrast. This resist system was used to exceed our imaging goal of 100 nm lines in a 130 nm thick film. Impressive 74 nm lines in a 130 nm thick film were achieved with this photoresist system. To further improve the imaging performance and reach our final two imaging goals, ester functionality was incorporated into the PNBHFA oligomers.

The oligomers of PNBHFA were deprotonated with sodium hydride and reacted with *tert*-butyl bromoacetate to produce **3.29** (**Figure 3.37**).

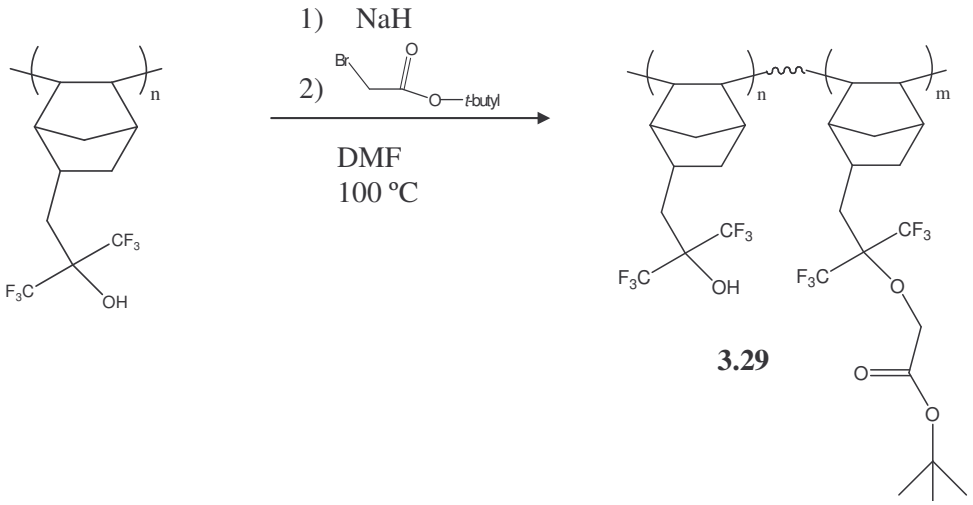

Figure 3.37: Synthesis of oligomeric DI 3.29.

The idea was to take advantage of the dissolution rate acceleration, due to the generation of carboxylic acid, observed in **Figure 3.33**. A loading of 30 wt% was required to inhibit the dissolution of the Asahi polymer. The contrast curve reveals that some top loss occurred and the contrast is not as high as with **3.28** as the DI. Finally, 100 nm lines in a 130 nm thick film were achieved with **3.29** in the Asahi polymer (**Figure 3.38**). Unfortunately both photoresist systems using the Asahi polymer and modified PNBHFA oligomers demonstrated poor imaging performance in 250 nm thick films.

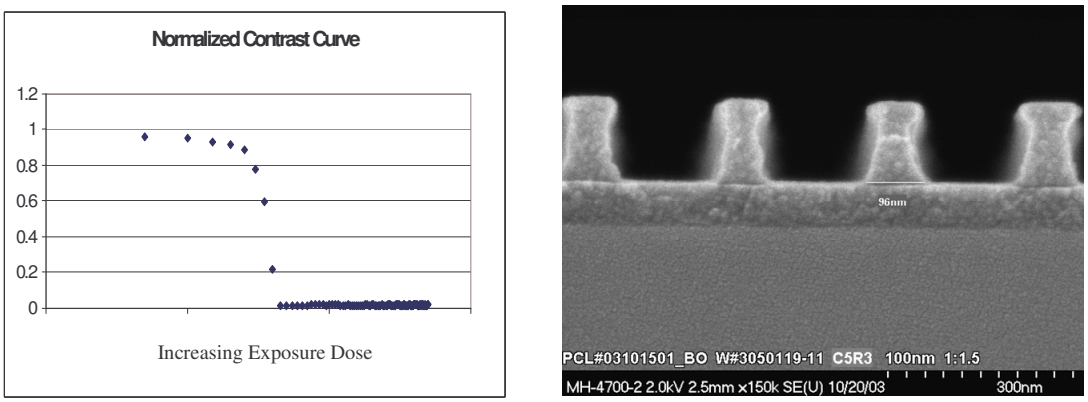

Figure 3.38: Contrast curve and imaging at 157 nm for 30 wt% 3.29 and 5 wt% PAG in the Asahi polymer.

The 157 nm imaging reported to this point was performed in films that were approximately 130-150 nm thick. The final project goals were to image in films 250 and 300 nm thick. Utilizing a photoresist with low absorbance is obviously more critical for imaging in thick films. The projected maximum absorbance of the fully formulated photoresist used for imaging in a 300 nm film is approximately 0.7 μm^{-1}. Even though the Asahi polymer was highly transparent, DI **3.29** had an absorbance of 3.3 μm^{-1} and 30 wt% was required to inhibit the dissolution of the Asahi polymer. Lower loadings of the DI could be used if either the 20% acetal protected polymer was used for imaging or if a PAG that also had a strong inhibition affect on the Asahi polymer was used.

PAG Dissolution Inhibition of Novolac and PHS

The inhibition of novolac by triphenyl sulphonium hexafluoroantinomate ($TPSSbF_6$) was reported by Hiroshi Ito at IBM. He reported that where as a 1 µm thick

film of the novolac resin dissolved away in 30 seconds, a 1 μm thick film containing a 4.8 wt% loading of the PAG in novolac retained 88% of its thickness after remaining in developer for 6 minutes. The PAG was a more efficient inhibitor of novolac than the diazonapthoquinones, like TDQ, used for 365 nm photolithography. The PAG-novolac system could be imaged at 254 nm as long as the films were very thin and the PAG concentration was kept low (Ito 1988).

Hiroshi Ito also reported the interaction between PHS and PAGs. ^{13}C NMR was used to examine the interaction between 4-isopropylphenol, as a model for PHS, and di-(*tert*-butylphenyl)iodonium triflate (tB-DBITf). The presence of the PAG caused a significant shift in the in the resonance of the phenolic compound. The interaction of PAG with phenolic functionality was also explored by FT-IR. The peak for the hydrogen bonded ester group in the IR spectrum of a film of poly(*para*-hydroxystyrene-co-*tert*-butyl acrylate) was greatly reduced by the addition of tB-DBITf. This suggests that the PAG interacts more strongly with the phenol group than the ester functionality (Ito 1997).

Ito also reported PAGs have a similar effect on polymers containing the bis-trifluoromethyl carbinol moiety. The trifluoromethyl groups of NBHFA are not magnetically equivalent and both endo and exo isomers are present. A significant shift in the ^{19}F NMR of the NBHFA monomer is observed upon the addition of tB-DBITf. The endo isomer was shifted shifted35 and 46 Hz and the endo was shifted 42 and 46 Hz. The fact that the exo isomer showed the greater shift is an indication of some interaction between the bis-trifluoromethyl carbinol and PAG. The same ^{19}F NMR experiment with

trimethylsilyl protected NBHFA resulted in shifts of only 5.7 and 6.9 Hz again indicating some interaction between the hexafluoro carbinol and PAG was responsible for the large shifts in the ^{19}F NMR resonances (Ito 2003).

TPSNf Inhibition of PNBHFA

The inhibition effect of triphenyl sulfonium nonafluoro-1-butanesulfonate (TPSNf) was first observed while preparing the Meyerhofer plot in **Figure 3.20**. The lines for the dissolution rate before and after exposure do not intersect at 0 wt% loading of the DI and the reason is the PAG has an effect on the dissolution rate of the polymer that it is different before and after exposure. A Meyerhofer plot similar to Figure 3. was prepared, but with TPSNf loading from 1 to 3 wt% (**Figure 3.39**).

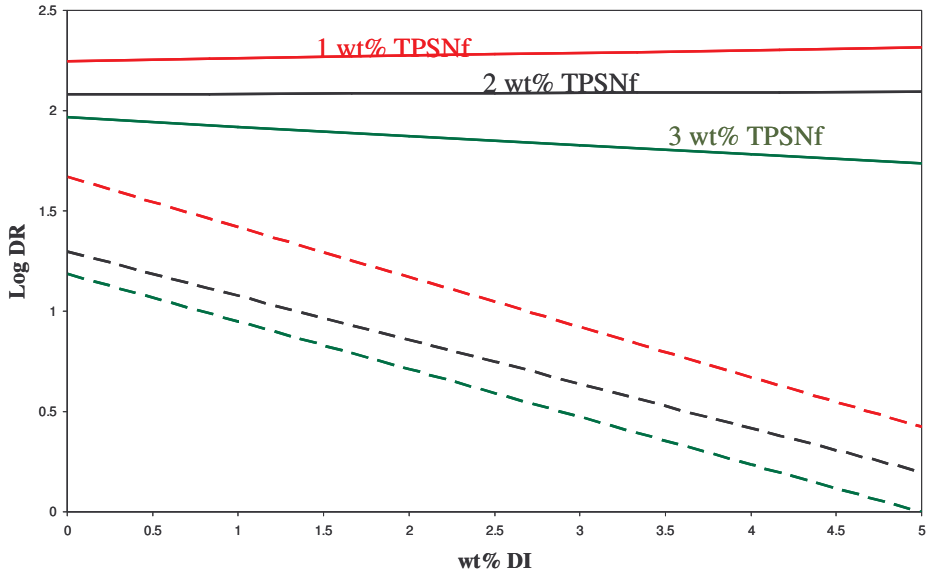

Figure 3.39: Meyerhofer plot of 3.10 with 1,2 and 3 wt% TPSNf in PNBHFA.

A similar shift in the plot is observed between increasing the TPSNf loading from 1 to 2 and 2 to 3 wt%. The observed dependence of the dissolution rate on PAG loading suggested that the three component system discussed earlier could be further simplified to a two component system by combining the DI and PAG into one compound. Unfortunately the inhibition effect of the TPSNf on PNBHFA or the Asahi polymer was not sufficient for a two component system using this PAG. The dissolution inhibition of several PAGs in PNBHFA and the Asahi polymers was investigated. **Figure 3.40** compares the dissolution rates of several PAGs at 3 wt% loading in novolac, PNBHFA and the Asahi polymer.

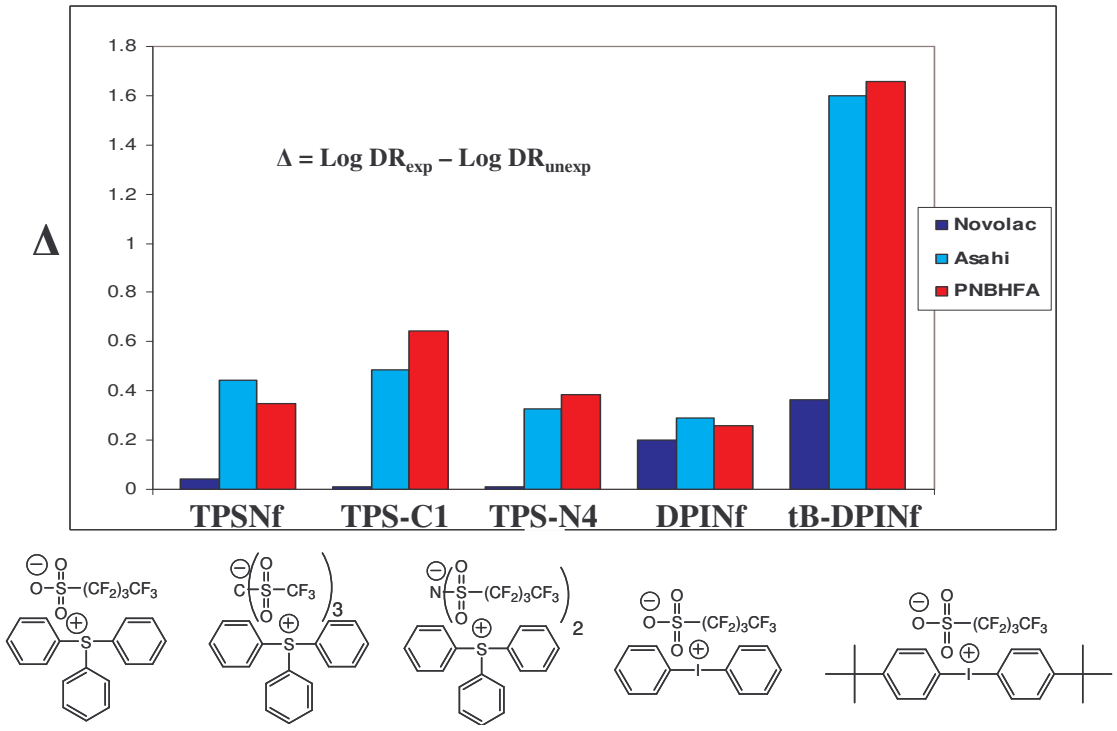

Figure 3.40: Inhibition effect of 3 wt% loading of PAGs in novolac, PNBHFA and the Asahi polymer.

The two important conclusions that can be drawn from **Figure 3.40** are: all the PAGs tested had an inhibition effect on the dissolution rate of all three polymers and the PAGs had different Δ values, which indicates that the structure of the PAG is important in determining inhibition effect due to the PAG. TPSNF, TPS-C1 and TPS-N4 are all triphenyl sulphonium salts, however TPS-C1 had a larger Δ in both PNBHFA and the Asahi polymer. Similarly, DPINf and tB-DFINf are both diphenyl iodonium nonaflates, but tB-DFINf has a much higher Δ in all three polymers**.** tB-DFINf. had the largest Δ in all three resins. Unfortunately, the iodonium salts based PAGs are more highly absorbing than sulphonium salts at 157 nm.

PAGs with Acid Labile Functionality

Sulfonium based PAGs with Δ values similar to tB-DFINf. in polymers PNBHFA ($\Delta_{3wt\%}$ = 1.65) and the Asahi polymer ($\Delta_{3wt\%}$ = 1.59) were required. The Δ could be increased by either increasing the inhibition effect of the PAG or by decreasing the inhibition effect of the photoproducts. The incorporation of acid labile inhibiting functional groups like carbonates or esters was considered as a method to increase the inhibition effect of the PAG.

A Δ of two orders of magnitude was believed to be attainable because the generation of some base soluble functional group in the photoproducts like a phenol or carboxylic acid after exposure would decrease the inhibition effect of the photoproducts on the film and increase the film's dissolution rate.

A commercially available PAG with *tert*-butyl ester functionality, (*tert*-butoxycarbonylmethoxyphenyl)diphenylsulfonium triflate (TPSTfE), was the first PAG investigated to improve the Δ of the sulphonium PAGs. The PAG had a strong inhibition effect on both polymers and more importantly the $\Delta_{3wt\%}$ values (1.97 and 1.37) were comparable to those achieved with 3 wt% of tB-DFINf. After exposure the dissolution rate of a film of PNBHFA with 3 wt% TPSTfE. was 122 nm/sec compared to 340 nm/sec for a film of the polymer alone. In order to further lessen the inhibiting effect of the photoproducts, a sulfonium PAG that would generate two base soluble functional groups after exposure was sought. No commercially available PAGs met these criteria. It was decided that we would synthesize a PAG with two phenolic alcohols protected by *tert*-butyl carbonates. The two phenols generated after exposure should impart base solubility to the photoproducts thereby reducing the inhibition effect even further and the two *tert*-butyl carbonates should further increase the inhibition effect the PAG has before exposure.

The synthesis of the initial functionalized PAG prepared is shown in **Figure 3.41**. The initial carbonate functionalized PAG investigated was prepared by the copper (II) catalyzed arylation of 4,4'-thiodiphenol with tB-DPITf (Crivello 1978) (**3.30**) followed by the deprotonation and reaction with di-*tert*-butyl dicarbonate (**3.31**)

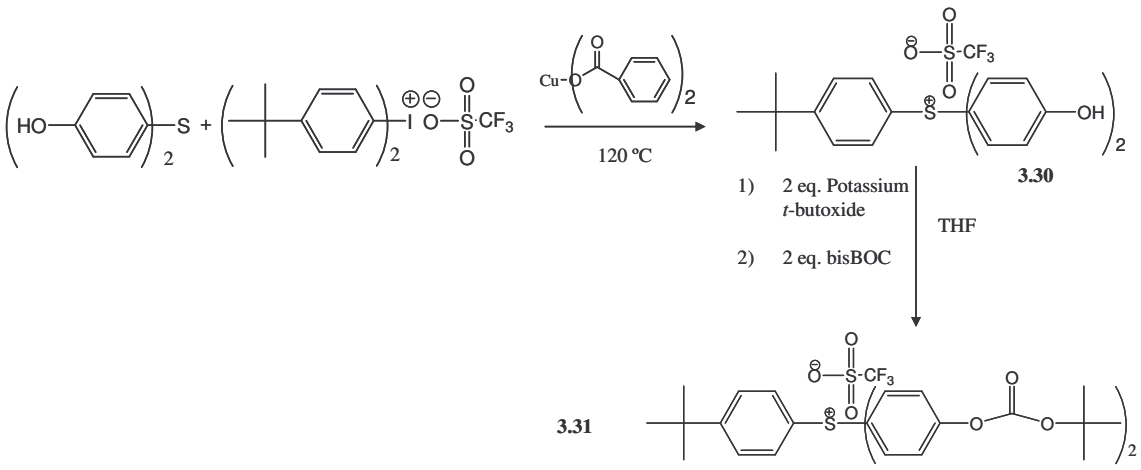

Figure 3.41: Synthesis of PAG functionalized with two *t*-butyl carbonate functionalities for improved dissolution inhibition.

The Δs achieved with **3.31**. in PNBHFA ($\Delta_{3wt\%}$ = 2.10) and the Asahi polymer($\Delta_{3wt\%}$ = 1.62) were greater than the ones achieved with tB-DPINf. A two component resist system, 5 wt% **3.31**in PNBHFA, was printed at 157 nm (**Figure 3.42**).

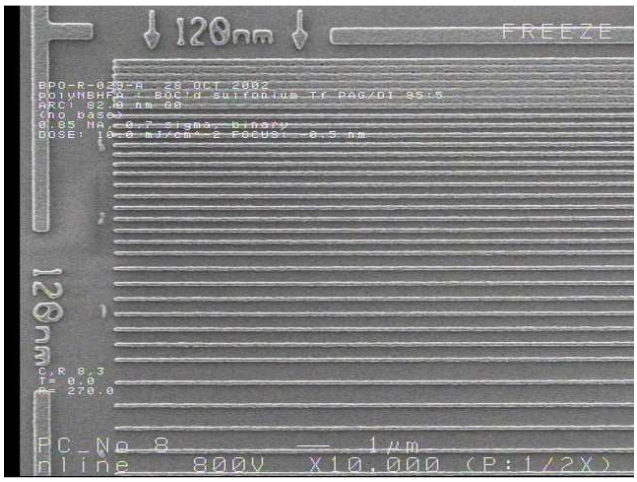

Figure 3.42: Imaging at 157 nm of two component resist system with 5 wt% 3.31 in PNBHFA.

A 5 wt% loading of **3.31**in PNBHFA slowed the dissolution rate of the film to 0.5 nm/sec, which means despite the strong inhibition effect some top lose in the unexposed areas occurs during development step. Increasing the PAG loading above 5 wt% led to film uniformity problems. A PAG with an even stronger inhibition effect was required.

Increasing the number of phenolic species protected by *tert*-butyl carbonate from two to three seemed the best way to further increase the inhibition effect of the PAG. A PAG with three phenolic sites protected by *tert*-butyl carbonate groups had been reported as an inhibiting PAG for 248 nm lithography by BASF (Schwalm 1991). The PAG was synthesized by the procedure of Dr. Reinhold Schwalm of BASF (**Figure 3.43**).

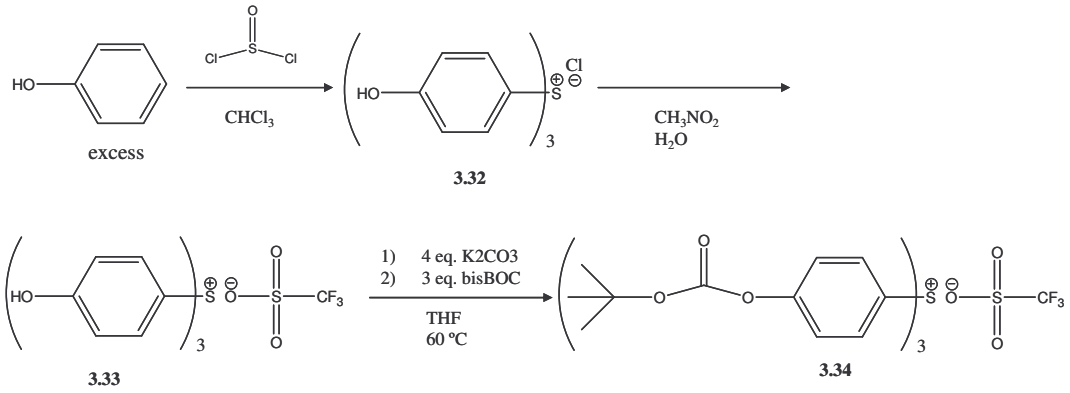

Figure 3.43: Synthesis of PAG functionalized with three *t*-butyl carbonate functionalities for improved dissolution inhibition.

Although **3.34** has a very strong dissolution inhibition effect, the Δs achieved. in PNBHFA. ($\Delta_{3wt\%}$ = 1.97) and the Asahi polymer ($\Delta_{3wt\%}$ = 1.53) were surprisingly less than the ones observed with **3.31** in these two resins.

Further increasing the PAG loading of either **3.31** or **3.34** would create coating uniformity problems or decrease the sensitivity of the photoresist.. In a typical photoresist the sensitivity is increased by increasing the PAG loading. Increasing the PAG loading increases the PAG to acid labile functional group ratio. In a 2 component photoresist system using either **3.31** or **3.34** the ratio of PAG to acid labile functional group ratio remains constant as the PAG loading is increased and since more PAG is added the exposure dose increases. It was decided that PAGs with inhibiting acid labile functional groups were not a viable option.

PAG Screening for Dissolution Inhibition of PNBHFA

Imaging films greater than 250 nm thick, at 157 nm required a PAG that had an inhibition effect stronger than the inhibition effect of TPSNf. Several sulphonium and iodonium ionic PAGs with varying cations and anions as well two nonionic PAGs were tested for dissolution inhibition of PNBHFA. Equal molar amounts of each PAG were tested in PNBHFA and the dissolution rates, in 0.26 N TMAH, of the resulting films were measured before and after being exposed 200 mJ/cm^2 at 248 nm. The high exposure dose was used to make sure the PAGs had completely reacted after exposure. PNBHFA was used as the resin for the PAG screening due to the expense and low availability of the Asahi polymer. **Table 3.3** shows the results of the PAG inhibition screening.

Table 3.3: results of PAG screening for dissolution inhibition in PNBHFA.

PAG structure and acronym	Unexposed DR (nm/s)	Δ	PAG structure and acronym	Unexposed DR (nm/s)	Δ
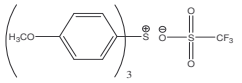 TMOPSTf	0.2	2.12	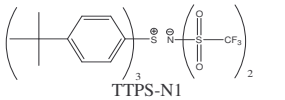 TTPS-N1	6.5	0.78
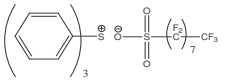 TPSPFOS	7	0.42	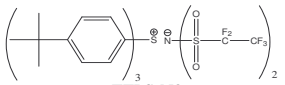 TTPS-N2	9.5	0.58
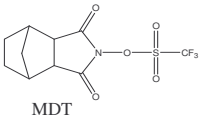 MDT	68.1	0.03	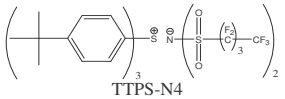 TTPS-N4	12	0.23
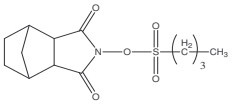 MDT-BuS	28	0.03	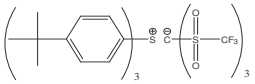 TTPS-C1	8.8	0.56
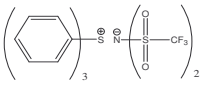 TPS-N1	5.2	0.85	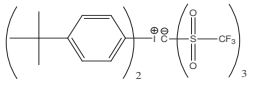 tBDPI-N1	0.01	3.37
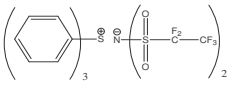 TPS-N2	6.3	0.72	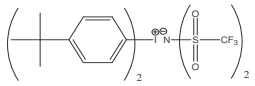 tBDPI-N2	1	1.51
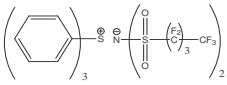 TPS-N4	7.3	0.54	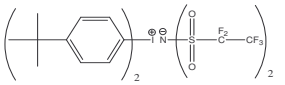 tBDPI-N4	0.08	2.65
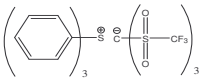 TPS-C1	5	0.77	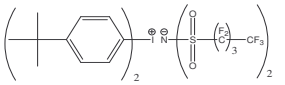 tBDPI-C1	0.4	1.8

The nonionic PAGs had the lowest Δ values of the PAGs tested. As expected the PAGs with the bis(4-*tert*-butylphenyl)iodonium cation had high Δ values and the strongest effect of the polymer's dissolution rate. The PAGs with the triphenyl sulphonium or tris(4-*tert*-butylpheny)sulphonium cations had reasonable Δ values.

Tris(4-methoxyphenyl)sulphonium triflate (TMOPSTf) had the largest dissolution inhibition effect of the sulphonium based PAGs tested. The Δ for TMOPSTf in PNBHFA was greater than two orders of magnitude making it the ideal PAG to use for imaging with the Asahi polymer in thick films.

Imaging with TMOPSTf

Figure 3.44. compares the inhibition effect of TPSNf and TMOPSTf on PNBHFA.

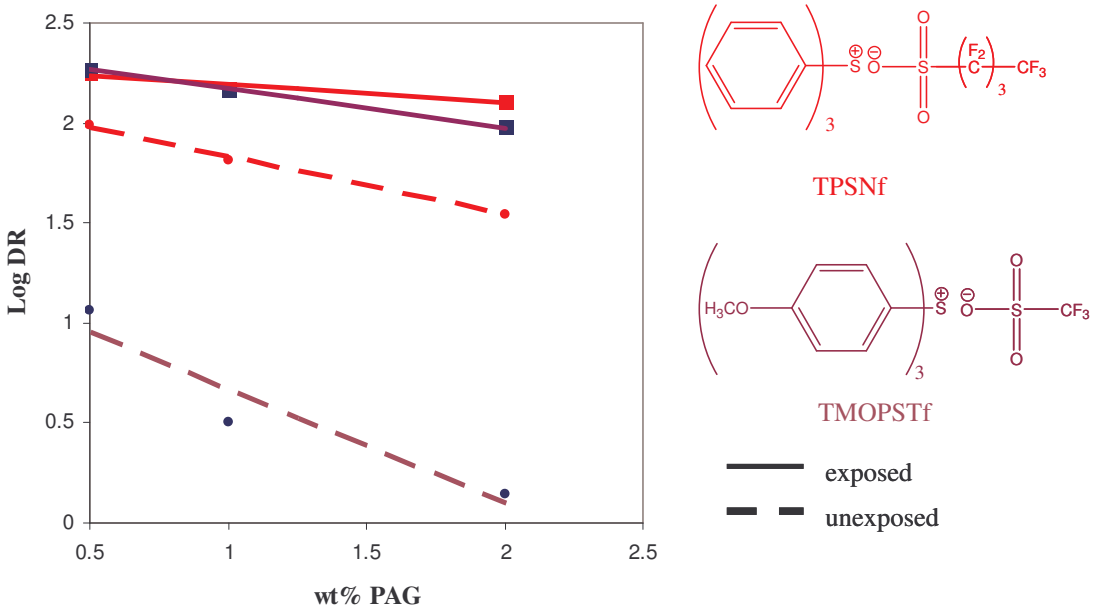

Figure 3.44: Meyerhofer plot of TPSNF and TMOPSTf in PNBHFA.

The inhibition effect of 2 wt% TMOPSTf on PNBHFA is two orders of magnitude. The Asahi polymer is also strongly inhibited by TMOPSTf. No dark loss is observed with 6 wt% loading of the PAG in the Asahi polymer. **Figure 3.45** compares the absorbance of TPSNf and TMOPSTf The absorbance of TMOPSTf is significantly less than that of TPSNf and only 2 wt% of was required in 20% acetal protected Asahi polymer. The fully formulated resist had an sbsorbance of 0.8 μm^{-1} and was used to print 120 nm features in 240 nm of resist (**Figure 3.46**).

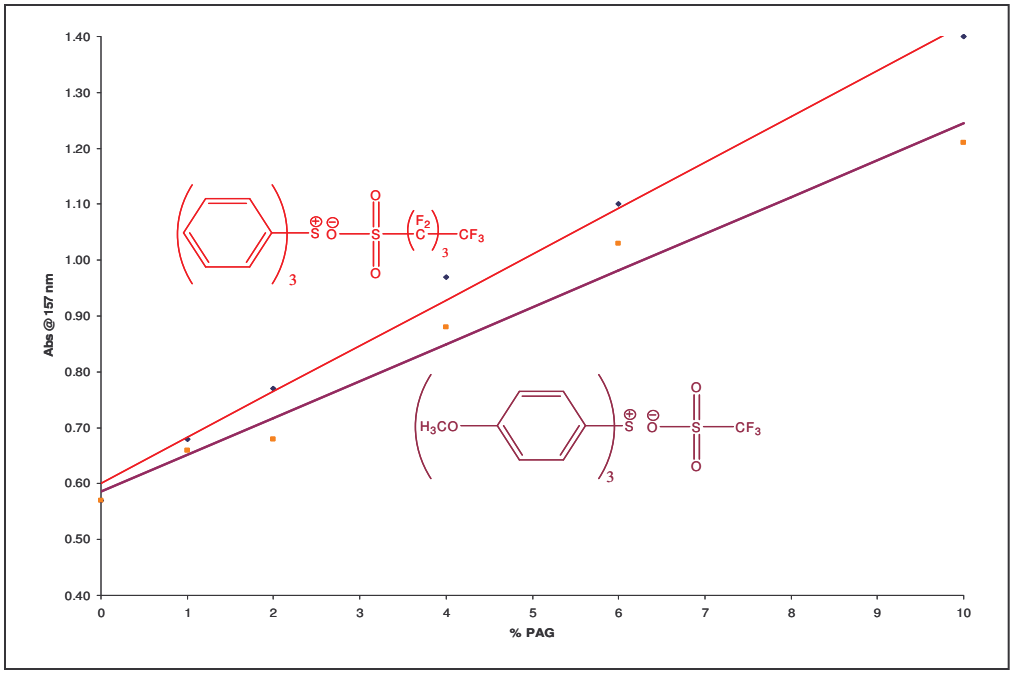

Figure 3.45: Absorbance comparison of TPSNF and TMOPSTf in PNBHFA.

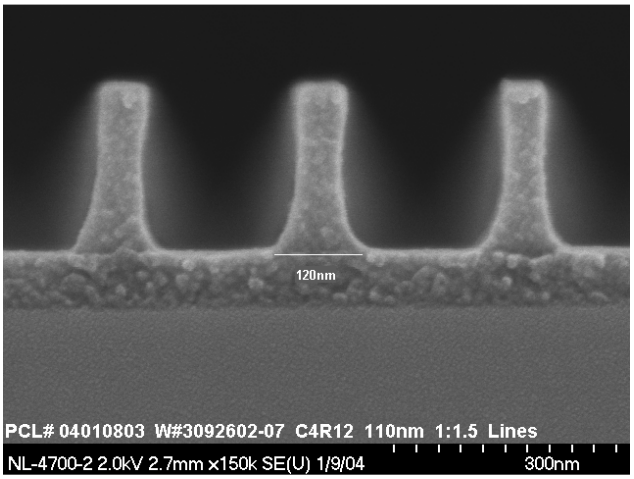

Figure 3.46: Imaging at 157 nm of two component resist system with 2 wt% TMOPSTf n 20% acetal protected Asahi polymer.

The final 157 nm image reported falls 10 nm short of the 130 nm lines in a 250 nm thick film goal. The plan was to used TMOPSTf and a low wt% loading of the PNBHFA oligomers in unprotected Asahi polymer to make a highly transparent photoresist formulation that could be used to used to achieve our last two imaging goals. Unfortunately the final two goals were never achieved.

The Death of 157 nm Photolithography

Despite the success finding highly transparent materials, incorporating them into 157 nm photoresists and imaging the photoresists at 157 nm, in the spring of 2003 Intel Corporation, the worlds largest chip producer, announced it would forgo 157 nm photolithography. The estimated 30 million dollar cost of the 157 nm stepper, the scarcity

of high purity calcium fluoride for the lenses of the optics as well as the lack of a pellicle material all contributed to Intel's decision.

The time and effort spent finding photoresist materials for 157 nm photolithography was not lost. The photoresist systems initially targeted for 157 nm are backwards compatible with 193 and 248 nm photolithography. Imaging of several 157 nm photoresist systems at 193 and 248 were reported in this thesis. The leading technology to replace 157 nm photolithography is 193 nm immersion lithography. The use of DIs in PNBHFA as a possible 193 nm immersion photoresist system has been investigated (Taylor 2005).

Appendix I: Immersion Lithography Extraction Experiments

Immersion Lithography

Immersion lithography at 193 nm has replaced dry 157 nm lithography as the leading technology for use at the 45 nm node (Dammel 2004) (http://public.itrs.net). Immersion lithography is an adaptation of traditional lithography where the gap between the silicon wafer and lens elements is filled with a liquid medium. When the liquid medium (Takanashi 1984) has a higher refractive index than air (as is present in traditional lithography), a larger depth of focus (DOF) is achieved.

The liquid also allows for the design of lenses with higher numerical apertures (NA) (Lin 1987) (Kawata 1989), which increases resolution and decreases the minimum feature size that can be printed (see the Rayleigh equation in Chapter 1). In traditional lithography the DOF degrades as the square of NA (**Eqn. 4.1**).

$$DOF = \frac{n\lambda}{2(NA)^2} \qquad \textbf{Eqn. 4.1}$$

In traditional lithography the n term is ignored because the refractive index of air is 1. Immersion lithography improves the DOF by n times compared to traditional lithography. While this improvement in DOF does not improve the resolution, or minimum feature

size that be achieved, it does off set the reduction in DOF when higher NA systems are used.

Water has been selected for the immersion fluid for 193 nm photolithography because of its compatibility with current manufacturing processes, its low absorbance (α_{193} = 0.036 cm^{-1} base 10) (Switkes 2002), and its high refractive index (n_{193} = 1.437) (Burnett 2003).

One of the major concerns with immersion lithography was the potential for resist components leaching out of the photoresist film into the immersion fluid. The extracted components can either contaminate the optics of the stepper or become deposited on the wafer's surface leading to fabrication and/or device performance problems. The components of concern were the photoacid generators (PAGs) and base quenchers (Switkes 2003). A method was needed to detect and quantify minute amounts of these components present in the immersion fluid. It was decided that liquid scintillation counting (LSC) would be a useful technique for both establishing the presence and quantity of leached components in the immersion fluid, after contact with the photoresist film (Lesuer 2004, Taylor 2004).

Synthesis of ^{14}C-Labeled Photoresist Components

^{14}C radio labeled versions of a PAG and base quencher were used in place of the non-radioactive photoresist components. The ^{14}C-labeled PAG and base, triphenyl

sulfonium nonafluoro-1-butanesulfonic acid (TPSNf) and tripentyl amine (TPA), were synthesized as shown in **Figure 4.1**.

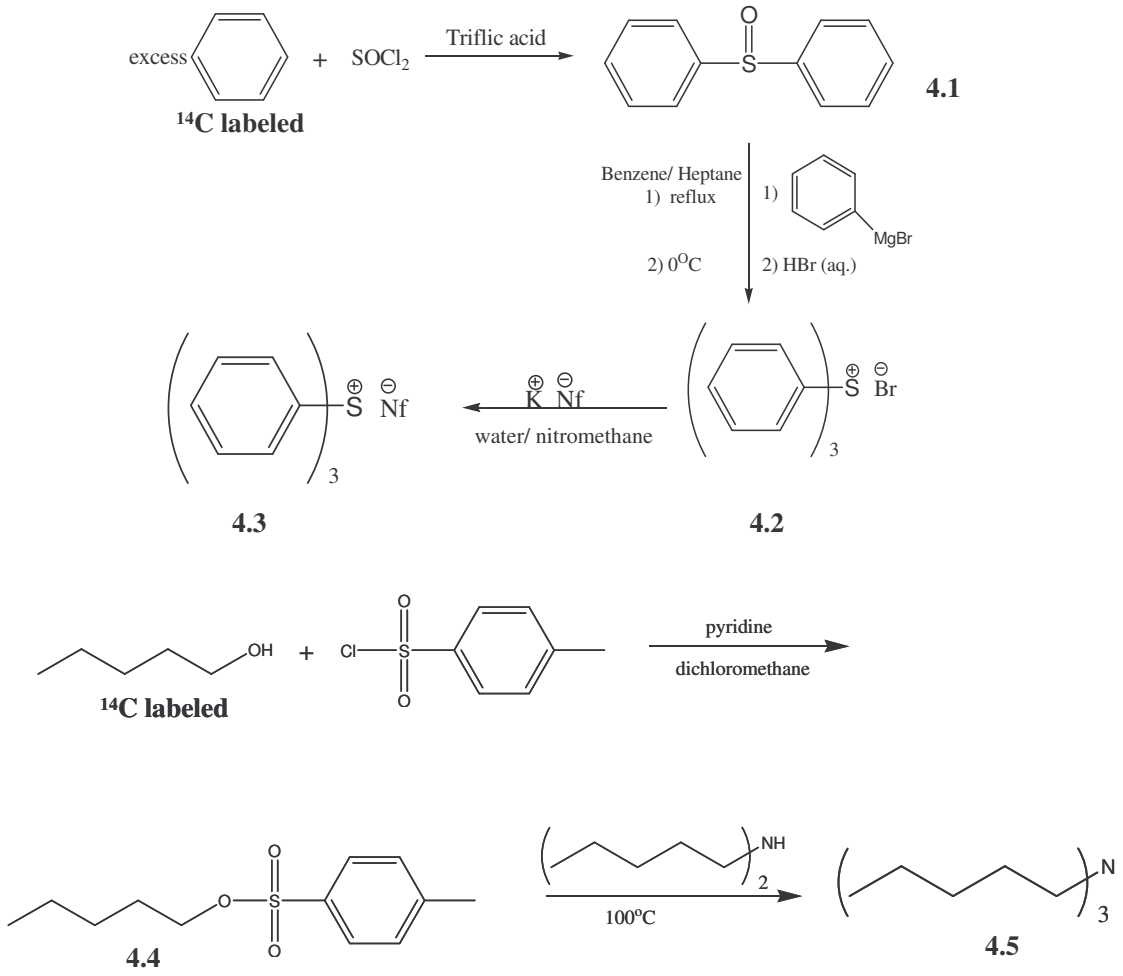

Figure 4.1: Synthesis of 14C labeled TPSNf and 14C labeled tripentyl amine.

The ^{14}C-labeled TPSNf was prepared using methods from the literature; first by reacting ^{14}C-labeled benzene with thionyl chloride in the presence of triflic acid to give the ^{14}C-labeled diphenyl sulfoxide (**4.1**) (Olah 1999). The diphenyl sulfoxide was then

reacted with a 5 molar excess of phenyl magnesium bromide in a 150 mL of a 2:1 refluxing heptane:benzene solution. After the addition of a 25% hydrogen bromide solution the triphenyl sulfonium bromide (**4.2**) (TPSBr) was isolated. Metathesis of TPSBr with potassium perfluoro-1-butanesulfonate in a 50:50 water:nitromethane mixture yielded the ^{14}C TPSNf (**4.3**) (Patterson 2000). The specific activity of the TPSNf was 8.60 ± 0.02 μCi/g. The ^{14}C-labeled TPA was synthesized starting with the tosylation of ^{14}C-labeled 1-petanol (**4.4**). The tosylate was then reacted with a four molar excess of dipentyl amine at 100ºC. The unreacted dipentyl amine was removed by vacuum distillation. The ^{14}C-labeled tripentyl amine (**4.5**) was then isolated by vacuum distillation. GC analysis shows the tripentyl amine to be 99% pure. The specific activity of the TPSNf was 49.8 ± 0.1 μCi/g

Resist Formulation and Film Preparation

Three commercially available 193 nm photoresist polymers were provided by Tokyo Ohka Kogya (TOK) Co. (polymers **A** and **B**) and AZ Electronic Materials (polymer **C**). The resists were formulated with a 6 wt% total solids concentration, a PAG loading of 5 wt% relative to the polymer, and a base loading of 0.3 wt% relative to the polymer, for a total mass of 20 g. Two samples of each resist were made one with ^{14}C-TPSNf and the other with ^{14}C-TPA. Resist films were cast onto 2 in silicon wafers. The films were then subjected to a post application bake for 90 s at 115 ºC, resulting in a film thickness of approximately 150 nm.

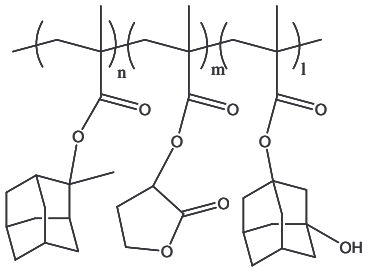

Polymer A

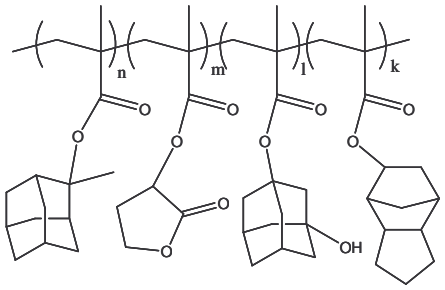

Polymer B

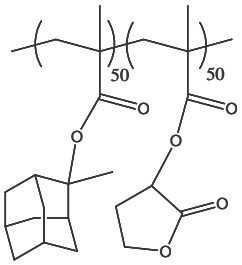

Polymer C

Extraction Experiments

Silicon wafers coated with the provided photoresists, containing radio labeled components, were placed into a 2 in glass Petri dish lid and covered with a 7 mL puddle of deionized (DI) water, for contact times ranging from 30 s to 30 min. The water was then transferred to a scintillation vial containing 12.5 mL Scintiverse BD scintillation cocktail (Fisher Scientific Co. Hampton, NH) and decay events were counted over 20 min using a Beckman 1801 liquid scintillation counter for the RCS and PAG samples. A Beckman LS 6500 counter was used to count the base samples for four to five hours. The scintillation counter also measured the extent to which the signal from the decay events was quenched by components in the vials.

A scintillation cocktail sample containing 7 mL of DI water was also counted to determine the level of background radiation present. To measure the amounts of radio

labeled components remaining in the films after immersion, the film was dissolved in 5 mL of unlabeled casting solvent. The wafer and Petri dish were rinsed two times with 5 mL and once with 4.5 mL of casting solvent to complete transfer of the sample into a scintillation vial for counting as described above.

The PAG extraction experiment on polymer A was repeated twice with slight variations. First, a 248 nm excimer laser was used to flood expose the resist films immediately after immersion. In the second repetition, a 30 sec pre-rinse immersion was performed before immersing four films from 30 sec to 5 min. The pre-rinse on polymer A was also performed for the base extraction. Thickness dependence on PAG and base leaching was measured using films of polymer B with thickness ranging from approximately 140 – 50 nm that were immersed for 30 s. A custom-built polycarbonate immersion cell based on a previously published design was used to improve time resolution to 10 s (Dammel 2004). A 4 mL aliquot of DI water was injected into the 2 mm high space in the cell over films of polymer C and was allowed to sit for a specified time before being collected with a 10 mL syringe.

Liquid scintillation counting was used to measure the number of radioactive decay events from ^{14}C-labeled photoresist components that leached into the immersion water (Howard 1976). The mass, in grams, of labeled material in a sample was determined using **Eqn. 5.2**.

$$Mass = \left(\frac{CPM - CPM_b}{Efficiency} \right) \left(\frac{1\mu Ci}{2.22 \times 10^6 DPM} \right) \Big/ SA \qquad \textbf{Eqn. 5.2}$$

CPM is the counting rate per minute of decay events, CPM_b is the level of background radiation, *Efficiency* is determined from the amount of quenching measured by the LSC instrumentation and the specific activity, *SA,* is given in μCi/g (Horrocks 1974) (Horrocks 1976).A detection limit for each was determined by **Eqn. 5.3**.

$$Mass_{\min} > \left(\frac{2\sqrt{CPM_b \times t}}{t} \right) \left(\frac{1\mu Ci}{2.22 \times 10^6 DPM} \right) \Big/ SA \qquad \textbf{Eqn. 5.3}$$

where *t* is the total time in minutes that the background level was counted and the first term on the right hand side is the 95% error limit of the CPM_b measurement (Howard 1976).

The results of the ^{14}C-PAG extraction experiments from unexposed films of all three resists showed a significant signal in each of the immersion water samples. **Figure 4.2** shows that after only 30 s immersion, a statistically significant amount of ^{14}C-TPSNf was detected. The amount of TPSNf extracted from each resist then remained essentially constant after 30 s, for increasing immersion times up to 30 min.

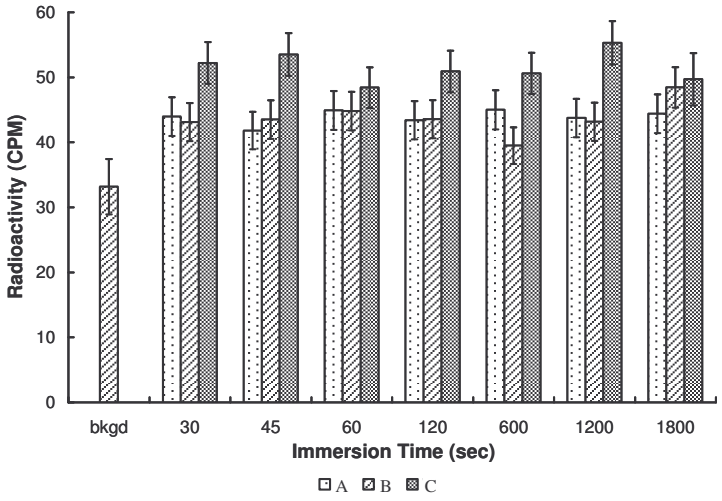

Figure 4.2: Radioactivity in CPM from LSC measurements of immersion water containing extracted ^{14}C-PAG vs. immersion time.

Figure 4.3 shows leaching from polymer **C** occurring primarily in the first 10 s of immersion. For a counting efficiency of 91%, the amounts of TPSNf extracted from films of polymers A and B, averaged over immersion time, was determined to be 30 ng/cm^2. Under the same conditions, 52 ng/cm^2 of TPSNf leached from polymer C. Detection limits for the PAG extraction experiments were determined from **Eqn. 5.3** to be 7 ng/cm^2.

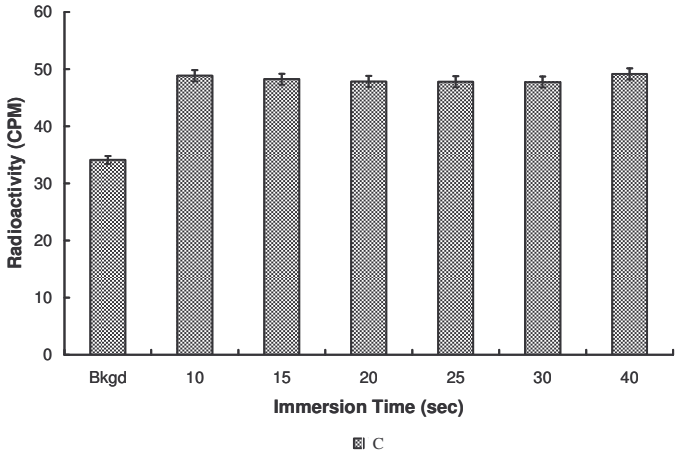

Figure 4.3: Radioactivity in CPM from LSC measurements of ^{14}C-PAG extracted from exposed and unexposed films of polymer A in immersion water vs. immersion time.

Figure 4.4 compares leaching of PAG and generated photoacid from unexposed and exposed samples of polymer A, with 5% TPSNf loading, respectively, as determined by LSC. No statistically significant difference between the amount of TPSNf extracted from the exposed resist, and that extracted from the unexposed samples, was observed using LSC. Several films of polymer A were also subjected to a 30 s pre-rinse before immersion.

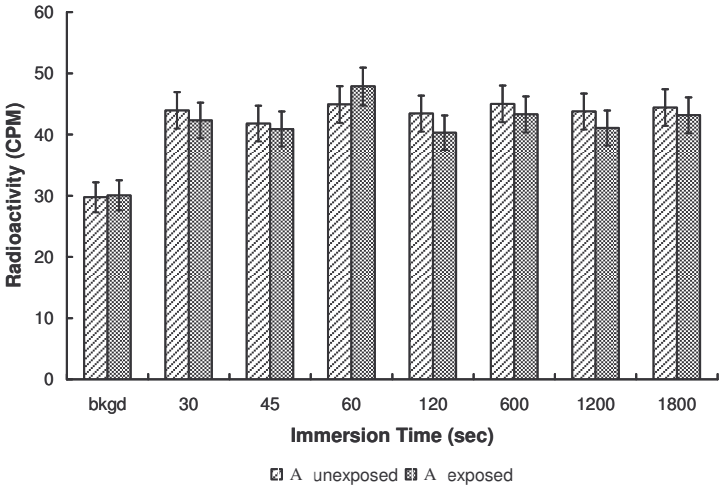

Figure 4.4: Radioactivity in CPM from LSC measurements of ^{14}C-PAG extracted from exposed and unexposed films of polymer A in immersion water vs. immersion time.

Figure 4.5 shows that the LSC measurements of the pre-rinse water showed radioactivity levels comparable to those initially reported for the PAG extraction experiments, but the activity level of the immersion water was no greater than background. This shows that essentially all the TPSNf that is extracted from a photoresist film is removed within the first 30 s of immersion.

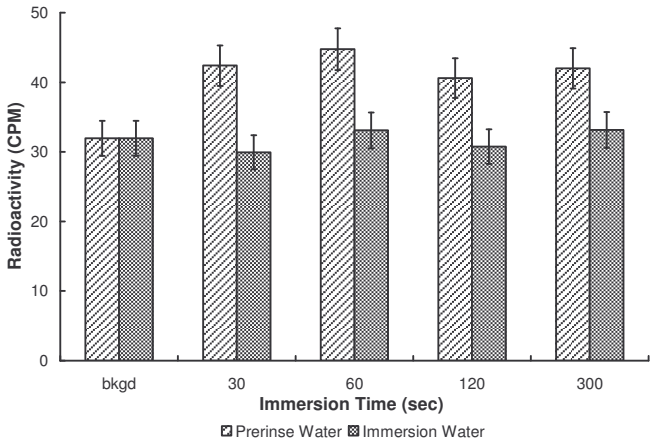

Figure 4.5: Radioactivity in CPM from LSC measurements of ^{14}C-PAG extracted from films of polymer A in 30 s pre-rinse water and immersion water vs. immersion time.

Figure 4.6 shows the thickness dependence of TPSNf extraction from films of polymer B. The radioactivity levels in the immersion water stay constant with decreasing film thickness, indicating that TPSNf is only being extracted from the uppermost surface of the film.

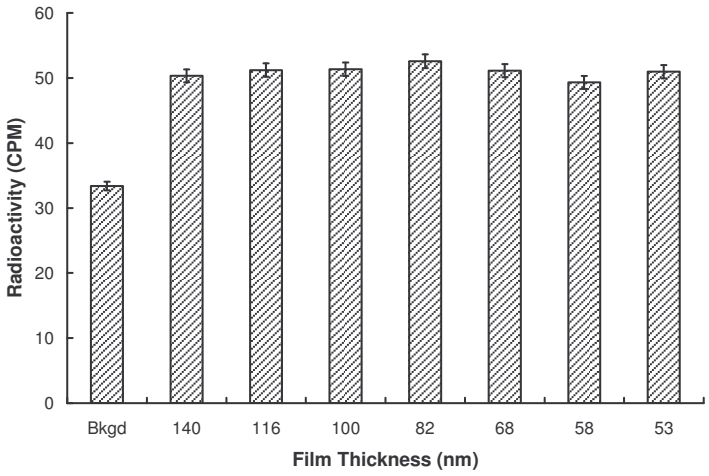

Figure 4.6: Radioactivity in CPM from LSC measurements of ^{14}C-PAG extracted from films of polymer B over decrease thickness during 30 s immersion.

The results of the ^{14}C-base extraction experiments are summarized in **Figure 4.6**. The radioactivity level in the immersion water shows that after 30 s of immersion a small, but detectable, amount of base was extracted from each resist. The level did not increase with immersion time, again indicating that the extraction is complete within the first 30 s. The amount extracted, with a counting efficiency of 96% and averaged over immersion time, was 0.04 μg or 2 ng/cm^2 of ^{14}C-TPA from each resist. Sub-30 s measurements showed no detectable signal from labeled base in the immersion water until 25 s of immersion time.

Figure 4.7 shows that LSC measurements of prerinse and immersion water from films of polymer A had similar levels of radioactivity from extracted base. The level again did not increase with immersion time and was consistent with those shown in **Figure 4.6**.

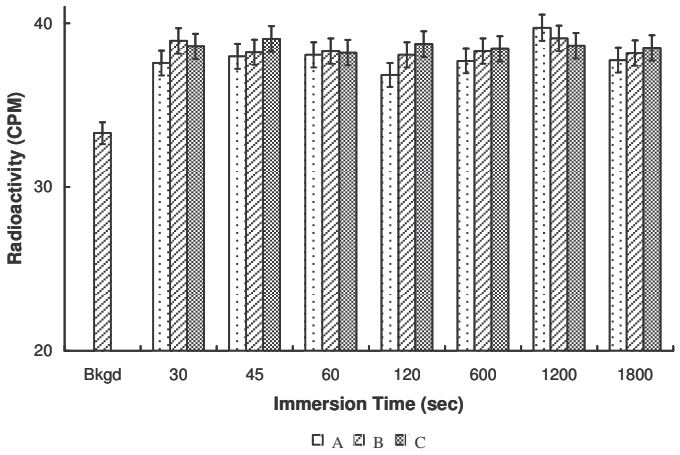

Figure 4.7: Radioactivity in CPM from LSC measurements of immersion water containing extracted ^{14}C-tripentylamine vs. immersion time.

Figure 4.7 suggests that base leaches from the entire resist film, not just the surface, and reaches an equilibrium with the water within 30 s. This is supported by the thickness dependence measurements. As the thickness of the polymer B films decreased, the radioactivity level in the immersion water increased, **Figure 4.8**, indicating that an increasing mass of TPA was extracted, as shown in **Figure 4.9**.

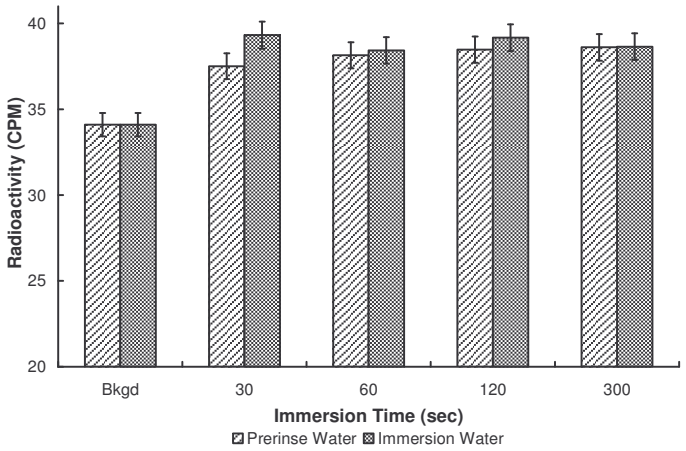

Figure 4.8: Radioactivity in CPM from LSC measurements of ^{14}C-tripentylamine extracted from films of polymer A in 30 s pre-rinse water and immersion water vs. immersion time.

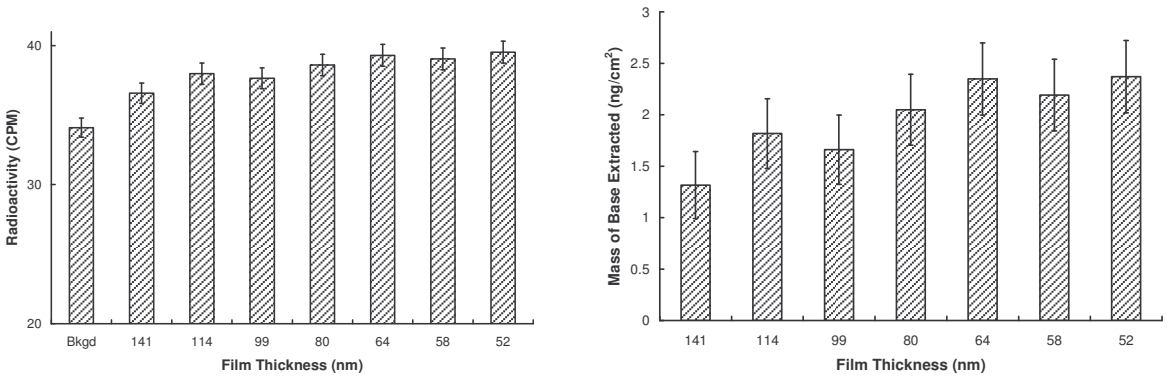

Figure 4.9: (a) Radioactivity in CPM from LSC measurements of ^{14}C-tripentylamine extracted from films of polymer B vs. film thickness during 30 s immersion. (b) Mass per unit surface area of extracted base vs. film thickness.

To our surprise, the thinner films allowed more base to diffuse into the water than the thicker films. This is contrary to bulk film properties. Typically more material will defuse out of a thicker film until at some thickness the amount of material diffusing out becomes constant. The mechanism for the PAG and base leaching appear to be very different

Experimental

Vacuum UV Spectroscopy

Gas-phase VUV measurements were made on an Acton CAMS-507 spectrophotometer fitted with a custom-made gas cell attachment. The details of the cell design and implementation are the subject of a separate paper (Brodsky 2000). VUV spectra of polymer films were calculated from measurements made with a J.A. Woollam VU301 variable angle spectroscopic ellipsometer. The films were cast on bare silica from solutions in propylene glycol monomethyl ether acetate (PGMEA) and baked at 110 ºC for at least 90 seconds prior to analysis. All absorbance data reported are in base 10.

Poly(2-(3,3,3-trifluoro-2-trifuoromethyl-2-hydroxypropyl)bicyclo[2.2.1]hept-5-ene)-co-2-trifluoromethyl-*tert* -butyl bicylco[2.2.1]hept-5-ene-2-carboxylate) (2.1).

To a solution of 2-trifluoromethyl-*tert*-butyl bicylco[2.2.1]hept-5-ene-2-carboxylate (1.230 g, 4.7 mmol) and di-*tert*-butyl peroxide (1.837g, 12.56 mmol), 3.000 g (11 mmol) of 2-(3,3,3-trifluoro-2-trifuoromethyl-2-hydroxypropyl)bicyclo[2.2.1]hept-5-ene was added. Three freeze-pump-thaw cycles were performed to deoxygenate the reaction mixture followed by backfilling with N_2. The reaction was heated to 135°C for 23 hours. The reaction mixture was diluted with 10 mL of THF and added slowly to 800 mL of rapidly stirred hexanes. The precipitate was isolated by filtration, redissolved in 5 mL of THF and added to rapidly stirred hexanes. The precipitate was isolated by filtration and dried under vacuum to give 1.134 g (27% yield). TGA analysis show the polymer is 15%

NBTBECF3. ^{1}H NMR ($CDCl_3$) δ 1.5 (s, 9H). ^{19}F NMR ($CDCl_3$) δ –66, -76. GPC (polystyrene standard) M_n 800/ M_w 1,600.

Poly(2-(3,3,3-trifluoro-2-trifuoromethyl-2-hydroxypropyl)bicyclo[2.2.1]hept-5-ene) (2.2).

To a 100 mL flask 2-(3,3,3-trifluoro-2-trifuoromethyl-2-hydroxypropyl)bicyclo[2.2.1]hept-5-ene (10.00 g, 36.5 mmol), 4.266 g (29.2 mmol) of di-*tert* -butyl peroxide was added. Three freeze-pump-thaw cycles were performed to deoxygenate the reaction mixture. The reaction was heated to 135°^{00}C for 48 hours. The reaction mixture was diluted with 15 mL of THF and added slowly to 1200 mL of rapidly stirred hexanes. The precipitate was isolated by suction filtration, redissolved in 10 mL of THF and added to rapidly stirred hexanes. The precipitate was isolated and dried to give 4.709 g (47% yield). ^{1}H NMR (d-DMSO) δ 7.6 (s, 1H), 3-0.4 (m, 13 H), (s, 9H). GPC (polystyrene standard) M_n 1,790/ M_w 3,020.

Poly(maleic anhydride-co-2-trifluoromethyl-*tert* -butyl bicylco[2.2.1]hept-5-ene-2-carboxylate) (2.3).

To a 100 mL round bottom flask with Teflon coated stir bar was added *tert* -butyl bicylco[2.2.1]hept-5-ene-2-carboxylate (4.196 g, 16.0 mmol), maleic anhydride (1.569 g, 16.0 mmol) and V601 (0.330 g, 0.16 mmol). Three freeze-pump-thaw cycles were

performed to deoxygenate the reaction mixture followed by backfilling with N_2. The reaction was heated overnight at 75°C. The resulting viscous mixture was diluted with 5 mL of THF and precipitated into 700 mL of rapidly stirred hexanes**.** The precipitate was isolated by filtration and dried under vacuum to give 2.310 g (40% yield). TGA analysis show the polymer is 35.4% NBTBECF3. ^{1}H NMR ($CDCl_3$) δ 1.5 (s, 9H). GPC (polystyrene standard) M_n 620/ M_w 1,800.

Poly(difluoromaleic anhydride-co-bicylco[2.2.1]hept-2-ene) (2.4).

To a solution of bicylco[2.2.1]hept-2-ene (1.449 g, 7.4 mmol) and V601 (0.3073 g, 1.5 mmol), 1.000 g (7.4 mmol) of difluoromaleic anhydride was added. The reaction mixture was sparged with nitrogen to deoxygenate the reaction mixture. The reaction was heated to $75^{0\circ0}$C for 12 hours. The reaction mixture was diluted with 1 mL of dichloromenthane and added slowly to 400 mL of rapidly stirred hexanes. The precipitate was isolated by suction filtration, redissolved in 1 mL of dichloromethane and added to rapidly stirred hexanes. The precipitate was isolated and dried to give 0.9774 g (40% yield). The GPC trace (M_n 120/ M_w 260) showed that the anhydride had openned up. The precipitate was dissolve in 20 mL of 4/1 benzene/methanol solution. The reaction was stirred for 1 hour before 1 mL of (trimethylsilyl)diazomethane was added dropwise. The reaction was stirred overnight. The benzene and methanol were removed using rotatory evaporation. The resulting powder was dried. ^{1}H NMR ($CDCl_3$) d 3.8 (s, 3H), 1.5 (s, 9H). GPC (polystyrene standard) M_n 320/ M_w 790.

Poly(trifluoromethyl maleic anhydride-co-bicyclo[2.2.1.]hept-2-ene) (2.5).

To a 10 mL round bottom flask was added 0.416 g (4.4 mmol) of bicylco[2.2.1]hept-2-ene, 0.700 g (4.4 mmol) of triflouromethyl maleic anhydride, 0.200 g AIBN, and 1 mL of 1,4-dioxane. Three feeze-pump-thaw cycles were performed. The reaction was heated to 75°C for 15 hours. The reaction was cooled to room temperature and precipitated into hexanes. Yellow solid was then dried overnight in a vacuum oven at 50°C to yield 0.14 g (12.6% yield). ^{19}F NMR ($CDCl_3$) δ –62, -63, -64, -66, -67. GPC (polystyrene) M_n 1,360/M_w 2,530.

Poly(3,3,3-trifluoropropene-co-bicyclo[2.2.1.]hept-2-ene) (2.6).

To a 22 mL stainless steel high pressure vessel was added 2.000 g (20.2 mmol) of bicylco[2.2.1]hept-2-ene, 0.400 g of *tert*-butyl peroxide and 5 mL of *tert*-butyl alcohol. The vessel was sealed and three freeze-pump-thaw cycles were performed. The 3,3,3-trifluoropropene (5 g, 52.1 mmol) was then condensed in the vessel by placing the vessel in liquid nitrogen. After an hour the vessel was warmed to room temperature before being heated to 155°C for 48 hours. The vessel was then cooled to room temperature, placed in liquid nitrogen and opened. The vessel contents were warmed to room temperature and allowed to degas. The reaction solution was then precipitated into methanol. The white polymer was dried in a vacuum oven over night at 50°C and 0.547 g (14% yield) was

obtained.^{19}F NMR shows two broad peaks around -67 and -69 ppm. GPC (polystyrene standard) M_n 4,200/M_w 4,880.

Poly(3,3,3-trifluoropropene-co-*tert*-butyl bicylco[2.2.1]hept-5-ene-2-carboxylate) (2.7).

To a 22 mL Parr reactor was added *tert*-butyl bicylco[2.2.1]hept-5-ene-2-carboxylate (NBTBE) (2.000 g, 10.3 mmol) and *tert*-butyl peroxide (0.400 g, 2.7 mmol) in 2.5 mL of freon 1,1,3 and 2.5 mL of *tert*-butyl alcohol, after three freeze-pump-thaw cycles were performed to deoxygenate the reaction mixture, 5 g (52 mmol) of 3,3,3-trifluoropropene was added. The reaction was heated to 155^{0}C for 12 hours. The unreacted NBTBE and solvents were removed by vacuum distillation to give 3 g (43% yield) of a viscous yellow oil. ^{1}H NMR ($CDCl_3$) δ 3.0-0.5 (m), 1.5 (s, 9H). ^{19}F NMR ($CDCl_3$) δ –66, -70. GPC (polystyrene standard) M_n 1,170/ M_w 1,380.

Poly(hexafluorocyclobutene-co-*tert*-butyl bicylco[2.2.1]hept-5-ene-2-carboxylate) (2.8)

To a 22 mL Parr reactor was added *tert*-butyl bicylco[2.2.1]hept-5-ene-2-carboxylate (NBTBE) (2.000 g, 10.3 mmol) and di-*tert*-butyl peroxide (0.400 g, 2.7 mmol) in 2.5 mL of freon 1,1,3 and 2.5 mL of *tert*-butyl alcohol, 5 g (30.9 mmol) of hexafluorocyclobutene was added. Three freeze-pump-thaw cycles were performed to

deoxygenate the reaction mixture. The reaction was heated to 155^{0}C for 12 hours. The unreacted NBTBE and solvents were removed under vacuum. The remaining yellow oil was dissolved in 4 mL of dichloromethane and added slowly to 300 mL of rapidly stirred hexanes. The precipitate was isolated by suction filtration and dried to give 0.736 g (11% yield). TGA analysis show the polymer is 77% NBTBE. ^{1}H NMR ($CDCl_3$) δ 3.0-0.5 (m), 1.5 (s, 9H). ^{19}F NMR ($CDCl_3$) δ –62, -130 (d). GPC (polystyrene standard) M_n 740/ M_w 1,430.

Poly(methyl -2-trifluoromethyl acrylate-co-bicyclo[2.2.1.]hept-2-ene) (2.9).

To a 10 mL round bottom flask was added 0.616 g (6.49 mmol) of methyl trifluoroacrylate, 1.000 g (6.49 mmol) of bicyclo[2.2.1.]hept-2-ene, 0.126 g V601, and 1.5 mL of 1,4-dioxane. Three feeze-pump-thaw cycles were performed. The reaction was heated to 75°C for 15 hours. The reaction was cooled to room temperature and precipitated into methanol and isolated by filtration. The white polymer was dried in a vacuum oven over night at 50°C and 0.400 g (24.8% yield) was obtained. ^{1}H NMR ($CDCl_3$) δ 3.0-1.0 (m), 3.9 (s, 3H). ^{19}F NMR ($CDCl_3$) δ –62, -64, -68. GPC (polystyrene standard) M_n 4,750/M_w 6,570.

Poly(methyl -2-trifluoromethyl acrylate-co-*tert*-butyl bicylco[2.2.1]hept-5-ene-2-carboxylate) (2.10).

To a 50 mL round bottom flask was added *tert*-butyl bicylco[2.2.1]hept-5-ene-2-carboxylate (NBTBE) (2.0000 g,10.3 mmol) of, 1.5863 g (10.3 mmol) of methyl 2-trifluoromethylacrylate, 0.35860 g (10 wt %) of V601 was added 1 mL of 1,4-dioxane in a 10 mL round bottom flask. The reaction was degassed through three freeze-thaw cycles. The reaction was then heated to 75°C with stirring for 17 hours. After cooling to room temperature the solution was diluted with 5 mL of THF and precipitated into hexane. The white polymer was allowed to dry before being redissolved in THF and reprecipitated into hexanes. The powder was then dried overnight in a vacuum oven at 50°C and 1.8100 g was obtained (50% yield). ^{1}H NMR ($CDCl_3$) δ 3.0-1.0 (m), 3.9 (s, 3H), 1.4 (s, 9H). ^{19}F NMR ($CDCl_3$) δ –62, -64, -68. GPC (polystyrene standard) M_n 1,950/M_w 2,490. TGA 40% NBTBE.

Poly(methyl trifluoroacrylate-co- bicyclo[2.2.1.]hept-2-ene) (2.11).

To a 10 mL round bottom flask was added 0.616 g (6.49 mmol) of methyl trifluoroacrylate, 1.000 g (6.49 mmol) of bicyclo[2.2.1.]hept-2-ene, 0.126 g V601, and 1.5 mL of 1,4-dioxane. Three feeze-pump-thaw cycles were performed. The reaction was heated to 75°C for 15 hours. The reaction was cooled to room temperature and precipitated into methanol. The white polymer was dried in a vacuum oven over night at 50°C and 0.400 g (24.8% yield) was obtained. ^{1}H NMR ($CDCl_3$) δ 3.0-1.0 (m), 3.8 (s,

3H). ^{19}F NMR ($CDCl_3$) δ –96, -111, -118. GPC (polystyrene standard) M_n 4,750/M_w 6,570.

Poly(methyl trifluoroacrylate-co-*tert*-butyl bicylco[2.2.1]hept-5-ene-2-carboxylate) (2.12).

To a 10 mL round bottom flask was added 1.417 g (10.1 mmol) of methyl trifluoroacrylate, 1.960 g (10.1 mmol) of *tert*-butyl bicylco[2.2.1]hept-5-ene-2-carboxylate (NBTBE), 0.337 g V601, and 1.5 mL of 1,4-dioxane. Three feeze-pump-thaw cycles were performed. The reaction was heated to 75°C for 15 hours. The reaction was cooled to room temperature and precipitated into deionized water. The residue was dissolved in acetone and precipitated into deionized water again. The white polymer was dried in a vacuum oven over night at 50°C and 0.272g (8% yield) was obtained. ^{1}H NMR ($CDCl_3$) δ 3.0-1.0 (m), 3.8 (s, 3H) 1.5 (s, 9H). ^{19}F NMR ($CDCl_3$) δ –96, -111, -118. GPC (polystyrene standard) M_n 1,430/M_w 2,360. TGA 46% NBTBE.

Poly(methyl-2-cyano acrylate-co-bicyclo[2.2.1.]hept-2-ene) (2.14).

In a glove bag under nitrogen was added 1.000 g (10.5 mmol) of bicyclo[2.2.1.]hept-2-ene, 1.170 g (10.5 mmol) of methyl-2-cyano acrylate, 2 mL of deoxygenated 1,4-dioxane and 0.217 g V601 to a 10 mL round bottom flask. Three feeze-pump-thaw cycles were performed. The reaction was heated to 75°C for 45 minutes before the reaction solidified.

The reaction was cooled to room temperature, dissolved in acetone and precipitated into methanol. The white solid was then dried overnight in a vacuum oven at 50°C and 1.610 g (74% yield) was isolated. GPC (polystyrene standard) M_n 8,340/M_w 37,800.

Poly(methyl-2-cyano acrylate-co-*tert*-butyl bicylco[2.2.1]hept-5-ene-2-carboxylate) (2.15).

In a glove bag under nitrogen was added 1.000 g (5.15 mmol) of *tert*-butyl bicylco[2.2.1]hept-5-ene-2-carboxylate (NBTBE), 0.571 g (5.15 mmol) of methyl-2-cyano acrylate, 1.5 mL of deoxygenated 1,4-dioxane and 0.157 g V601 to a 10 mL round bottom flask. Three feeze-pump-thaw cycles were performed. The reaction was heated to 75°C and stirred for 9 hours. The reaction was cooled to room temperature, dissolved in acetone and precipitated into methanol. The white solid was then dried overnight in a vacuum oven at 50°C and 0.9647 g (61.5% yield) was isolated. ^{1}H NMR ($CDCl_3$) δ 3.3-0.8 (m), 3.8 (s, 3H), 1.4 (s, 9H). GPC (polystyrene standard) M_n 12,300/M_w 23,700. TGA 32% NBTBE.

Poly(methyl-2-cyano acrylate-co-2-trifluoromethyl *tert*-butyl bicylco[2.2.1]hept-5-ene-2-carboxylate) (2.16).

In a glove bag under nitrogen was added 1.181 g (4.5 mmol) of 2-trifluoromethyl *tert*-butyl bicylco[2.2.1]hept-5-ene-2-carboxylate (NBTBECF3), 0.500 g (4.5 mmol) of

methyl-2-cyano acrylate, 1.5 mL of deoxygenated 1,4-dioxane and 0.168 g V601 to a 10 mL round bottom flask. Three feeze-pump-thaw cycles were performed. The reaction was heated to 75°C for 20 hours. The reaction was cooled to room temperature, dissolved in acetone and precipitated into methanol. The white solid was then dried overnight in a vacuum oven at 50°C and 0.335 g (20% yield) was isolated. The polymer was bimodal. ^{1}H NMR ($CDCl_3$) δ 3.3-0.8 (m), 3.8 (s, 3H), 1.4 (s, 9H). GPC (polystyrene standard) M_n 9,970/M_w 15,800 and M_n 531,100/M_w 1,268,000. TGA 21% NBTBECF3.

Poly(acrylonitrile-co-bicyclo[2.2.1.]hept-2-ene) (2.17)

To a 10 mL round bottom flask was added 2.000 g (21 mmol) of bicyclo[2.2.1.]hept-2-ene, 1.118 g (21 mmol) of acrylonitrile, 3 mL of 1,4-dioxane and 0.312 g V601. Three feeze-pump-thaw cycles were performed. The reaction was heated to 75°C for 15 hours. The reaction was cooled to room temperature and precipitated into hexanes twice. The yellow solid was then dried overnight in a vacuum oven at 50°C and 1.25 g (40% yield) was isolated. IR (KBr, cm-1) 3238. ^{1}H NMR ($CDCl_3$) δ 3.3-1.0 (m). GPC (polystyrene standard) M_n 2,330/M_w 3,590.

Poly(acrylonitrile-co-*tert*-butyl bicylco[2.2.1]hept-5-ene-2-carboxylate) (2.18).

To a 10 mL round bottom flask was added 1.830 g (9.4 mmol) of bicylco[2.2.1]hept-5-ene-2-carboxylate (NBTBE), 0.500 g (9.4 mmol) of acrylonitrile, 2 mL of 1,4-dioxane

and 0.230 g V601. Three freeze-pump-thaw cycles were performed. The reaction was heated to 75°C for 20 hours. The reaction was cooled to room temperature and precipitated into hexanes twice. Yellow solid was then dried overnight in a vacuum oven at 50°C and 0.630 g (27% yield) was isolated. IR (KBr, cm-1) 3238. ^{1}H NMR ($CDCl_3$) δ 3.3-1.0 (m), 1.4 (s, 9H). GPC (polystyrene standard) M_n 1,500/M_w 2,180. TGA 32% NBTBE.

Poly(acrylonitrile-co-2-trifluoromethyl *tert*-butyl bicylco[2.2.1]hept-5-ene-2-carboxylate) (2.19).

To a 10 mL round bottom flask was added 5.840 g (22.3mmol) of 2-trifluoromethyl *tert*-butyl bicylco[2.2.1]hept-5-ene-2-carboxylate (NBTBECF3), 1.200 g (22.3 mmol) of acrylonitrile, 5 mL of 1,4-dioxane and 0.702 g V601. Three freeze-pump-thaw cycles were performed. The reaction was heated to 75°C for 13 hours. The reaction was cooled to room temperature and precipitated into hexanes. The polymer was then dissovled in acetone and precipitated in isopropyl alcohol. Yellow solid was then dried overnight in a vacuum oven at 50°C and 0.937g (13% yield) was isolated. ^{1}H NMR ($CDCl_3$) δ 3.3-1.0 (m), 1.4 (s, 9H). GPC (polystyrene standard) M_n 1,620/M_w 2,430. TGA 14.5% NBTBECF3.

General procedure for carbon monoxide copolymerization

To a 300 mL Parr bomb were added monomer(s) (15 mmol), palladium (II) acetate (3.4 mg, 0.015 mmol), copper (II) tosylate (0.061 g, 0.15 mmol), 2,2'-bipyridine (0.070 g, 0.45 mmol), benzoquinone (0.324 g, 3.00 mmol), methanol (15 mL), and carbon monoxide (440 psi). The bomb was stirred at 80 to 90 °C overnight. Then, the remaining carbon monoxide was vented. A red solution was obtained. Ether (100 mL) was added to the solution (sometimes small amount of THF was used to transfer the material) and the solution was washed with 5% Na_2CO_3 aqueous solution (100 mL x 6) and brine (100 mL x 2). Charcoal (ca. 2 g) was added to the organics and stirred for ca. 15 min. Then, $MgSO_4$ was added. The resulting solution was filtered through filter paper, condensed to ca. 20 mL, filtered through 0.2µm PTFE membrane, evaporated, and dried *in vacuo* overnight at 50 °C to yield a solid.

Poly(carbon monoxide-co- 2-(3,3,3-trifluoro-2-trifuoromethyl-2-hydroxypropyl)bicyclo[2.2.1]hept-5-ene) (3.1).

This polymer was made by following the above general procedure using NBHFA (4.00g, 14.6 mmol). A pale yellow solid was obtained (3.76 g, 85 %). ^{1}H NMR (300 MHz, DMSO, δ): 7.7 (br m, OH), 3.6-3.4 (br m), 3.4-0.4 (br m). ^{13}C NMR (75.5 MHz, CD_2Cl_2 with $Cr(acac)_3$, δ): 210 (br, ketone), 180-170 (br, lactone and ester), 150 (br, olefin), 123.4 (q, J = 289 Hz, CF_3), 118 (br, spiroketal), 108 (br, olefin), 76.8 (br s, $C(CF_3)_2$), 60-

30 (br). ^{19}F NMR (282 MHz, CD_2Cl_2, δ): -76 (br m), -77 (br m). FTIR (cm^{-1}): 3416 (m), 2970 (m), 2882 (w), 1752 (m), 1712 (m), 1627 (w), 1456 (m), 1285 (s), 1214 (vs), 1143 (s). GPC: Mw = 1940, Mn = 1360, Pd = 1.43. MALDI-MS: 1209, 1267, 1510, 1569, 1870, 2171, 2473, 2775, 3076, 3377, 3679, 3980, 4282.

Poly(carbon monoxide-*co*-2-trifluoromethyl *tert*-butyl bicylco[2.2.1]hept-5-ene-2-carboxylate) (3.2).

Protection ratio 100% (by TGA). GPC: Mw = 1590, Mn = 1100, Pd = 1.45. IR (cm^{-1}): 2982 (m), 1795 (w), 1739 (s), 1372 (m), 1295 (s), 1171 (s).

2,2,3,3,4,4,5,5-Octafluorohexamethylene dibicyclo[2.2.1]hept-5-ene-2-carboxylate (2-2) (3.3).

To a 50 mL flask containing a stir bar and equipped with a reflux condenser was added 2,2,3,3,4,4,5,5-octafluorohexamethylene diacrylate (2.00 g, 5.40 mmol), tetrahydrofuran (2.1 g), and freshly cracked cyclopentadiene (0.88 g, 13.3 mmol). The mixture was refluxed for 1 h. The resulting solution was evaporated and purified by column chromatography on silica gel using n-hexanes, then ethyl acetate / hexane (5 / 95) as eluents to give 2.3 g of colorless liquid (4.6 mmol, 85%). The product contains a mixture of the *endo* and *exo* configuration of bicyclo[2.2.1]heptene system. Assignment of the

major isomer is indicated as α and minor as β. ^{1}H NMR (500 MHz, $CDCl_3$, δ): 6.18 (dd, *J* = 5.7 and 3.1 Hz, H-5α, 2α H), 6.13 (dd, *J* = 5.6 and 3.0 Hz, olefinic β, 2β H), 6.09 (dd, *J* = 5.6 and 3.0 Hz, olefinic β, 2β H), 5.89 (dd, *J* = 5.8 and 2.8 Hz, H-6α, 2α H), 4.57 (q, *J* = 13 Hz, OC*H*$\alpha_2$$CF_2$ and OC*H*$\beta_2$$CF_2$, 2α H and 2β H), 4.43 (q, *J* = 13 Hz, OC*H*$\alpha_2$$CF_2$ and OC*H*$\beta_2$$CF_2$, 2α H and 2β H), 3.23 (br m, H-1α, 2α H), 3.06 (br m, H-1β or H-4β, 2β H), 3.01 (m, H-2α, 2α H), 2.90 (br m, H-4α and bridgehead-β, 2α H and 2β H), 2.29 (m, bridgehead-β, 2β H), 1.91 (m, H-3α and H-3β, 2α H and 2β H), 1.47 (br d, *J* = 8.6 Hz, H-7β, 2β H), 1.45-1.35 (m, H-3α, H-3β, H-7α, and H-7β, 4α H and 4β H), 1.27 (br d, *J* = 8.2 Hz, H-7α, 2α H). ^{13}C NMR (126 MHz, $CDCl_3$, δ): 174.70 (*C*β=O), 173.15 (*C*α=O), 138.23 (C-5β or C-6β), 138.09 (C-5α or C-6α), 135.49 (C-5β or C-6β), 132.02 (C-5α or C-6α), 114.64 (tt, *J* = 258 and 31 Hz, *C*$\alpha$$F_2$ and *C*$\beta$$F_2$), 111.12 (tt, *J* = 267 and 33 Hz, *C*$\alpha$$F_2$ and *C*$\beta$$F_2$), 59.55 (t, *J* = 26 Hz, O*C*$\beta$$H_2$), 59.43 (t, *J* = 27 Hz, O*C*$\alpha$$H_2$), 49.63 (C-7α), 46.58 (C-1β or C-4β), 46.30 (C-7β), 45.78 (C-1α), 43.00 (C-2α), 42.82 (C-2β), 42.50 (C-4α), 41.65 (C-1β or C-4β), 30.36 (C-3β), 29.12 (C-3α). ^{19}F NMR (282 MHz, $CDCl_3$, δ): -120.10 (m, CF_2, 4 F), -124.16 (m, CF_2, 4 F). HRMS-CI (m/z): $[M + H]^+$ calcd for $C_{22}H_{23}F_8O_4$, 503.1469; found, 503.1475.

Borane reduction of poly(carbon monoxide-co-3-(bicyclo[2.2.1]hept-5-ene-2-yl)-1,1,1-trifluoro-2-(trifluoromethyl) propan-2-ol).

To a 25 mL flask containing a stir bar were added poly(NBHFA-*co*-carbon monoxide) (TC2040, 0.72 g, 2.38 mmol as repeating unit) and tetrahydrofurane (3.5 mL). Borane-tetrahydrofurane complex (1 *M* solution, 2 mL) was added dropwise and the solution was stirred overnight. A pale yellow solution turned colorless. The resulting solution was poured into 50 mL diethyl ether, washed with water (50 mL x 2), dried over magnesium sulfate, filtered, evaporated, and dried *in vacuo* overnight at 150 °C. ^{1}H NMR (300 MHz, CD_2Cl_2, δ): 4-3.2 (br m), 3.2-0.4 (br m). ^{13}C NMR (75.5 MHz, CD_2Cl_2 with $Cr(acac)_3$, δ): 210 (br, ketone), 180-170 (br, lactone and ester), 150 (br, olefin), 123.4 (q, J = 289 Hz, CF_3), 118 (br, spiroketal), 108 (br, olefin), 76.8 (br s, $C(CF_3)_2$), 60-30 (br). ^{19}F NMR (282 MHz, CD_2Cl_2, δ): -76 (br m), -77 (br m). FTIR (cm^{-1}): 3429 (m), 2968 (m), 2882 (w), 1752 (w), 1716 (m), 1623 (w), 1456 (m), 1285 (s), 1217 (vs), 1144 (s).

***tert*-butyl carbonate protection of oly(carbon monoxide-co-3-(bicyclo[2.2.1]hept-5-ene-2-yl)-1,1,1-trifluoro-2-(trifluoromethyl) propan-2-ol) (3.5).**

To a 250 mL flask were added 3.1 (6 g, 22 mmol as a monomer), THF (80 mL), di-*tert*-butyl dicarbonate (6 g, 0.028 mol), and 4-(*N*,*N*-dimethylamino)pyridine (DMAP) (0.36 g, 3.0 mmol). The solution was stirred overnight at room temperature, then extracted with 5% NaOH aqueous solution. The resulting solution was evaporated and ether (100 mL)

was added. The organics were washed with 0.05*N* HCl (100 mL x 3) and brine (100 mL x 2), dried over $MgSO_4$, filtered, evaporated, and dried *in vacuo* overnight at 50 °C to yield 7.79 g of a pale yellow solid. Protection ratio 92.5% (by TGA). GPC: Mw = 2890, Mn = 1720, Pd = 1.68. IR (cm-1): 2983 (s), 2879 (m), 1774 (s), 1737 (m), 1374 (s), 1247 (s), 1133 (s).

1,4-di-*tert*-butoxycarbonyloxy tetrafluorohydroquinone (3.6).

To a 100 mL round bottom flask was added 1.000 g (5.49 mmol) of tetrafluorohydroquinone, 2.994 g (13.73 mmol) of di-*tert*-butyl dicarbonate, and 10 mL of dried (sodium/benzophenone) THF. The reaction was stirred for a few minutes before 0.134 g (1.10 mmol) of DMAP was added. Gas evolution was observed after a few minutes and lasted about five minutes. The reaction was stirred over night. The THF was removed by rotary evaporation. The yellowish solid was dissolve in chloroform and rinsed with: 1 M hydrochloric acid (2 X 30 mL), saturated sodium bicarbonate solution (2 X 30 mL) and saturated sodium chloride solution (1 X 30 mL). The organic layer was dried over sodium sulfate, filtered and evaporated off using rotary evaporation. The yellow solid was then dried using the vacuum of an oil pump to afford 1.360 g (65% yield). ^{1}H NMR (CDCl3) δ: 1.5 (s, 18 H).^{19}F NMR (CDCl3) δ: -154 (s, 4 F). ^{13}C NMR (CDCl3) δ: s, 149.1; d, 142.8,*J*= 15 Hz; t, 139.5, *J*= 39.8 Hz; s,127.5; s, 86.2; s, 27.4.

IR (KBr, cm^{-1}) 1780.

1,4-bis(ethoxymethoxy) tetrafluorobenzene (3.7).

To a solution of 1,4-tetrafluorohydroquinone (1.000 g, 5.5 mmol) in THF (15 mL) at 0^0C, 5 mL (12.6 mmol) of 2.5 M butyllithium in hexanes was added dropwise. The reaction warmed to room temperature and stirred for an hour. The reaction was then cooled to 0°C and 1.2 mL (1.246 g, 13.2 mmol) of chloromethyl ethyl ether in 10 mL of THF was added dropwise. The reaction warmed to room temperature and stirred for 24 hours. The reaction was poured into 100 mL of 1 M HCl. The aqueous layer was extracted with 3x40 mL of chloroform. The combined organic layers were extracted with 1x100 mL of deionized water, 3x30 mL of saturated bicarbonate solution, and 1x30 mL of saturated brine solution. The organic layer was dried over magnesiun sulfate and concentrated using rotatory evaporation to afford a yellow oil (1.614 g). The product was collected as a yellow oil (0.853 g, 52% yield). Bp.120^0C@ 5 Torr. GC_{rt}= 8.648. IR (KBr, cm^{-1}) 2986, 2934, 2904, 1511, 1408, 1388, 1285, 1183, 1152, 1122, 1009 917 871, 840. ^{1}H NMR ($CDCl_3$) δ: 5.1 (s, 4H), 3.8 (q, 4H), 1.2 (t, 6H). ^{13}C NMR ($CDCl_3$) δ: dm, 142.37; m,130.95; s, 97.843; s,65.47; s,14.75. ^{19}F NMR ($CDCl_3$) δ: s, –58.

1,3-bis(2- *tert*-butoxycarbonyloxy hexafluoroisopropyl) benzene (3.8).

To a solution of hydrogenated 1,3-HFAB (2.00 g, 4.8 mmol) in 20 mL of THF, 2.66 g (12.2 mmol) of di-*tert*-butyl dicarbonate was added. The reaction was stirred for a few minutes before 0.120 g (0.96 mmol) of DMAP was added. Gas evolution was observed after a few minutes and lasted about five minutes. The reaction was stirred over night.

The THF was removed by rotary evaporation to give a white solid. The white solid was dissolve in chloroform and rinsed with 1 M hydrochloric acid (2 X 30 mL), saturated sodium bicarbonate solution (2 X 30 mL) and saturated sodium chloride solution (1 X 30 mL). The organic layer was dried over sodium sulfate, filtered and the solvent removed using rotary evaporation. The product was recrystallized from hexanes and isolated by suction filtration. The white solid was then dried to give 2.065g (70% yield). ^{1}H NMR (CDCl3) δ: 3.1 (t, 2H); 2.1-1.8 (m, 6H); 1.7-1.3 (m, 20H). ^{13}C NMR ($CDCl_3$) δ: q, 123.2, *J*= 286.2; m, 77.7; s, 42.4; s, 35.8; s, 26.6; s, 26.3. IR (KBr, cm^{-1}) 1780.

1,4-bis(2- *tert*-butoxycarbonyloxy hexafluoroisopropyl) benzene (3.9).

To a 100 mL round bottom flask was added 2.000 g (4.8 mmol) of reduced 1,4-HFAB, 2.62 g (12 mmol) of di-*tert*-butyl dicarbonate, and 20 mL of dried (sodium/benzophenone) THF. The reaction was stirred for a few minutes before 0.117 g (0.96 mmol) of DMAP was added. Gas evolution was observed after a few minutes and lasted about five minutes. The reaction was stirred over night. The THF was removed by rotary evaporation. The white solid was dissolve in chloroform and rinsed with: 1 M hydrochloric acid (2 X 30 mL), saturated sodium bicarbonate solution (2 X 30 mL) and saturated sodium chloride solution (1 X 30 mL). The organic layer was dried over sodium sulfate, filtered and evaporated off using rotary evaporation. The white solid was then dried using the vacuum of an oil pump to afford 2.879 g (97% yield). ^{1}H NMR (CDCl3)

δ: 1.4 (s, 18 H); 1.6 (m, 4); 1.9 (m, 4H); 3.1 (s, 2H) ^{13}C NMR (CDCl3) δ: d, 149.0; q, 122.2,*J*= 288 Hz; m, 85.0; s,38.1; s, 32.8; q, 27.4; s, 21.5.

IR (KBr, cm^{-1}) 1780.

Bisphenol A di-*tert*-butyl carbonate(3.10)

To a solution of bisphenol A (1.00 g, 4.38 mmol) in 10 mL of THF, 2.40 g (11 mmol) of di-tert-butyl dicarbonate was added. The reaction was stirred for a few minutes before 0.054 g (0.44 mmol) of DMAP was added. Gas evolution was observed after a few minutes and lasted about five minutes. The reaction was stirred over night. The THF was removed by rotary evaporation to give an oil. The oil was dissolve in chloroform and rinsed with 1 M hydrochloric acid (2 X 30 mL), saturated sodium bicarbonate solution (2 X 30 mL) and saturated sodium chloride solution (1 X 30 mL). The organic layer was dried over sodium sulfate, filtered and the solvent removed using rotary evaporation. The product was recrystallized from hexanes and isolated by suction filtration. The white solid was then dried to give 2.065g (73% yield). ^{1}H NMR (d-acetone) δ: 7.3 (d, 4H); 7.1 (d, 4H); 1.7 (s, 6H), 1.5 (s, 18H). ^{13}C NMR (d-acetone) δ: s, 153; s, 150; s, 149; s, 128 s, 122; s, 83; s, 43; s, 31; s, 28.

Bisphenol A di-tetrahydro-pyran (3.11)

To a solution bisphenol A (2.00 g, 8.76 mmol) and 3,4-dihydro-2H-pyran (DHP) (2.213 g, 26.28 mmol) in 20 mL of dichloromethane, 0.440 g (1.75 mmol) of pyridinium *para*-

toluene sulfonate (PPTS) was added. The reaction stirred over night. The reaction was extracted with 50 mL of brine solution, 3 x 33 mL of 5 wt% NaOH solution, and 25 mL of deionized water. The organic layer was dried over magnesiun sulfate and concentrated using rotary evaporation to afford a white solid. The solid was recrystallized from isopropyl alcohol, isolated by suction filtration and dried to give 1.0249 g (29%, yield).^{1}H NMR (d-acetone) δ: 7.1 (d, 4H), 6.9 (d, 4H), 5.4 (t, 2H), 3.8 (m, 2H), 3.5 (m, 2H), 2.1-1.5 (m, 18H). ^{13}C NMR (d-acetone) δ: s, 156; s, 144; s, 128; s, 114; s, 97; s, 62; s, 42; m, 30; s, 26; s, 20.

1,3-Bis(2-hydroxyhexafluoroisopropyl)cyclohexane (3.12)

To a solution of 1,3-HFAB (8.00 g, 19.5 mmol) in 25 mL of isopropyl alcohol in a 300 mL high pressure vessel (bomb) under a nitrogen atmosphere, 1.0 g of 5% rhodium on carbon was added. The bomb was sealed and pressurized to 600 psi with hydrogen gas. The reaction was heated at 150°^{00}C for 24 hours. The rhodium on carbon was removed by filtration. The isopropyl alcohol was removed using rotatory evaporation. The product was collected as a clear oil. (7.75 g, 95% yield). Bp.100^{0}C@ 10 Torr. ^{1}H NMR ($CDCl_3$) δ: 3.1 (s, 2H), 2.5 (m, 2H), 2.4 (m, 2H), 2.0 (m, 4H), 1.7 (m, 2H), 1.5 (m, 2H). ^{13}C NMR ($CDCl_3$) δ: q, 123.2, *J*= 286.2; m, 77.7; s, 42.4; s, 35.8; s, 26.6; s, 26.3. ^{19}F NMR ($CDCl_3$) δ: s, -58.

1,4-Bis(2-hydroxyhexafluoroisopropyl)cyclohexane (3.13).

Under a nitrogen atmosphere, 1,4-bis(2-hydroxyhexafluoroisopropyl)benzene (15.0 g, 37.0 mmol), rhodium catalyst (5 wt% on carbon, 2.0 g), and isopropanol (30 mL) were added to a 300 mL Parr pressure reactor equipped with a stir bar. The reactor was sealed and charged with hydrogen gas (ca. 600 psi at room temperature). The reaction mixture was stirred overnight at 135°C (ca. 650 psi). The resulting mixture was filtered to remove the catalyst, and the isopropanol solution was concentrated *in vacuo*. The product was purified by fractional distillation (48-52°C / 0.15 mm Hg) to give a clear oil that is a mixture of cis/trans isomers (13.0 g, 84%) that are presumably 10% cis and 90% trans (by GC analysis). ^{1}H NMR ($CDCl_3$, 300 MHz, ppm): δ 1.30-2.28 (m, cyclohexyl-H), 2.91 (s, OH). ^{13}C NMR ($CDCl_3$, 75.4 MHz, ppm): δ 23.4 (s, alicyclic), 26.6 (s, alicyclic), 36.3 (s, alicyclic), 41.6 (s, alicyclic), 77.8-79.9 (m, $\underline{C}$-CF_3), 123.4 (q, $\underline{C}F_3$). IR (KBr, cm^{-1}): 3600, 3482, 2983, 2896, 1464, 1363, 1207, 1141, 1078, 969, 897.

1,3-Bis(2- *tert*-butoxycarbonyloxy hexafluoroisopropyl)cyclohexane (3.14).

To a solution of hydrogenated 1,3-HFAB (2.00 g, 4.8 mmol) in 20 mL of THF, 2.66 g (12.2 mmol) of di-tert-butyl dicarbonate was added. The reaction was stirred for a few minutes before 0.120 g (0.96 mmol) of DMAP was added. Gas evolution was observed after a few minutes and lasted about five minutes. The reaction was stirred over night. The THF was removed by rotary evaporation to give a white solid. The white solid was dissolve in chloroform and rinsed with 1 M hydrochloric acid (2 X 30 mL), saturated

sodium bicarbonate solution (2 X 30 mL) and saturated sodium chloride solution (1 X 30 mL). The organic layer was dried over sodium sulfate, filtered and the solvent removed using rotary evaporation. The product was recrystallized from hexanes and isolated by suction filtration. The white solid was then dried to give 2.065g (70% yield). ^{1}H NMR (CDCl3) δ: 3.1 (t, 2H); 2.1-1.8 (m, 6H); 1.7-1.3 (m, 20H). ^{13}C NMR ($CDCl_3$) δ: q, 123.2, *J*= 286.2; m, 77.7; s, 42.4; s, 35.8; s, 26.6; s, 26.3. IR (KBr, cm^{-1}) 1780.

1,3-Bis(2- *tert*-butoxycarbonyloxy hexafluoroisopropyl)cyclohexane (3.15).

To a 100 mL round-bottom flask equipped with a stir bar were added 1,4-HFAB (**15**, 2.00 g, 4.80 mmol) and di-*tert*-butyl dicarbonate (2.62 g, 12.0 mmol) in freshly distilled THF (20 mL). The resulting mixture was stirred for 5 min before the addition of 4-(*N*,*N*-dimethylamino)pyridine (117 mg, 0.960 mmol). Gas evolution was observed after a few minutes and lasted about 5 min. The resulting mixture was stirred overnight at room temperature and then concentrated *in vacuo*. The resulting white solid was dissolved in chloroform (30 mL) and washed with 1 *M* HCl (2 x 30 mL), saturated sodium bicarbonate (2 x 30 mL), and brine (30 mL). The organic layer was dried over Na_2SO_4, filtered, concentrated *in vacuo*, and dried under reduced pressure to yield a white solid (2.88 g, 97%). ^{1}H NMR ($CDCl_3$, 300 MHz, ppm): δ 1.40 (s, 18H, t-Bu), 1.60 (m, 4H, aliphatic), 1.90 (m, 4H, aliphatic), 3.10 (m, 2H, aliphatic). ^{19}F NMR ($CDCl_3$, 282 MHz, ppm): δ -68.3, -74.2. IR (KBr, cm^{-1}): 2986, 2893, 1771 (C=O), 1604, 1484, 1464, 1402, 1371, 1274, 1216, 1165, 1142, 1115, 1006, 959, 862, 769, 715.

3,5-bis-(2-hydroxyhexafluoro-2-propyl) bromobenzene (3.16)

To a 500 mL three-neck round bottom flask fitted with a magnetic stir bar, pressure equalizing addition funnel and reflux condenser(fitted with gas adapter connected to a potassium hydroxide-water trap) was added 200 g (490 mmol) of 1,3-bis-(2-hydroxyhexafluoro-2-propyl) benzene and 32.6 g (245 mmol) of aluminum trichloride. The flask was then warmed to 44-46 ºC before 86 g (540 mmol) of bromine was added dropwise over 2 hours. After the addition of the bromide was complete the reaction stirred for three hours at 44-46 ºC before the flask was cooled to room temperature. The reaction mixture was washed five times with 600 mL portions of an aqueous 3% $NaHSO_3$ solution. The aqueous layer was extracted with 250 mL of CH2Cl2. The combined organics were washed with two 500 mL portions of a saturated brine solution, dried over $MgSO_4$, filtered and concentrated *in vacuo* to give 214 g of crude product as a red solution. Distillation at 77-78.5 C/5 torr gave 116 g (49% yield) of product as a colorless oil. ^{1}H NMR ($CDCl_3$, 300 MHz, ppm): δ 3.54 (s, 2H, OH), 8.02-8.03 (m, 3H, Ph). ^{19}F NMR ($CDCl_3$, 282 MHz, ppm): δ -76.

3,5-bis-(2-ethoxymethoxy-hexafluoro-2-propyl) bromobenzene (3.17)

To a 200 mL three-neck round bottom flask fitted with a magnetic stir bar, pressure equalizing addition funnel and reflux condenser (fitted with gas adapter connected nitrogen source 20 g (41mmol) of 3,5-bis-(2-hydroxyhexafluoro-2-propyl) bromobenzene

in 100 mL of dry THFwas added dropwise to a solution of 2.35 g (98 mmol) of NaH in 20 mL of THF at 0 ºC. After the addition was complete, the reaction was refluxed for two hours. Chloromethyl ethyl ether (8.32 g, 88 mmol) in 60 mL of THF was added to the reaction and the reaction was refluxed for two additional hours. The reaction was cooled to roomtemperature before it was poured into 600 mL of water and extracted with 200 mL of ether. The organic layer was washed with 500 mL of a saturated brine solution, dried over $MgSO_4$, filtered and concentrated *in vacuo* to give 23 g (93% yield) of product as a pale yellow oil. ^{1}H NMR ($CDCl_3$, 300 MHz, ppm): δ 1.27 (t, 6H, J = 7.2 Hz 2xCH_3), 3.81 (q, 4H, J = 7.1 Hz 2xCH_2), 4.91 (s, 4H, 2xCH_2), 7.92 (m, 3H, Ph),. ^{19}F NMR ($CDCl_3$, 282 MHz, ppm): δ -71.8.

1,3,5-tris-(hexafluoro-2-propyl) benzene (3.18).

To an oven dried 250 mL three-neck round bottom flask fitted with a magnetic stir bar, pressure equalizing addition funnel and reflux condenser (fitted with gas adapter connected nitrogen source) was added 0.47 g (19 mmol) of magnesium turnings and 10 mL of dry THF. An iodine crystal was added and the reaction heated to 50 ºC before 12.59 g (19 mmol) of 3,5-bis-(2-ethoxymethoxy-hexafluoro-2-propyl) bromobenzene in 10 mL of THF was added dropwise. After the addition was complete the reaction was heated to reflux for three hours and cooled to room temperature. An additional 15 mL of THF was added to the reaction to dissolve a solid precipitate that formed. The reaction was placed in a water bath before hexafluoroacetone was slowly bubbled through the

reaction for 15 minutes. The reaction stirred for one hour before 60 mL of 2 M HCl was added and the mixture was extracted with two 60 mL portions of diethyl ether. The combined organics were washed with two 60 mL portions of a saturated brine solution, dried over $MgSO_4$, filtered and concentrated *in vacuo* to give 14.34 g of clear oil. ^1H NMR showed the presence of the methyl-ethyl acetal protecting group. The clear oil was added to a 100 mL round bottom flask with 20 mL of deionized water and 1 mL of trifluoroacetic acid. The round bottom was fitted with a reflux condenser and heated to 60 ºC over night. The mixture was extracted with two 60 mL portions of diethyl ether. The combined organics were washed with two 60 mL portions of a saturated brine solution, dried over $MgSO_4$, filtered, concentrated *in vacuo* and recrystallized from hexanes to give 4.8 g (40% yield) of the product as a crystalline white solid. mp 105 ºC; ^1H NMR (300 MHz, $CDCl_3$, δ): 8.27 (s, H). ^{19}F NMR (282 MHz, $CDCl_3$, δ): -76.5 (s), IR (KBr) 3620, 3519 (OH stretchs).

1,3,5-tris-(*tert*-butoxycarbonyloxy hexafluoro-2-propyl) benzene (3.19).

To a 100 mL round bottom flask with a stir bar was added **3.18** (0.17 g, 0.1 mmol) in 2 mL of dry THF, 0.33 g (1.5 mmol) of di-*tert*-butyl dicarbonate was added. The reaction was stirred for a few minutes before 0.013 g (0.10 mmol) of DMAP was added. The reaction was stirred over night. The THF was removed by rotary evaporation to give a pale yellow solid. The solid was dissolve in dichloromethane and rinsed with dilute acetic acid (2 x 30 mL), saturated sodium bicarbonate solution (2 x 30 mL) and saturated brine

solution (1 x 30 mL). The organic layer was dried over $MgSO_4$, filtered, concentrated *in vacuo* and recrystallized from hexanes to give 0.061g (70% yield) of product. ^{1}H NMR (300 MHz, $CDCl_3$, δ): 8.0 (s, H), 1.4 (s, 9H). ^{19}F NMR (282 MHz, $CDCl_3$, δ): -74 (s).

2-[3-{1-[3,5-bis-(2,2,2-trifluoro-1-hydroxy-1-trifluoromethyl-ethyl)-phenyl]-2,2,2-trifluoro-1-hydroxy-ethyl}-5-(2,2,2-trifluoro-1-hydroxy-1-1trifluoromethyl-ethyl)-phenyl]-1,1,1,3,3,3-hexafluoro propan-2-ol (3.20).

To an oven dried 100 mL three-neck round bottom flask fitted with a magnetic stir bar, pressure equalizing addition funnel and reflux condenser (fitted with gas adapter connected nitrogen source) was added 0.245 g (10 mmol) of magnesium turnings and 30 mL of dry THF. An iodine crystal was added and the reaction heated to reflux before 6.052 g (10 mmol) of 3,5-bis-(2-ethoxymethoxy-hexafluoro-2-propyl) bromobenzene in 10 mL of THF was added dropwise. After the addition was complete the reaction was refluxed until it became a clear pale yellow (typically over night) and was then cooled to room temperature. The reaction was placed in a water bath before ethyl trifluoroacetate was added dropwise. The reaction stirred for one hour before 30 mL of 2 M HCl was added and the mixture was extracted with two 30 mL portions of diethyl ether. The combined organics were washed with two 30 mL portions of a saturated brine solution, dried over $MgSO_4$, filtered and concentrated *in vacuo* to give 5.9 g of a yellow semisolid. ^{1}H NMR showed the presence of the methyl-ethyl acetal protecting group. The yellow solid was added to a 100 mL round bottom flask with 20 mL of deionized water and 1

mL of trifluoroacetic acid. The round bottom was fitted with a reflux condenser and heated to 60 ºC over night. The mixture was extracted with two 60 mL portions of diethyl ether. The combined organics were washed with two 60 mL portions of a saturated brine solution, dried over $MgSO_4$, filtered, concentrated *in vacuo* and recrystallized from hexanes to give 1.4 g (24.4% yield) of the product as a white solid. ^{1}H NMR (300 MHz, $CDCl_3$, δ): 8.14 (s, 2H), 7.90 (s, 4H). ^{19}F NMR (282 MHz, $CDCl_3$, δ): -76.1 (s, 24 F, 8 x CF_3), -74.9 (s, 3F, CF_3).

2-[3-{1-[3,5-bis-(2,2,2-trifluoro-1-*tert*-butoxycarbonyloxy -1-trifluoromethyl-ethyl)-phenyl]-2,2,2-trifluoro-1-*tert*-butoxycarbonyloxy -ethyl}-5-(2,2,2-trifluoro-1-*tert*-butoxycarbonyloxy -1-trifluoromethyl-ethyl)-phenyl]-1,1,1,3,3,3-hexafluoropropan-2-*tert*-butoxycarbonyloxy (3.21)

To a 100 mL round bottom flask with a stir bar was added **3.20** (0.55 g, 0.6 mmol) in 5 mL of dry THF, 0.56 g (2.52 mmol) of di-*tert*-butyl dicarbonate was added. The reaction was stirred for a few minutes before 0.034 g (0.28 mmol) of DMAP was added. The reaction was stirred over night. The THF was removed by rotary evaporation to give a pale yellow solid. The solid was dissolve in dichloromethane and rinsed with dilute acetic acid (2 x 30 mL), saturated sodium bicarbonate solution (2 x 30 mL) and saturated brine solution (1 x 30 mL). The organic layer was dried over $MgSO_4$, filtered, concentrated *in vacuo* to give 0.695 g of impure white solid. Column chromatography (silica gel,

dichloromethane) yielded 6 g (76% yield) of product as a white solid. ^{1}H NMR (300 MHz, $CDCl_3$, δ): 7.86 (s, 2H), 7.75-7.73 (d, 4H), 1.3-1.4 (s, 36H). ^{19}F NMR (282 MHz, $CDCl_3$, δ): -70.9 (s, 24 F, 8 x CF_3), -70.5 (s, 3F, CF_3).

Synthesis of 5-Hydroxy-2-trifluoromethyl-bicyclo[2.2.1]heptane-2-carboxylic acid *t*-butyl ester (3.22).

To a 250 mL round-bottomed flask, was added 7.87 g (30 mmol) of 2-Trifluoromethyl-bicyclo[2.2.1]hept-5-ene-2-carboxylic acid *t*-butyl ester and 60 mL of dry THF under nitrogen and mixture was allowed to stir for 10 minutes. To this mixture, was added 30.0 mL (30 mmol) of borane-tetrahydrofuran complex (1.0M soln. in THF) dropwise and stirred under nitrogen atmosphere for 17 h at room temperature. After adding 15 mL of 6M sodium hydroxide aqueous solution (90 mmol), the reaction mixture was stirred for 10 minutes. To this solution, was added11.9 mL of 30 wt.% hydrogen peroxide (99 mmol) and mixture was refluxed for 1 h. The mixture was extracted with AcOEt (3 x 50 mL). The combined organic phase was washed with water and dried over $K2CO_3$. Removal of the solvent in vaccuo, gave colorless liquid (7.97 g, 94.8%). According to the GC analysis, product has four isomers (t_R = 9.33, 9.63, 9.72 and 9.76 min). ^{1}H NMR (300 MHz, $CDCl_3$, δ): 4.31, 3.89-3.87 (m, H-2, 1H), 2.68-2.86 (m, OH, 1H), 1.20-1.88, 2.02-2.10, 2.24-2.55 (m, H-1, 3, 4, 5, and 7, 8H), 1.490, 1.494, and 1.507 (s, t-Bu, 9H). IR (Salt plate) 1732cm^{-1} (C=O), 3359cm^{-1}(OH).

Synthesis of Bis-(6-trifluoromethyl-6-*t*-buthoxycarbonyl-bicyclo[2.2.1]heptyl)-sulfate (3.23).

To a 100 mL round-bottomed flask, was added 1.40 g (5.0 mmol) of 5-Hydroxy- 2-trifluoromethyl-bicyclo[2.2.1]heptane-2-carboxylic acid *t*-butyl ester, 0.56g (5.5 mmol) of triethylamine and 20 mL of dry THF and the mixture was cooled to below 5ºC in ice-bath. To this mixture, was added 2.50 mL of sulfuryl chloride in dichloromethane (2.5 mmol) dropwise, and stirred for 2 h below 5ºC. Then mixture was allowed to warm up to room temperature and stirred for 20 h. After removal of the insoluble salt by filtration, the reaction mixture was evaporated. The brown oil obtained was subjected to flash column chromatography (silica gel, CH_2Cl_2), which afforded colorless oil (233.2 mg, 14.7%). According to the GC analysis, product has 1 isomer (t_R = 7.92 min). ^{1}H NMR (300 MHz, $CDCl_3$, δ): 4.85 (dd, H-2, 2H), 1.14-3.60 (m, H-1, 3, 4, 5, and 7, 16H), 1.47 (s, t-Bu, 18H). ^{19}F NMR (282 MHz, $CDCl_3$, δ): -72.9 (s, CF_3). IR (Salt plate) 1736, 1794cm^{-1} (C=O), 1197, 1059, 1038, 924, 891cm^{-1}(S=O).

Synthesis of Bis-(6-trifluoromethyl-6-*t*-buthoxycarbonyl-bicyclo[2.2.1]heptyl)-carbonate (3.24).

To a 100 mL round-bottomed flask, was added 7.01 g (25.0 mmol) of 5-Hydroxy-2-trifluoromethyl-bicyclo[2.2.1]heptane-2-carboxylic acid *t*-butyl ester **(3)**, 2.53g (25.0 mmol) of triethylamine and 40 mL of dry toluene and the mixture was cooled to below 5ºC in ice-bath. To this mixture, was added 6.61 mL of phosgene (12.5 mmol) in toluene

dropwise and stirred for 2 h below 5ºC. Then mixture was allowed to warm up to room temperature and stirred for 20 h. After removal of the insoluble salt by filtration, the reaction mixture was washed with ice-HCl and 5% aqueous Na_2CO_3 solution. The organic layer was dried over anhydrous $MgSO_4$, and subsequent evaporation gave pale yellow oil. This material was subjected to flash column chromatography (Si-gel, CH_2Cl_2), which afforded colorless oil (2.86 g, 39.0%). The GC analysis shows that product has three isomers (t_R = 14.26, 16.33, 18.04 and 10.88 min). ^{1}H NMR (300 MHz, $CDCl_3$, δ): 5.11, 4.75, 4.65(d, H-2, 2H), 1.06-3.36 (m, H-1, 3, 4, 5, and 7, 16H), 1.47, 1.48, and 1.54 (s, t-Bu, 18H). ^{19}F NMR (282 MHz, $CDCl_3$, δ): -64.5, -64.8, -67.7 (s, CF_3). IR (Salt plate) 1735, 1702cm^{-1} (C=O).

Sublimation of Bis-(6-trifluoromethyl-6-*t*-buthoxycarbonyl-bicyclo[2.2.1]heptyl)-sulfate (3.23).

To a sublimation apparatus, was added Bis-(6-trifluoromethyl-6- *t*-buthoxycarbonyl-bicyclo[2.2.1]heptyl)-sulfate (3.23) and the apparatus was evacuated to 5 Torr. The cold finger was cooled with dry-ice IPA and the outside was heated to 80ºC. The condensed white semisolid was identified as Bis-(6-trifluoromethyl-6-*t*-buthoxycarbonyl-bicyclo[2.2.1]heptyl)- sulfate **(3.23)** by NMR and IR analysis. ^{1}H NMR (300 MHz, $CDCl_3$, δ): 4.85 (dd, H-2, 2H), 1.14-3.60 (m, H-1, 3, 4, 5, and 7, 16H), 1.47 (s, t-Bu, 18H). ^{19}F NMR (282 MHz, $CDCl_3$, δ): -72.9 (s, CF_3). IR (Salt plate) 1736, 1794cm^{-1} (C=O), 1197, 1059, 1038, 924, 891cm^{-1}(S=O).

Sublimation of Bis-(6-trifluoromethyl-6-*t*-buthoxycarbonyl-bicyclo[2.2.1]heptyl)-carbonate (3.24).

To a sublimation apparatus, was added Bis-(6-trifluoromethyl-6- *t*-butoxycarbonyl-bicyclo[2.2.1]heptyl)-carbonate **(3.24)** and the apparatus was evacuated to 5 Torr. The cold finger was cooled with dry-ice IPA and the outside was heated to 80ºC. The condensed white semisolid was identified as Bis-(6-trifluoromethyl-6-*t*-buthoxycarbonyl-bicyclo[2.2.1]heptyl)-sulfate **(3.24)** by NMR and IR analysis. ^{1}H NMR (300 MHz, $CDCl_3$, δ): 5.11, 4.75, 4.65(d, H-2, 2H), 1.06-3.36 (m, H-1, 3, 4, 5, and 7, 16H), 1.47, 1.48, and 1.54 (s, t-Bu, 18H). ^{19}F NMR (282 MHz, $CDCl_3$, δ): -64.5, -64.8, -67.7 (s, CF_3). IR (Salt plate) 1735, 1702cm^{-1} (C=O).

Synthesis of 5-Formyl-2-trifluoromethyl-bicyclo[2.2.1]heptane-2-carboxylic acid *t*-butyl ester (3.25).

To a 100 mL three-necked round-bottomed flask equipped with a gas inlet, was added 93 mg (0.125 mmol, 10 mmol/L) of tetrarhodium dodecacarbonyl and 50 mL of degassed dry toluene under nitrogen atmosphere. To this clear orange colored solution, was added 98 mg of triphenylphosphine (0.375 mmol, L/M=3), dissolved in dry toluene, under vigorous stirring. As triphenylphosphine ligand was added, the reaction mixture turned to a dark brown color. The reactor was evacuated, filled with the carbon monoxide and hydrogen 1:1 mixed gas, and warmed up to 70ºC. To this mixture, was added 7.87 g of

deoxygenated 2-Trifluoromethyl- bicyclo[2.2.1]hept-5-ene-2-carboxylic acid *t*-butyl ester (30 mmol), and reaction mixture was held at 70ºC and maintained under CO/H_2 mixed gas flow. The reaction was periodically tested by GC analysis checked for residual starting material. After 48 h, all of the starting material was consumed, and reaction mixture was subjected to distillation. Distillation at 104°C (2 Torr) afforded the desired product as a colorless liquid (4.76 g, 52.0%). According to the GC analysis, product has 4 isomers (t_R = 9.44, 9.70, 9.92, and 10.06 min). ^{1}H NMR (300 MHz, $CDCl_3$, δ): 9.62, 9.66, and 9.69 (s, -CHO, 1H), 1.07-3.21 (m, H-1, 3, 4, 5, and 7, 9H), 1.476, 1.488, and 1.493 (s, t-Bu, 9H). ^{19}F NMR (282 MHz, $CDCl_3$, δ): -64.48, -65.06, -67.76, and –67.81 (s, CF_3). IR (Salt plate) 2819, 2711cm^{-1}(-CHO), 1736cm^{-1}(C=O).

5-Hydroxymethyl-2-trifluoromethyl-bicyclo[2.2.1]heptane-2-carboxylic acid *t*-butyl ester (3.26)

To a 50 mL round-bottomed flask, was added 30 mg (0.67 mmol) of sodium hydroxide and 10 mL of dry IPA and mixture was cooled to 0°C in an ice bath. To this mixture, was added 50 mg (1.40 mmol) of sodium borohydride and warmed up to room temperature. Then 1.46 g (5.0 mmol) of 5-Formyl-2-trifluoromethyl-bicyclo[2.2.1]heptane- 2-carboxylic acid *t*-butyl ester dissolved in 10 mL of IPA was added drop-wise to the mixture and stirred overnight. After addition of 15 mL of 1N aqueous NaOH, the reaction mixture was acidified with 1N HCl. Resulted cloudy solution was extracted with 25 mL of CH_2Cl_2 twice. The combined organic layers were washed with 50 ml of water

twice and dried over anhydrous MgSO4. Removal of the solvent by evaporation gave a colorless liquid (1.17 g, 79.2%). According to the GC analysis, the product has 4 isomers (t_R = 10.49, 10.84, 10.99, and 11.19 min). ^{1}H NMR (300 MHz, $CDCl_3$, δ): 3.36-3.44 (m, O-CH_2-, 2H), 0.96-2.84 (m, H-1, 2, 3, 4, 5, 7 and OH, 9H), 1.47, 1.48, and 1.49 (s, t-Bu, 9H). ^{19}F NMR (282 MHz, $CDCl_3$, δ): -63.34, -64.95, -67.36, and –67.89 (s, CF_3). IR (Salt plate) 3355cm^{-1}(OH), 1736cm^{-1}(C=O). CIMS (m/z): $[M+H]^+$ calcd for $C_{14}H_{22}F_3O_3$, 295; found, 295.

Bis-(6-trifluoromethyl-6-*t*-buthoxycarbonyl-bicyclo[2.2.1]heptylmethyl)-carbonate (3.27)

To a 50 mL round-bottomed flask, was added 0.94 g (3.2 mmol) of 5-Hydroxymethyl- 2-trifluoromethyl-bicyclo[2.2.1]heptane-2-carboxylic acid *t*-butyl ester, 0.32g (3.2 mmol) of triethylamine and 20 mL of dry THF and the mixture was cooled to below 5ºC in ice-bath. To this mixture, was added 0.85 mL of phosgene 20% toluene solution (1.6 mmol) dropwise and stirred for 2 h below 5ºC. Then mixture was allowed to warm up to room temperature and stirred for 20 h. After removal of the insoluble salt by filtration, reaction mixture was evaporated and dissolved into CH_2Cl_2. This mixture was washed with ice-HCl, 5% aqueous Na_2CO_3 solution, and water. The organic layer was dried over anhydrous $MgSO_4$, and subsequent evaporation gave pale yellow oil. This material was subjected to flash column chromatography (Si-gel, CH_2Cl_2), which afforded a colorless oil (349 mg, 35.5%). The GCMS analysis shows that product contains three isomers (t_R

= 9.61, 9.82, 10.14 and 10.47 min). ^{1}H NMR (300 MHz, $CDCl_3$, δ): 3.81-4.14(m, O-CH_2-, 4H), 1.00-2.88 (m, H-1, 3, 4, 5, and 7, 18H), 1.474, 1.479, and 1.498 (s, t-Bu, 18H). ^{19}F NMR (282 MHz, $CDCl_3$, δ): -63.7, -65.1, -67.5, and 68.0 (s, CF_3). IR (Salt plate) 1736, 1779cm^{-1} (C=O).

***tert*-butyl carbonate protection of PNBHFA oligomers (3.28)**

To a 100 mL flask was added 2.0 g (7.3 mmol as a monomer) of NBHFA oligomers, 10 mL of dry THF, 1.28 g (5.84 mmol) of di-*tert*-butyl dicarbonate, and 0.065 g (0.5 mmol) of DMAP. The solution was stirred overnight at room temperature. The resulting solution was evaporated and dichloromethane (20 mL) was added. The organics were washed with dilute acetic acid (10 mL x 3) and brine (10 mL x 2), dried over $MgSO_4$, filtered, evaporated, and dried *in vacuo* overnight at 50 °C to yield 1.785 g of a white semicrystaline solid. Protection ratio 81% (by ^{19}F NMR). ^{19}F NMR NMR (chloroform) δ: -72 to -75 (6F, protected alcohol), -76 to -79 (6F, alcohol).

***tert*-butyl ester protection of PNBHFA oligomers (3.29)**

To an oven dried 100 mL three neck round bottom flask equipped with a stir bar, pressure equalizing addition funnel and reflux condesor (with adapter to nitrogen source) was added 0.087 g (3.6 mmol) of NaH and 5 mL of dry THF. PNBHFA oligomers (1 g, 3.65 mmol) were added to the addition funnel and dissolved in 10 mL of THF. The PNBHFA

oligomers/ THF solution was added dropwise to the round bottom flask. The reaction stirred for one hour after the addition was complete. *t*-butyl bromoacetate (0.712 g, 3.6 mmol) was added to the flask via syringe. The reaction was refluxed for 24 hours, cooled to room temperature and poured into an aqueous ammonium chloride solution. The solution was extracted with dichloromethane (3 x 20 mL) and the combined organics were dried over $MgSO_4$, filtered, and evaporated to yield the crude product as a yellow semisolid. Column chromatography (silica gel and 1:4 ethyl acetate:hexanes) afforded 1.1 g of 83% protected material (by ^{19}F NMR). ^{19}F NMR NMR (chloroform) δ: -71 to -74 (6F, protected alcohol), -76 to -79 (6F, alcohol).

di-(*p*-hydroxyphenyl)-*p*-*tert*-butylphenyl sulfonium triflate (3.30).

In a 50 ml round bottom flask was added 3.0 g (5.53 mmol) of di-(p-tert-butylphenyl) iodonium triflate, 1.207 g (5.53 mmol) of 4,4'-thiodiphenol, and 44.2 mg (0.14 mmol, catalytic) of copper (II) benzoate. The flask was fitted with a condensor and purged with nitrogen for 15 minutes. The flask was heated to 120-125C for 3 hours. After the flask cooled to room temperature, 2 x 20 mL of ether was used to extract the reaction. The material remaining in the flask was dried under vacuum to yield 2.43 g (80%) of a tan solid. ^1H NMR (DMSO) δ: 7.8 (d, 2H) 7.6 (m, 6H), 7.1 (d, 4H), 1.3 (s, 9H); ^{19}F NMR (DMSO) δ: -78.1 (s, 3F)

di-*tert*-butyl carbonate of di-(*p*-hydroxyphenyl) *p*-*tert*-butylphenyl sulfonium triflate (3.31).

To an oven dried 100 mL 3 neck round bottom flask with gas adapter, stopper, septum and stir bar was added (under a nitrogen blanket) 1.0 g (2.00 mmol) of di-(*p*-hydroxyphenyl) p-*tert*-butylphenyl sulfonium triflate and 25 mL of dry THF. When all the solids dissolve 0.448 g (4.0 mmol) of potassium *t*-butoxide was added. When the solid dissolved, 0.872 g (4.0 mmol) of di-tert-butyl dicarbonate was added. The reaction stirred overnight. The THF was removed by rotary evaporation. The viscous yellow oil was dissolved in DCM and extracted with 2 x 15 mL of a saturated sodium carbonate solution. The organic layer was dried over sodium sulfate, filtered, and concentrated using rotary evaporation. Ether was added to the yellow oil and after heating ether to 35ºC a white powder forms. The powder was isolated by filtration and dried under vacuum. Mp 135-138 ºC. ^{1}H NMR (DMSO) δ: 7.8 (d, 4H) 7.7 (s, 4H), 7.1 (d, 4H), 1.5 (s, 18H), 1.3 (s, 9H).

tri-(*p*-hydroxyphenyl) sulfonium chloride (3.32).

To a 3 neck 500 mL 3 neck round bottom flask was added 52.5 g (557 mmol) of phenol, and 28 mL of chloroform. The flask is cooled in ice water before 11.7 g (98.3 mmol) of thionyl hloride is added dropwise. The reaction mixture is stirred for 20 hours. The chloroform was removed by rotary evaporation. The excess phenol was removed by vacuum distillation. The bath temperature was increased up to 125ºC. The hot reaction

mixture was poured into75ºC concentrated acetic acid and then cooled to 10ºC. The white powder was then isolated by filtration and washed with acetone to yield 35 g (26%) of the white salt: Mp 268-270 ºC, ^{1}H NMR (DMSO) δ: 7.5 (d, 6H) 7.0 (d, 6H).

tri-(*p*-hydroxyphenyl) sulfonium nonafluoro-1-butanesulfonate (3.33): In a 100 mL round bottom flask was placed 3 g (8.6 mmol) tri-(*p*-hydroxyphenyl) sulfonium chloride and 2.925 g (8.6 mmol) nonafluoro-1-butanesulfonate. To this mixture was added 50 mL deionized water and 50 mL of nitromethane. After stirring vigorously for one hour, the phases were separated, and the organic phase extracted 3 x 100 mL of deionized water followed by drying over $MgSO_4$. Removal of solvent *in vacuo* gave a viscous oil. After digesting the oil in hot hexanes several times a crystalline product was isolated. Filtration gives the desired product as a white solid. Yield: 1.15 g (22 % yield). Mp 152-155 ºC ^{1}H NMR (DMSO) δ: 7.6 (d, 6H), 7.2 (d, 6H). ^{19}F NMR (DMSO) δ: -80 (3F), -115 (2F), -121 (2F), -126 (2F).

tri-*tert*-butyl carbonate of tri-(*p*-hydroxyphenyl) sulfonium nonafluoro-1-butane sulfonate (3.34).

To an oven dried 100 mL 3 neck round bottom flask with gas adapter, stopper, septum and stir bar was added (under a nitrogen blanket) 0.81 g (1.33 mmol) of tri-(*p*-hydroxyphenyl) sulfonium nonaflate and 25 mL of dry THF. When all the solids dissolve 0.83 g (6.0 mmol) of potassium carbonated and 0.872 g (4.0 mmol) of di-*tert*-butyl

dicarbonate were added. The reaction was refluxed over night. The THF was removed by rotary evaporation. The viscous yellow oil and solids was dissolved in DCM and extracted with 2 x 30 mL of deionized water and 2 x 30 mL of saturated sodium carbonate solution. The organic layer was dried over sodium sulfate, filtered, and concentrated using rotary evaporation. Ether was added to the yellow oil and after heating ether to 35ºC a white powder forms. The powder was isolated by filtration and dried under vacuum to give 0.85 g (71% yield). ^{1}H NMR (DMSO) δ: 7.8 (d, 6H) 7.5 (d, 6H), 1.5 (s, 27H). ^{19}F NMR NMR (DMSO) δ: -80 (3F), -115 (2F), -121 (2F), -126 (2F).

^{14}C-labeled Diphenyl Sulfoxide (4.1).

Break-seal ampules containing ^{14}C labeled benzene (Sigma-Aldrich, Inc., 1.4mCi, SA of 10.3 mCi/mmol) were cooled in an ice bath. The ampules were ruptured and rinsed with 20 mL of benzene. The benzene was transferred to an oven dried 100 mL three neck round bottom flask under nitrogen. Thionyl chloride (0.6 mL, 8.2 mmol) was added and the flask was cooled to 0 ºC before triflic acid (3.1 mL, 35.3 mmol) was added. The ice bath was removed after 1 hour and the reaction stirred for 24 hours at room temperature. The reaction was quenched by pouring the solution over ice and neutralizing with sodium bicarbonate. The neutralized solution was extracted with four 30 mL portions of methylene chloride. The combined organics were dried over magnesium sulfate. The solution was filtered to remove the magnesium sulfate and distilled to remove methylene chloride and benzene. The residue was dissolved in boiling hexanes and decanted away

from the hexane insoluble yellow oil. The yellow oil was extracted with boiling hexanes once more. The combined hexanes solutions were cooled in an ice bath and diphenyl sulfoxide precipitated out as a white solid that was isolated by filtration and dried under vacuum. Yield: 1.32 g (80%). Mp: 69-72 ºC. ^{1}H NMR ($CDCl_3$, ppm): δ 7.4 (m, 6H), δ 7.6 (m, 4H).

Triphenylsulfonium Bromide (^{14}C-TPS bromide) (4.2).

A 875 mg (36 mmol) portion of powdered magnesium was suspended in 20 mL of dry diethyl ether in a oven-dried 500 mL three-neck flask equipped with a Teflon coated stir bar, reflux condenser, and dropping funnel. A positive pressure of dry nitrogen was maintained throughout the reaction. The dropping funnel was charged with 5.9 g (37.5 mmol) of bromobenzene and 10 mL of diethyl ether of which 1-2 mL were added immediately. An iodine crystal was added to initiate the reaction and the remaining bromobenzene solution was added drop wise at a rate to maintain reflux. The solution was allowed to stir overnight under a nitrogen atmosphere. The ether solvent was removed by heating in an 80 °C bath *in vacuo* with stirring for two hours, giving a semi-solid brown residue. Freshly distilled heptane, 50mL, was added to the flask was removed by heating in an 80 °C bath *in vacuo*. This was repeated three times. Dry heptane, 100 mL, and 50 mL of dry benzene were added to the flask and the reaction was heated to reflux. A 1.32 g (6.5 mmol) portion of diphenyl sulfoxide was dissolved in 30 mL freshly distilled benzene and added dropwise to the refluxing phenyl magnesium

bromide mixture. After addition was complete, the mixture was maintained at reflux over night, followed by cooling to 0 °C with an ice bath. HBr, 80 mL of 25%, was added slowly to maintain a temperature below 20 °C, and allowed to stir overnight. The aqueous phase was collected, and the organic phase washed with two 30 mL portions of 5% HBr. The combined aqueous phases were extracted with four 30 mL portions of dichloromethane. The organics were dried over $MgSO_4$ and removed *in vacuo* to give a tan powdered product. Yield: 0.324 g (15%). Melting point = 284-286 °C. ^{1}H NMR ($CDCl_3$, ppm): δ 7.6 (m, 9H), δ 7.8 (m, 6H).

Triphenylsulfonium Perfluoro-1-butanesulfonate (^{14}C-TPS nonaflate) (4.3).

In a 100 mL round bottom flask was placed 0.324 g (0.94 mmol) TPS bromide and 0.319 g (0.94 mmol) potassium perfluoro-1-butanesulfonate. To this mixture was added 10 mL deionized water and 10 mL of nitromethane. After stirring vigorously for one hour, the phases were separated, and the organic phase extracted 3x30 mL of deionized water followed by drying over $MgSO_4$. Removal of solvent *in vacuo* gave a viscous oil. After extracting the oil with ice cold diethyl ether several times a crystalline product was isolated. Filtration gives the desired product as a white solid. Yield: 0.23 g (43 %). MP = 88-89 ºC. ^{1}H NMR ($CDCl_3$, ppm): δ 7.6 (m, 9H), δ 7.8 (m, 6H). ^{19}F NMR ($CDCl_3$, reference = $CFCl_3$, ppm): δ -80.8 (3F, CF_3), -114.4 (2F, $CF_3\mathbf{CF_2}CF_2CF_2SO_3^-$), -121.1 (2F, $CF_3CF_2\mathbf{CF_2}CF_2SO_3^-$), -125.6 (2F, $CF_3CF_2CF_2\mathbf{CF_2}SO_3^-$). The SA was 8.60 ± 0.02 μCi/g.

^{14}C-Tripentylamine (**4.5**).

Tosylation of ^{14}C-labeled 1-Pentanol: A break-seal ampule containing ^{14}C-labeled 1-pentanol (American Radiolabeled Chemicals, Inc., 1 mCi, SA of 5 mCi/mmol) was cooled in a dry ice-isopropyl alcohol bath. The ampule was ruptured and rinsed with 2.5 mL of 1-pentanol. The 1-pentanol (2.5 mL, 23 mmol) was distilled from calcium hydride directly into the oven dried 3 neck round bottom flask used for the tosylation reaction. Dichloromethane (20 mL) and pyridine (2.3 mL, 28 mmol) were added to the flask. The flask was cooled in an ice bath before tosyl chloride (4.83 g, 25.3 mmol) was added. The reaction was warmed to room temperature and stirred over night, then filtered through a celite plug to remove the pyridinium chloride that formed. The solution was then extracted with water (3 x 15 mL) and once with 20 mL of brine solution. The organic layer was dried over $MgSO_4$ and removed in vacuo to give a clear oil (**4.4**). The oil was used for the next reaction without any further purification. The oil from the tosylation reaction was added to a 100 mL round bottom flask with dipentylamine (14.1 mL, 69 mmol), and K_2CO_3 (6.36 g, 46 mmol). The flask was heated and held at 100 ºC overnight, then cooled and filtered through a celite plug to remove any solids. The plug was then rinsed with ethyl acetate. The organics were dried over $MgSO_4$ and the ethyl acetate removed in vacuo. The unreacted dipentylamine was removed by vacuum distillation at 37 ºC @ 540 mtorr. The tripentylamine (2.4g, 46% yield) was isolated at 66-69 ºC @ 540

mtorr. ^{1}HNMR ($CDCl_3$, ppm): δ 2.4 (t, 6H), δ 1.2-1.5 (m, 18H), δ 2.4 (t, 9H). The SA was 49.8 ± 0.1 μCi/g.

Bibliography

Allcock, H. R., Lampe, F. W. Contemporary Polymer Chemistry. New Jersey: Prentice Hall, **1990**, Chap. 12.

Brodsky, Colin; Byers, Jeff; Conley, Will; Hung, Raymond; Yamada, Shintaro; Patterson, Kyle; Somervell, Mark; Trinque, Brian; Tran, H. V.; Cho, Sungseo; Chiba, Takashi; Lin, Shang-Ho; Jamieson, Andrew; Johnson, Heather; Vander Heyden, Tony; Willson, C. Grant. *Journal of Vacuum Science & Technology, B: Microelectronics and Nanometer Structures* (**2000**), 18(6), 3396-3401.

Clecak, Nicholas J.; McKean, Dennis R.; Miller, Robert D.; Tompkins, Terry C.; Twieg, Robert J.; Willson, Carlton G. **Positive resist compositions.** U.S. (**1983**).

Crawford, Michael K.; Feiring, Andrew E.; Feldman, Jerald; French, Roger H.; Periyasamy, Mookkan Peri; Schadt, Frank L., III; Smalley, Robert J.; Zumsteg, Fredrick C., Jr.; Kunz, Roderick R.; Rao, Veena; Liao, Ling; Holl, Susan M. *Proc. SPIE-Int. Soc. Opt. Eng* (**2000**), 3999, 357-364.

Crivello, J. V., Lam, J. H. W. *J. Org. Chem.*, Vol. 43, No. 15, **1978,** 3055-30058**.**

Dammel, R. R.; Houlihan, F. M.; Sakamuri, R.; Rentkiewicz, D.; Romano, A. *J. Photopolym. Sci. Technol.*, **2004**, *17(4)*, 587.

Dektar, J. L.; Hacker, N. P. *J. Am. Chem. Soc.* **1990**, *112*, 6004.

Dixon,Dave at Pacific Northwest National Labs

Drent, E; Broehhoven, J. A. M. and Doyle, M. J. *J. Org. Chem.* **1991**, 417, 235.

Drent, E. and Budzelaar, P.H. M. *Chem. Rev.* **1996**, 96(663).

Frechet, J. M. J.; Eichler, E.; Ito, H. and Willson, C. G. *Polymer* **1983**, 24, 995.

Gaylord, N. G., Deshpande, A B., Mandal, B. M., Martin, *Micheal J Macromol. SCI.-Chem.*, A11(5), pp. 1053-1070 (**1977**).

Gokan, H.; Esho, S.; Ohnishi, Y. J. *Electrochem. Soc*. **1983**, 130, 143.

Goldschmidt, A. *Journal of the Ameican Chemical Society* 73 (**1951**) 2940.

Horrocks, D. L. *Applications of Liquid Scintillation Counting*; Academic Press, Inc: New York, **1974**.

Horrocks, D. L. in *Liquid Scintillation, Science and Technology*; Academic Press, Inc: New York, **1976**.

Howard, P. L. *Basic Liquid Scintillation Counting*; American Society of Clinical Pathologists: Chicago, **1976**.

Hung, Raymond Jui-Pu; Tran, Hoang Vi; Trinque, Brian C.; Chiba, Takashi; Yamada, Shintaro; Sanders, Daniel; Connor, Eric F.; Grubbs, Robert H.; Klopp, John M.; Frechet, Jean M. J.; Thomas, Brian H.; Shafer, Gregory J.; DesMarteau, Darryl D.; Conley, Will; Grant, Willson C. *Proc. SPIE-Int. Soc. Opt. Eng* (**2001**), 385-395.

Hung, R. J. *Organic Material for Microelectronics: 157 nm Photoresist and Electrooptic Liquid Crystals*, The University of Texas at Austin: Austin, **2001**.

Ishikawa, Takuji; Kodani, Tesuhiro; Yoshida, Tomohiro; Moriya, Tsukasa; Yamashita, Tsuneo; Toriumi, Minoru; Araki, Takayuki; Aoyama, Hirokazu; Hagiwara, Takuya; Furukawa, Takamitsu; Itani, Toshiro; Fujii, Kiyoshi. *Journal of Fluorine Chemistry* (**2004**), 125(11), 1791-1799.

Ito, H; Miller, D. C.; Willson, C. G. *Macromolecules* **1982**, 15, 915.

Ito, H.; Willson, C. G. and Frechet, J. M. J. *Digest of Technical Papers of 1982 Symposium on VLSI Technology* **1982**, 86-87.

Ito, Hiroshi; Flores, Elizabeth. *Journal of the Electrochemical Society* (**1988**), 135(9), 2322-7.

Ito, Hiroshi; Alexander, Debra-Fenzel; Breyta, Greg *Journal of Photopolymer Science and Technology* (**1997**), 10(3), 397-408.

Ito, H. Miller, D. C., Sherwood, M., *Journal of Photopolymer Science and Technology*. 13 (**2000**) 559.

Ito, H.; Allen, R.D.; Opitz, J.; Wallow, T. I.; Truong, H.D.; Hofer, D.C.; Varanasi, P.R.; Jordhamo, G.M.; Jayaraman, S. and Vicari, R. *Proc. SPIE* **2000**, 3999, 2.

Ito, H.; Wallraff, G. M.; Brock, P. J.; Fender, N.; Truong, H. D.; Breyta, G.; Miller, D. C.; Sherwood, M. H.; Allen, R. D. *Proc. SPIE-Int. Soc. Opt. Eng*. **2001**, 4345, 273.

Ito, Hiroshi; Hinsberg, William D.; Rhodes, Larry F.; Chang, Chun. *Proc. SPIE-Int. Soc. Opt. Eng* (**2003**), 5039 70-79.

Iwatsuki, S.; Kondo, A.; Harashina, H. *Macromolecules* **1984**, 17, 2473.

Judge, J. M. and Price, C. C., *Joournal of Polymer Science* (**1959**) 41 435-43.

Knights, Evord F.; Brown, Herbert C. *JACs* (1968), 90(19), 5281-3.

Kodama, Shun-ichi; Kaneko, Isamu; Takebe, Yoko; Okada, Shinji; Kawaguchi, Yasuhide; Shida, Naomi; Ishikawa, Seiichi; Toriumi, Minoru; Itani, Toshiro. *Proc. SPIE* **2000**, 4690, 76-83.

Kunz, R. R. *Proc. Spie* **1999**, 13, 3678.

Mack, C.A. "Inside Prolith: A complete Guide to Optical Lithography," FINLE Technologies, Inc., Austin, Texas, **1997**, 75.

Maruno, T.; Nakamura, K.; Murata, N. *Macromolecules*, **1996**, 29, 2006-2010.

McAdams, C. L.*Polymers and Photoactive Compounds for Nonchemically Amplified Deep-UV Photoresists*; The University of Texas at Austin: Austin, 2000.

McKean, Dennis R.; MacDonald, Scott A.; Clecak, Nicholas J.; Willson, C. Grant. *Proc. SPIE* **1988**, 920, 60-6.

Meyerhofer, D. *IEEE Trans. Electron Devices*, ED-27, pp. 921, (**1980**).

Moore, G. E., *Electronics*, 38 (1965), 8.

Okoroanyanwu, U. Ph.D. Thesis, University of Texas at Austin, **1997**.
Olah, G. A.; Marinez, E. R.; Prakash, G. K. S. *Synlett* **1999**, *9*, 1397.

Osborn, B. P *Vacuum Ultraviolet Directed Design, Synthesis and Developement of 157 nm Photoresist Materials*, The University of Texas at Austin: Austin, **2004**.

Patterson, K. W. *PhD Thesis*; The University of Texas at Austin, **2000**.

Regel, W. and Canessa, G. *Makromol. Chem*. 181 (**1980**) 1703.

Schlegel, Leo; Ueno, Takumi; Shiraishi, Hiroshi; Hayashi, Nobuaki; Hesp, Simon; Iwayanagi, Takao. *Japanese Journal of Applied Physics, Part 1*: Regular Papers, Short Notes & Review Papers (**1989**), 28(10), 2114-19.

Schwalm, R. et all. *J. Chem. Soc. Perkin Trans 2*. **1991**, 1803-1808.

Schwalm, Reinhold (Procedure provided by Reinhold Schwalm)

Shirai, M. and Tsunooka, M. *Bull. Chem. Soc. Japan* **1998**, 71, 2483.

Soulen, R. L. and Griffith, J. R. *Journal of Fluorine Chemistry*, 44 (**1989**) 203-210.

Takanashi, A.; Harada, T.; Akeyama, M.; Kondo, Y.; Kurosaki, T.; Kuniyoshi, S.; Hosaka, S.; Kawamura, Y. *US Patent No. 4480910* **1984.**

Tran, H. V.; Hung, R. J.; Chiba, T.; Yamada, S.; Mrozek, T.; Hsieh, Y.-T.; Chambers, C. R.; Osborn, B. P.; Trinque, B. C.; Pinnow, M. J.; Sanders, D. P.; Connor, E. F.; Grubbs, R. H.; Conley, W.; MacDonald, S. A.; Willson, C. G. *Journal of Photopolymer Science and Technology* **2001**, *14*, 669-674.

Tran, Hoang V.; Hung, Raymond J.; Chiba, Takashi; Yamada, Shintaro; Mrozek, Thomas; Hsieh, Yu-Tsai; Chambers, Charles R.; Osborn, Brian P.; Trinque, Brian C.; Pinnow, Matthew J.; MacDonald, Scott A.; Willson, C. Grant; Sanders, Daniel P.; Connor, Eric F.; Grubbs, Robert H.; Conley, Will. *Macromolecules* (**2002**), 35(17), 6539-6549.

Trefonas, P., III; Daniels, B. K.; Fischer, R. L., Jr. *Solid State Technology* (1987), 30(8), 131-7.

Trinque, Brian C.; Osborn, Brian Philip; Chambers, Charles R.; Hsieh, Yu-Tsai; Corry, Schuyler Boon; Chiba, Takashi; Hung, Raymond Jui-Pu; Tran, Hoang Vi; Zimmerman, Paul; Miller, Daniel; Conley, Will; Willson, C. Grant *Proc. SPIE-Int. Soc. Opt. Eng* (**2002**), 4690, 58-68.

Trinque, B. C. *Synthesis, Copolymerization Studies and 157 nm Photolthography Applications of 2-trifluoromethylacrylates*, The University of Texas at Austin: Austin, **2003**.

Willson, C. G.; Ito, H.; Frechet, J. M. J.; Tessier, T. G. and Houlihan, F. M. *J. Electrochem*. Soc. **1986**, 133, 181.

Yamada, S. *Design and Study of Advanced Photoresist Materails: Positive Tone Photoresists with Reduced Environmental Impact and Materials for 157 nm Lithography*. The University of Texas at Austin: Austin, **2000**.

Zurkova, E.; Bouchal, K.; Kalal, J.; Dedek, V. *Die Angewandte Makromolekulare Chemie* 155 (**1987**) 101-115.

VITA

Charles Ray Chambers Jr. was born in Freeport, Texas on November 14, 1974, the son of Charles and Rose Lee Chambers. After graduating from West Columbia High School, West Columbia, Texas in May 1993, he entered Wharton County Junior College for one year followed by Brazosport Community College for one year. He enrolled at Southwest Texas State University, San Marcos, Texas in August of 1995 and received the degree of Bachelor of Science in Chemistry in May 1998. In August 2000, he entered the Graduate School of the University of Texas at Austin, working in the Department of Chemistry, Organic Division under the supervision of Professor C. Grant Willson.

Permanent Address: 236 Mustang Street, Prairie Lea, TX 78661

This dissertation was typed by the author.